FLORIDA INTERNATIONAL UNIVERSITY

Miami, Florida

BIOSYNTHESIS AND TRANSPORT OF THE ARSENIC-CONTAINING ANTIBIOTIC ARSINOTHRICIN (AST)

A dissertation submitted in partial fulfillment of

the requirements for the degree of

DOCTOR OF PHILOSOPHY

in

BIOMEDICAL SCIENCES

by

Patience Ngozi Paul

2023

To: Dean Juan Cendan
Herbert Wertheim College of Medicine

This dissertation, written by Patience Ngozi Paul, and entitled Biosynthesis and Transport of the Arsenic-containing Antibiotic Arsinothricin (AST), having been approved in respect to style and intellectual content, is referred to you for judgment.

We have read this dissertation and recommend that it be approved.

_____

Toby Rossman

_____

Xiaotang Wang

_____

Charles Dimitroff

_____

Masafumi Yoshinaga, Co-Major Professor

_____

Barry Rosen, Co-Major Professor

Date of Defense: May 16, 2023

The dissertation of Patience Ngozi Paul is approved.

_____

Dean Juan Cendan

Herbert Wertheim College of Medicine

_____

Andrés G. Gil

Vice President for Research and Economic Development

and Dean of the University Graduate School

Florida International University, 2023

This dissertation (Chapter 1-3) is based in full on the previously published articles listed below with slight changes. I have copies of all copyright permissions.

1. Paul NP, Galván AE, Yoshinaga-Sakurai K, Rosen BP, Yoshinaga M. Arsenic in medicine: past, present and future. Biometals. 2022 Feb 21:1–19. doi: 10.1007/s10534-022-00371-y. PMID: 35190937; PMCID: PMC8860286.
2. Galván AE, Paul NP, Chen J, Yoshinaga-Sakurai K, Utturkar SM, Rosen BP, Yoshinaga M. Identification of the Biosynthetic gene cluster for the organoarsenical antibiotic arsinothricin. Microbiol Spectr. 2021 Sep 3;9(1):e0050221. doi: 10.1128/Spectrum.00502-21. PMID: 34378964; PMCID: PMC8552651.
3. Paul NP, Viswanathan T, Chen J, Yoshinaga M, Rosen BP. The ArsQ permease and transport of the antibiotic arsinothricin. Mol Microbiol. 2023 Feb. 13. doi: 10.1111/mmi.15045. PMID: 36785875.

DEDICATION

To my beloved mother, Cecilia Paul; your resilience inspires me

ACKNOWLEDGMENTS

My heartfelt thanks and appreciation go to my Major Professor, Dr. Barry Rosen. Your enthusiastic commendation after my first presentation during the lab rotation made me feel valued. You took a chance on me when you accepted me into your lab, and I don't think I ever lived up to your expectations, but you never stopped supporting and looking out for me. Thank you for this opportunity of a lifetime. I will never be able to repay you. I am very grateful. My Co-Mentor, Dr. Masafumi Yoshinaga, thank you for always being present, for your patience and guidance, and for being very considerate with me. The truth is, I don't make a lot of sense most of the time, but you have been so kind and gracious. Thank you. I had the great privilege of learning from Emilce Galvan, Jian Chen, Luis Garbinski, Venkadesh Nadar, Kunie Sakurai-Yoshinaga, Thiruselvam Viswanathan, and Manohar Radhakrishnan. There is no lab in FIU I would rather be in than the Rosen Lab.

Special thanks to my committee members, Dr. Toby Rossman, Dr. Xiaotang Wang, and Dr. Charles Dimitroff, for their time and effort in guiding me through the process, reviewing my dissertation, and for their helpful suggestions that made my dissertation successful. Thanks to the Program Coordinator, Dr. Alexander Agoulnik, the amazing Program Specialist, Odalys Delarosa, and all my Professors in the Program. I am grateful to the entire faculty and staff of the College of Medicine for the support and opportunities granted to me to grow professionally.

The University Graduate School awarded me the DEA and DYF Fellowships for the completion of my dissertation. The Student Government Association awarded me a scholarship in aid of research, and the Division of Diversity, Equity, and Inclusion awarded me a fellowship for two semesters. Thank you for making my Ph.D. journey worthwhile.

I have a tremendous support system, My NIGERIAN/AFRICAN FAMILY at FIU. Miami feels like home because of you. The InterVarsity Graduate and Faculty Christian Fellowship and my church Family, Christ Fellowship, Doral, provided moral and spiritual support throughout these years. Mama Mary and Papa Rick Tuttle, your home is a haven to which I can always retreat when I need some rest. Dr. Debbie Able and Debbie Hew, your consistent prayers and care worked many wonders. With my friends from Manna House, I can always be myself. I enjoy every bit of time with you.

To my parents, Paul, and Cecilia Obeta, I owe you a great deal. To Daddy William Anyebe, words are not enough to express my gratitude to you. You held my hands from start to finish of the Ph.D. journey. I will not try to repay you because I cannot. My siblings, Ifeoma, Ebere, Nnamdi, and Chinenye, I am thankful for the gift of you all. My wonderful nieces and nephews lighten me up with their stories and laughter over the phone. I was never alone.

ABSTRACT OF THE DISSERTATION

BIOSYNTHESIS AND TRANSPORT OF THE ARSENIC-CONTAINING ANTIBIOTIC ARSINOTHRICIN (AST)

by

Patience Ngozi Paul

Florida International University, (2023)

Miami, Florida

Professor Masafumi Yoshinaga, Co-Major Professor

Professor Barry Rosen, Co-Major Professor

Arsenicals are one of the oldest treatments for a variety of human disorders. Although infamous for its toxicity, arsenic is paradoxically a therapeutic agent that has been used since ancient times for the treatment of multiple diseases. In the 1970s, arsenic trioxide (ATO), the active ingredient in a traditional Chinese medicine, was shown to produce dramatic remission of acute promyelocytic leukemia (APL) similar to the effect of all-*trans* retinoic acid (ATRA). The discovery of the pentavalent arsenic-containing antibiotic arsinothricin (AST), which is effective against multidrug-resistant pathogens, illustrates the future potential of this new class of organoarsenical antibiotics. The goal of this dissertation is to identify the AST biosynthetic pathway and the mechanism of transport of AST and related compounds into and out of the cells of bacteria. In the first study, three genes, *arsQML*, in an arsenic resistance operon were shown to be a biosynthetic gene cluster responsible for synthesis of AST and its precursor, hydroxyarsinothricin (2-amino-4-(dihydroxyarsinoyl) butanoate or AST-OH). The

arsL gene product is a noncanonical radical *S*-adenosylmethionine (SAM) enzyme that is predicted to transfer the 3-amino-3-carboxypropyl (ACP) group from SAM to the arsenic atom in inorganic arsenite, forming the reduced trivalent form of AST-OH (R-AST-OH), which is methylated by the *arsM* gene product, an arsenic SAM methyltransferase, to produce the reduced trivalent form of AST (R-AST). ArsQ is an efflux permease that was proposed to transport AST or related species out of the cells. In a follow-up study, *B. gladioli arsQ* was expressed in *Escherichia coli* and shown to confer resistance to AST and related arsenicals. Cells of *E. coli* expressing *arsQ* transport R-AST-OH and R-AST, with little transport of their pentavalent forms. Transport is independent of cellular energy and appears to be equilibrative. A structural homology model of ArsQ suggests that Ser320 is in the substrate binding site. A S320A mutant exhibits reduced R-AST-OH transport, suggesting that it plays a role in ArsQ function. The ArsQ permease is proposed to be an energy-independent uniporter responsible for downhill transport of the trivalent form of AST out of cells, which is oxidized extracellularly to the active form of the antibiotic.

TABLE OF CONTENTS

CHAPTER PAGE

LIST OF TABLES

CHAPTER PAGE

LIST OF FIGURES

FIGURE PAGE

CHAPTER 3

CHAPTER 4

CHAPTER 5

ABBREVIATIONS AND ACRONYMS

ABBREVIATIONS

ACP: 3-amino-3-carboxypropyl

AML: Acute myeloid leukemia

APL: Acute promyelocytic leukemia

AQP: Aquaporin/aquaglyceroporin

ArsM: As(III) *S*-adenosylmethionine methyltransferase

ART: Antiretroviral therapy

As(III): Arsenite

As(V): Arsenate

AST: Arsinothricin

AST-OH: Hydroxyarsinothricin

ATL: Adult T-cell leukemia/lymphoma

ATO: Arsenic trioxide

ATRA: All-trans retinoic acid

BGC: Biosynthetic gene cluster

DASS: Divalent anion sodium symporter family

DMAs(III): Dimethylarsenite

DMAs(V): Dimethylarsenate

EBV: Epstein–Barr virus

EGCG: (-)-Epigallocatechin-3-gallate

FCCP: carbonyl cyanide 4-(trifluoromethoxy)phenylhydrazone

FDA: Food and Drug Administration

GOE: Great Oxidation Event

GS: Glutamine synthetase

HAT: Human African trypanosomiasis

HCV: Hepatitis C virus

HIV-1: Human immunodeficiency virus-1

HPLC: High pressure liquid chromatography

HPV: Human papillomavirus

ICP-MS: Inductively coupled plasma-mass spectrometry

INF: Interferon

LB: Lysogeny broth

LRA: Latency reversing agent

MAs(III): Methylarsenite

MAs(V): Methylarsenate

MSMA: Monosodium methylarsenate

MSO: Methionine sulfoximine

MurA: UDP-*N*-acetylglucosamine enolpyruvyl transferase

Nit(V): Nitarsone

PAGE: Polyacrylamide gel electrophoresis

p-ASA: *p*-Arsanilic acid

Pin1: Peptidyl-prolyl cis–trans isomerase NIMA (never in mitosis A) interacting1

PML: Promyelocytic leukemia

PT: Phosphinothricin

RARα: Retinoic acid receptor α

R-AST: Reduced trivalent form of AST

R-AST-OH: Reduced trivalent form of AST-OH

ROS: Reactive oxygen species

Rox(V): Roxarsone

SAM: *S*-Adenosylmethionine

SARS-CoV-2: Severe acute respiratory syndrome coronavirus 2

SDS: Sodium dodecyl sulfate

SIV: Simian immunodeficiency virus

TB: Tuberculosis

TM: Transmembrane spanning helix

UDP: Uridine diphosphate

WHO: World Health Organization

CHAPTER 1: ARSENIC IN MEDICINE: PAST, PRESENT AND FUTURE

1.1 Abstract

Arsenicals are among the oldest treatments for a variety of human disorders. Although infamous for its toxicity, arsenic is paradoxically a therapeutic agent that has been used since ancient times for the treatment of multiple diseases. The use of most arsenic-based drugs was abandoned with the discovery of antibiotics in the 1940s, but a few remained in use such as those for the treatment of trypanosomiasis. In the 1970s, arsenic trioxide, the active ingredient in a traditional Chinese medicine, was shown to produce dramatic remission of acute promyelocytic leukemia similar to the effect of all-*trans* retinoic acid. Since then, there has been a renewed interest in the clinical use of arsenicals. Here I review the ancient and modern medicinal uses of inorganic and organic arsenicals. Included are antimicrobial, antiviral, antiparasitic and anticancer applications. In the face of increasing antibiotic resistance and the emergence of deadly pathogens such as the severe acute respiratory syndrome coronavirus 2 (SARS-CoV-2), we propose revisiting arsenicals with proven efficacy to combat emerging pathogens. Current advances in science and technology can be employed to design newer arsenical drugs with high therapeutic index. These novel arsenicals can be used in combination with existing drugs or serve as valuable alternatives in the fight against cancer and emerging pathogens. The discovery of the pentavalent arsenic-containing antibiotic arsinothricin (AST),

which is effective against multidrug resistant pathogens, illustrates the future potential of this new class of organoarsenical antibiotics.

Keywords Arsenic · Metalloids · Metallodrugs · Anticancer drugs · Antivirals · Antimicrobials

1.2 Introduction

1.2.1 History of arsenic in medicine

Here I review the history and present use of arsenicals in medicine. The origin of the name “arsenic” traces back to the Greek word “*arsenikon*” meaning “*potent*” (Jollife 1993; Hoonjan et al. 2018). Arsenic was known empirically as a potent medicinal agent as early as 2000 BC (Fig. 1), when arsenic trioxide (ATO, As_2O_3, also known as white arsenic) (Fig. 2A) obtained from copper smelting was used as both a drug and a poison (Jollife 1993). Orpiment (As_2S_3, yellow arsenic) and realgar, (As_4S_4, red arsenic) (Fig. 2B), described as early as the 4th Century BC by the Greek philosopher Aristotle (384–322 BC), were the earliest arsenic minerals in recorded history (Fig. 1) (Gorby 1988; Bentley and Chasteen 2002). Although arsenic-containing minerals were known in antiquity, it was not until 1250 that elemental arsenic was conclusively identified by the German alchemist Albertus Magnus (1193–1280) (https://pubchem.ncbi.nlm.nih.gov/element/Arsenic). History is rife with stories of arsenic used as a poison for both royalty and commoners. Odorless and tasteless ATO has been used as a poison for millennia due to its availability and low cost

(Jollife 1993; Hoonjan et al. 2018; Gorby 1988; Hughes et al. 2011). One of the earliest recorded cases of arsenic poisoning was in the year 55 AD, when the fifth Roman emperor Nero ordered the poisoning of his 13-year-old stepbrother Britannicus to secure his Roman throne (Jollife 1993; Gorby 1988; Bentley and Chasteen 2002; Doyle 2009). Pope Alexander VI (1431–1503), a member of the Borgia family, one of the most eminent dynasties of the Italian Renaissance, used the infamous powder called *cantarella*, which is widely believed to have consisted mainly of arsenic, to murder cardinals for their property and wealth (Gorby 1988). A well-known example of arsenic poisoning is "*The Affair of the Poisons*" in the French court of Louis XIV, where Catherine Deshayes provided the arsenic-based poison *La Poudre de Succession* or "*inheritance powder*" to women to help them rid themselves of their husbands (Gorby 1988; Bentley and Chasteen 2002). The inheritance powder continued to be popular in France until the nineteenth century, when it became the most favorite poison, as recorded by early forensic toxicologists (Gorby 1988). The incidence of arsenic poisoning dramatically waned after the advent of the Marsh test, a sensitive forensic test for arsenic developed in 1836 by the English chemist James Marsh (Gorby 1988; Hughes et al. 2011).

Behind its inglorious history as a poison, however, arsenic has an even more prestigious history as a pharmaceutical agent. Arsenic has been in use as therapeutics since ancient times in the Greek and Roman civilizations, as well as in Chinese and Indian traditional medicine (Doyle 2009). Hippocrates (460–377 BC), the Greek physician, often referred to as the Father of Medicine, is

thought to have administered the arsenic minerals orpiment and realgar as escharotics and remedies for ulcers and abscesses (Fig. 1) (Jollife 1993; Hoonjan et al. 2018; Hughes et al. 2011; Bentley and Chasteen 2002; Waxman and Anderson 2001; Zhu et al. 2002; Riethmiller 2005). Aristotle and the Roman author Pliny the Elder (23–79 AD) both wrote on the medicinal properties of arsenicals (Fig. 1) (Jollife 1993; Gorby 1988). The Greek physician Galen (129–210 AD) recommended the use of arsenic sulfide to treat ulcers (Jollife 1993; Riethmiller 2005). The first book on Chinese traditional medicine, *Shen Nong Ben Cao Jing*, compiled in the Eastern Han dynasty (25–220 AD), traces the use of arsenic in traditional Chinese medicine as far back as 200 BC (Fig. 1) (Liu et al. 2008), which agrees with the fact that the Chinese Nei Jing Treaty (263 BC) recorded the use of arsenic pills for treatment of periodic fever (Hoonjan et al. 2018; Zhu et al. 2002; Chen and Chen 2017). Sun Si-Miao (581–682 AD), a Chinese physician called China's King of Medicine, used a combination of realgar, orpiment and ATO for treatment of malaria (Hoonjan et al. 2018; Zhu et al. 2002; Chen and Chen 2017). Shi Zhen Li (1518–1593 AD), a Chinese physician in the Ming dynasty, wrote *Ben Cao Gang Mu*, or *Compendium of Materia Medical*, a major pharmacopoeia in Chinese history, where he described the use of ATO as a remedy for various diseases (Zhu et al. 2002; Chen and Chen 2017; Gibaud and Jaouen 2010). In traditional Indian medicine, the three main arsenicals used in Ayurveda, an alternative system of medicine originating from the ancient Indian subcontinent several thousand years ago, are orpiment, realgar and ATO (Panda and Hazra 2012). In Arabia, Avicenna (980–1037 AD),

a Persian physician, introduced the internal use of ATO for the treatment of fevers (Zhu et al. 2002). Paracelsus (1493–1541 AD), a Swiss physician recognized as the Father of Toxicology and Pharmacology, is known to have used elemental arsenic extensively (Fig. 1) (Jollife 1993; Hoonjan et al. 2018; Gorby 1988; Waxman and Anderson 2001; Zhu et al. 2002; Borzelleca 2000). He advocated for the use of minerals and chemicals, including arsenic, in medicine, emphasizing that the dosage makes the difference between a drug and a poison. In 1786 Thomas Fowler (1736–1801 AD), a British physician and pharmacist, reported the effects of a favored solution of 1% potassium arsenite named "*liquor mineralis*" for malaria, remittent fevers, and periodic headaches (Fig. 1). This medicine, renamed "***Fowler's solution***", once introduced into the London Pharmacopoeia in 1809, became popular in Western countries throughout the Victorian Era as a main therapeutic option for a wide variety of ailments and diseases, including asthma, chorea, eczema, psoriasis, rheumatism, syphilis, tuberculosis and ulcers (Jollife 1993; Hoonjan et al. 2018; Gorby 1988; Hughes et al. 2011; Bent ley and Chasteen 2002; Doyle 2009; Waxman and Anderson 2001; Zhu et al. 2002; Gibaud and Jaouen 2010; Thomas and Troncy 2009).

There is some concern over the present-day use of arsenicals in traditional medicine (Ernst 2002), leading to evaluation of the bioavailability of arsenic species in their prescriptions. In Indian traditional ayurvedic medicine, for example, a special subset of herbal medicines called *Rasa Shastra* involves

intentional use of toxic elements including arsenic, which are believed to be converted into non-toxic forms called *bhasmas* via the preparation procedures. However, the bioaccessibility of arsenic in several traditional Indian medicines was suggested to lead to accumulation of arsenic above the acceptable daily limit if consumed at recommended doses (Koch et al. 2011). More recently a similar concern was raised about some traditional Chinese medicines (Liu et al. 2018). To exploit the full potential of arsenic as medicine, therefore, further evaluation is required to develop regulations for the proper dosage of arsenic containing traditional medicines.

Applications of arsenicals extend beyond drugs and poisons. They have been used in agriculture, metallurgy, cosmetics, electronics semiconductors, and other industries (Bentley and Chasteen 2002). Monosodium methylarsenate (MSMA) and sodium dimethylarsenate (cacodylate) have been used as post-emergent herbicides on cotton fields and other non-food crops (Matteson et al. 2014). Although banned for general use by the US Environmental Protection Agency (EPA), MSMA is still in limited use in the United States for cotton fields, new golf courses and highway medians, and it is still applied as an herbicide on rice, cotton, fruit trees and coffee in Asian countries.

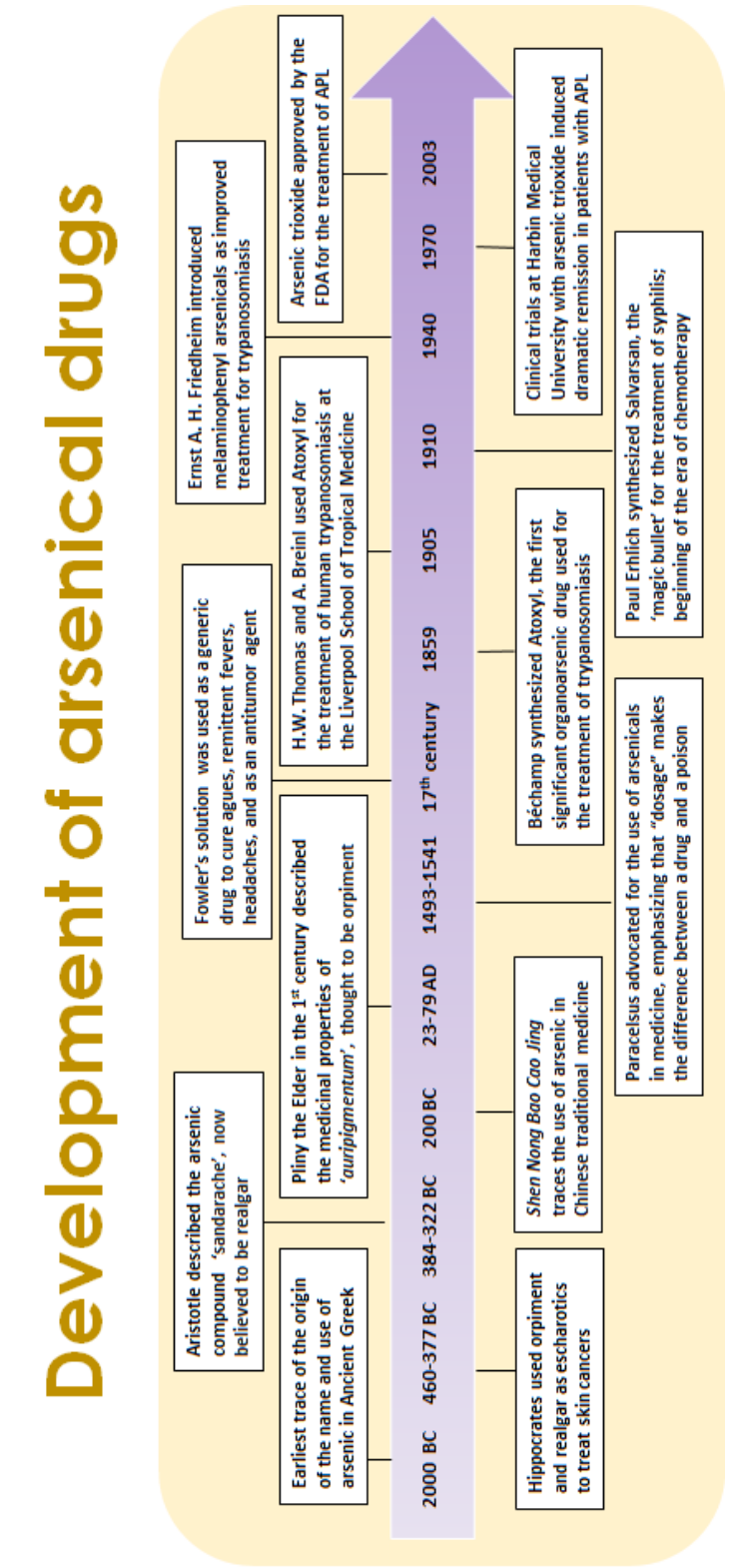

Fig 1: Milestones of the use and development of arsenicals in medicine

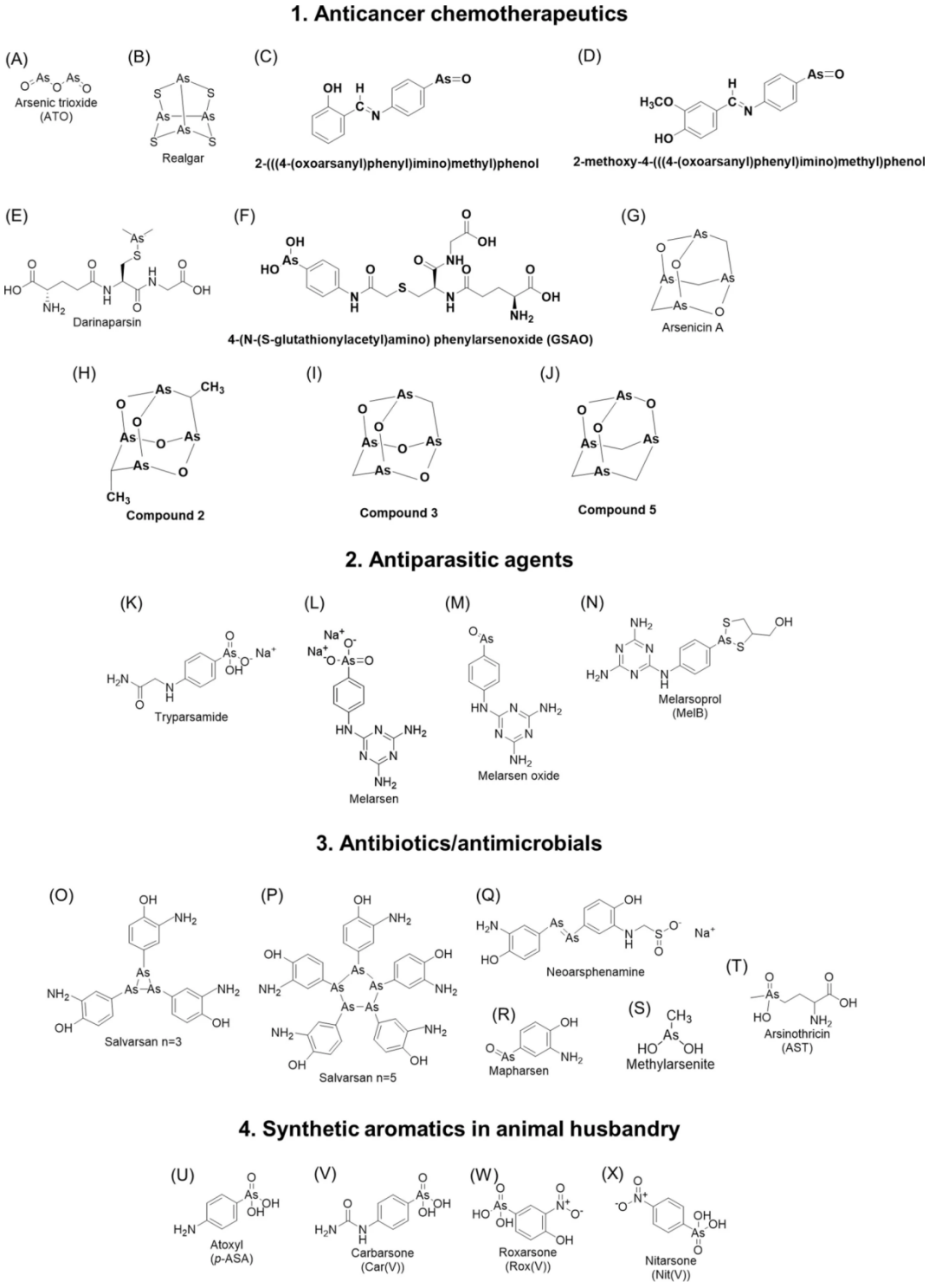

Fig 2: Chemical structure of arsenicals

1.3 Inorganic and organic arsenic-containing drugs

1.3.1 Development of arsenical drugs

In the modern era, the use of arsenicals as drugs has alternated between successes and failures. As described below, arsenical drugs can be generally grouped into inorganic, for example, ATO (Fig. 2A), and organic compounds, such as atoxyl (*p*-aminophenylarsenate or *p*-arsanilic acid (*p*-ASA)) (Fig. 2U). Atoxyl, the first effective artificial organoarsenic drug, was synthesized by the French scientist Antoine Béchamp (1816–1908 AD), in 1859 by heating a mixture of aniline and arsenic acid (Fig. 1) (Riethmiller 2005; Gibaud and Jaouen 2010). Its clinical effectiveness was not demonstrated until some forty years later, when the physicians Canadian Harold W. Thomas (1875–1931 AD) and Australian Anton Breinl (1880–1944 AD) at the Liverpool School of Tropical Medicine first used it in 1905 to treat human trypanosomiasis (Fig. 1) (Jollife 1993; Gibaud and Jaouen 2010). Although it causes optic atrophy due to its high arsenic content (Jollife 1993), the trypanocidal effects of Béchamp's atoxyl inspired Paul Ehrlich (1854–1915), the German Nobel Laureate known as the Father of Chemotherapy, to initiate an extensive synthesis of organic arsenicals to find a drug against the syphilis spirochaete (Jollife 1993). Arsphenamine was the 606th aromatic arsenical he synthesized in 1910 (Fig. 1). Compound 606 was later called the *magic bullet* Salvarsan, the first effective chemotherapeutic drug for the treatment of syphilis (Jollife 1993; Gorby 1988; Hughes et al. 2011; Bentley and Chasteen 2002). The composition of Salvarsan was a question of debate for

almost a century. In 2005, Nicholas and colleagues provided evidence based on electrospray ionization mass spectrometric data that Salvarsan in solution exists as cyclic species $(RA)_n$, with n=3 (Fig. 2O) and *n*=5 (Fig. 2P) (Lloyd et al. 2005). Like atoxyl, however, Salvarsan treatment was lengthy, and the side effects unpleasant. Less toxic derivatives such as neoarsphenamine (Neosalvarsan) (Fig. 2Q) and oxophenarsine hydrochloride (Mapharsen) (Fig. 2R) made treatment more bearable (Jollife 1993; Bentley and Chasteen 2002; Gibaud and Jaouen 2010). Ehrlich's work with Salvarsan ushered in the modern era of chemotherapy.

1.3.2. Arsenical anticancer chemotherapeutic agents

1.3.2.1 *Arsenic trioxide (ATO)*

Arsenicals have a long history of use as cancer chemotherapeutic agents. ATO (Fig. 2A) was a favorite compound in traditional ancient Chinese medicine for over 2000 years (Bentley and Chasteen 2002). ATO is an amphoteric oxide that readily dissolves in alkaline solutions. It was originally made from orpiment by roasting and purifying the smoke (Gibaud and Jaouen 2010). In 1878, the related formulation, Fowler's solution, was found to be effective for the treatment of leukemia, and, in addition, Fowler pastes were applied topically potentially for the treatment of skin and breast cancers (Hoonjan et al. 2018; Hughes et al. 2011; Waxman and Anderson 2001; Gibaud and Jaouen 2010). Arsenic therapy was the mainstay of antileukemia treatment until the advent of radiation therapy in the early twentieth century (Hoonjan, et al. 2018; Waxman and Anderson 2001). Despite its

toxicity, arsenic remained in use in traditional Chinese medicine (Bentley and Chasteen 2002). Taking inspiration from this traditional medicine, investigators at Harbin Medical University showed that a solution of ATO produced complete remission of acute promyelocytic leukemia (APL) in about two-thirds of patients in the 1970s (Fig. 1) (Zhu et al. 2002; Chen and Chen 2017). The ATO used in those clinical studies contained trace amounts of mercury, so it was possible that the anticancer effects were due to mercury rather than arsenic. Clinical trials with pure ATO began in 1994, and, by 1996, its effectiveness was confirmed in other countries. In 2003 ATO, marketed as Trisenox®, was approved by the U.S. Food and Drug Administration (FDA) for treatment of APL refractory to all-trans retinoic acid (ATRA) (Gibaud and Jaouen 2010). The revival of ATO for treatment of APL and other specific hematological malignancies has sparked renewed interest in arsenic-based drugs (Hoonjan et al. 2018; Hughes et al. 2011; Gibaud and Jaouen 2010).

Since ATO was approved as an effective drug for clinical treatment of hematological malignancies, including APL and multiple myeloma, its mechanism as anticancer agent has been under active investigation. The mechanism of action of ATO is not clear, and there are a number of potential targets. Like most trivalent arsenicals, it has the potential to bind to thiols in metabolites such as glutathione, vicinal thiol pairs in lipoamide and in proteins such as lipoamide dehydrogenase, inhibiting cellular energy production and increasing production of intracellular reactive oxygen species (ROS) (Carney

2008; Emadi and Gore 2010). ATO treatment results in demethylation of DNA, affecting the promoters of many genes and also binds to oncoproteins/transcription factors (Emadi and Gore 2010; Dawood et al. 2018; Huynh et al. 2019). These alterations affect multiple cellular processes in a variety of cancers, resulting in cell cycle arrest, apoptosis and mesenchymal to epithelial transition through a variety of molecular targets (Chen et al. 1997; Bao et al. 2016; Miller et al. 2002; Shao et al. 1998). The final outcome depends on the cell type as well as the concentrations of administration and duration of ATO exposure (Chen et al. 1997).

However, those are rather nonspecific effects of ATO and do not explain its selective ability to treat APL. APL is characterized by chromosomal translocation t(15;17) (q24;q21), which produces a fusion promyelocytic leukemia (PML) protein-retinoic acid receptor alpha (RARα) gene that is found in over 98% of patients (Borrow et al. 1990; de Thé et al. 1990; Golomb et al. 1980). The PML-RARα fusion gene consists of the PML gene on chromosome 15 and the RARα gene on chromosome 17. The production of the PML-RARα oncoprotein alters myeloid differentiation at the promyelocytic stage, leading to accumulation of immature cells (Grisolano et al. 1997). In addition, PML-RARα increases cell survival and increases proliferation of leukemic cells, resulting in progressive leukemogenesis (Grignani et al. 1993; Pandolf 2001; Puccetti and Ruthardt 2004). PML-RARα appears to be a target of ATO, which binds to the PML-RARα oncoprotein in NB4 cells, a human APL cell line, and alters SUMOylation of the

PML moiety, leading to protein degradation (Zhang et al. 2010). Although the effect of ATO on the PML-RARα leukemic stem cells appears to be mainly through inhibition of proliferation (Testa and Lo-Coco 2015), this PML-RARα degradation is also thought to induce apoptosis or differentiation to myeloid cells, leading to a decrease in leukemic cells (Zhang et al. 2010; Rojewski et al. 2002). Another putative target of ATO is the Wip1 phosphatase. ATO has been reported to activate the Chk2 and/or p38 MAPK apoptotic pathways in various chronic myelogenous leukemia cells (Giafs et al. 2006; Shim et al. 2002; Verma et al. 2002) as well as APL cells (Yoda et al. 2008) by inhibiting Wip1 phosphatase activity. Since expression of Wip1 is amplified in a number of cancers, including breast, papillary thyroid, colorectal and prostate cancers and other types (Emelyanov and Bulavin 2015; Li et al. 2002; Natrajan et al. 2009), ATO is potentially a therapeutic agent for other tumor types.

ATO may also be a treatment for other forms of leukemia via its function as a pro-oxidant factor, disrupting redox pathways in cancer cells. The combination of ATO with ascorbate (vitamin C), a dietary antioxidant that also possesses pro-oxidant activity in high concentrations (Kaźmierczak-Barańska et al. 2020), selectively killed blasts from APL patients and was also effective against approximately one-third of primary acute myeloid leukemia (AML) samples examined, presumably due to apoptosis induced by overproduction of ROS (Noguera et al. 2017). This pro-oxidant activity provides a rationale for testing the combination of ATO and ascorbate in advanced cases of AML and APL (Noguera et al. 2017).

Pin1, the peptidyl-prolyl *cis–trans* isomerase NIMA (never in mitosis A)-interacting 1, has been reported to be another target of ATO, enhancing its anti-cancer effects against multiple tumor types (Kozono et al. 2018). Pin1 is a major regulator of cancer signaling networks. It catalyzes *cis–trans* isomerization at phosphorylated Ser/Thr–Pro motifs, resulting in changes of protein conformation, function and stability, which in turn activates numerous cancer-driving pathways. Pin1 is overexpressed in various cancers and cancer stem cells (Ayala et al. 2003; Bao et al. 2004; Luo et al. 2015; Rustighi et al. 2014; Wulf et al. 2004) and involved in regulation of more than 50 oncogenes and 20 tumor suppressor factors (Lu and Hunter 2014; Zhou and Lu 2016). ATO inhibits Pin1 via direct and noncovalent binding to the active site, inducing degradation of Pin1. Interestingly, the anticancer effects of ATO are indirectly enhanced by co-treatment with ATRA, another well-known Pin1 inhibitor, which increases cellular ATO uptake via induction of aquaporin-9 (AQP9) expression, in addition to directly inhibiting and degrading Pin1 (Kozono et al. 2018).

However, a higher dose of ATO is required for the treatment of solid tumors compared to soft tumor hematologic malignancies, which raises concerns about toxicity. Methods to effectively deliver ATO to the cells without the accompanying toxicity are under development. For example, liposomal-encapsulated ATO delivered to HeLa cells, which are derived from human papillomavirus (HPV)-cervical carcinoma, effectively reduced levels of HPV-E6 proteins and induced

apoptosis with reduced toxicity compared to free ATO. Encapsulation of ATO using this liposomal nanotechnology was shown to decrease membrane permeability to ATO by allowing its gradual release (Wang et al. 2016). The O'Halloran group developed a nanoparticulate formulation of ATO encapsulated in "nanobins" (liposomal vesicles) (Chen et al. 2006). The cytotoxicity of the encapsulated ATO was evaluated against a panel of human breast cancer cell lines and was found to be much less compared to the free ATO. In contrast, the nanobins potentiated the antitumor efficacy of ATO *in vivo* in an orthotopic model of triple-negative breast cancer (Ahn et al. 2010). The group has also developed a synthesis method that combines ATO and cisplatin (*cis*-diamminedichloroplatinum(II)), a compound commonly used in the treatment of solid tumors, to form a stable aqueous complex, arsenoplatin, having a distinct biological activity from ATO and cisplatin individually (Miodragović et al. 2013). Arsenoplatin can be loaded in liposomal drug delivery systems and has been shown to possess significant biological activity against several cancer cell lines. When compared to cisplatin, it showed greater activity in breast, leukemia, colon, and central nervous system cancer cell lines (Miodragović et al. 2019). Other systems have been investigated for the effective delivery of arsonium compounds in cancer therapeutics, such as the triphenylarsonium-functionalised gold nanoparticles (Lalwani et al. 2015). The gold nanoparticles are decorated with the triphenylarsonium groups to serve as potential nanocarriers for intracellular therapeutics. The development of delivery systems for slow dosing

with arsenical drugs can modulate toxicity, significantly expanding medical applications of arsenic.

1.3.2.2 *Realgar*

Another form of inorganic arsenic, realgar (As_4S_4, red arsenic) (Fig. 2B), has been used as a therapeutic agent since the days of ancient China (Wu et al. 2011). Inspired by nano-drug, lately, realgar nano particles (an average particle size of <100 nm) have been employed in studies rather than coarse realgar. This approach is adopted to overcome the problem of limited solubility of realgar particles in aqueous solutions, and to increase their bioavailability (Shi et al. 2016). Several *in vitro* studies demonstrated that realgar nanoparticles significantly decreased cell proliferation and promoted apoptosis in B16 melanoma cells (Zhao et al. 2010) and rat C6 glioma cells (An et al. 2011). Furthermore, in tumor bearing C57BL/6 mice, transdermal delivery of the realgar nanoparticles markedly decreased the tumor volumes with little toxicity to the mice (Zhao et al. 2010). Recently the effect of realgar nanoparticles was compared with ATO against several multiple myeloma cell lines and primary cell lines from multiple myeloma patients (Cholujova et al. 2017). The realgar nanoparticles were prepared by milling realgar into nano-sized dimensions under high energy. Both forms of inorganic arsenic were cytotoxic, but the realgar nanoparticles were two- to four-fold more effective than ATO in the cell lines, xenograft and multiple myeloma patient-derived myeloma mouse models. Mechanistic studies showed that the effects of the realgar nanoparticles and ATO on the multiple myeloma models

included pronounced apoptosis and G2/M cell cycle arrest. In this study, realgar nanoparticles but not ATO could significantly deplete the amount and clonogenicity of multiple myeloma stem-like side population in bone marrow stromal cells. Also, there was synergistic anti-multiple myeloma activity when realgar and ATO were combined with lenalidomide or melphalan, both of which have been approved for treatment of multiple myeloma. In an attempt to increase the uptake of realgar and prolong the retention time in cancer cells, (-)-epigallocatechin-3-gallate (EGCG), another natural medicine that inhibits cancer cell growth, was used as a drug carrier to encapsulate realgar nanoparticles (Fang et al. 2019). Compared with realgar nanoparticles, the EGCG-realgar nanoparticles significantly inhibited the proliferation of APL HL-60 cells. In subcutaneous solid tumor model mice, EGCG-realgar nanoparticles decreased tumor volumes at an inhibitory rate of 60.18% at a dose of 70 mg/kg. More recently, the effect of realgar nanoparticles on lung cancer stem cells was also examined. The nano-realgar was shown to inhibit tumor growth both *in vitro* and *in vivo* by repressing metabolic reprogramming via downregulation of HIF-1α expression and PI3K/Akt/mTOR pathway (Yang et al. 2021).

1.3.2.3 *Organoarsenicals*

Organic arsenicals are under current examination for potential therapeutic use. Several synthetic organoarsenicals were tested for antitumor activity against HL-60 (leukemia), SGC 7901 (gastric cancer) and MCF-7 (breast cancer) human cancer cell lines (Fan et al. 2016). 2-(((4-(oxoarsanyl)phenyl)imino)methyl)phenol

($C_{13}H_{10}AsNO_2$) (Fig. 2C) and 2-methoxy-4-(((4-(oxoarsanyl)phenyl)imino)methyl) phenol ($C_{14}H_{12}AsNO_3$) (Fig. 2D) exhibited the highest growth inhibition of HL-60 cells, with IC_{50} values of 0.77 μM and 0.51 μM, respectively. Both induced apoptosis via oxidative stress in HL-60 cells (Fan et al. 2016). Another organoarsenical that is being evaluated for the treatment of solid tumors is the glutathione conjugate of dimethylarsenite, darinaparsin (L-γ glutamyl-S-(dimethylarsino)-L-cysteinyl-glycine) (Fig. 2E). The injectable form of darinaparsin, SP 02L, is currently in phase 2 clinical trial in patients with relapsed or refractory peripheral T-cell lymphoma (https://clinicaltrials.gov/ct2/show/NCT02653976). Analysis of data from two phase 1 clinical trials in Japan and Korea showed that darinaparsin has good potential efficacy and high safety profile (Ogura et al. 2021). A related glutathione conjugate, 4-(N-(S-glutathionylacetyl)amino) phenylarsenoxide or GSAO (Fig. 2F), is in phase 1 clinical trial in patients with advanced solid tumors (Horsley et al. 2013). It is noteworthy that darinaparsin (Darvias®), the DMAs(III)-glutathione conjugate, has been approved in Japan as a novel mitochondrial-targeted anticancer agent for the treatment of relapsed or refractory peripheral T-cell lymphoma in 2022 (Frampton JE 2022), after this review article was published.

1.3.2.4 *Polyorganoarsenicals*

Another class of organoarsenicals with potential clinical value is polyarsenicals. The first reported is arsenicin A (2,4,6-trioxa-1,3,5,7-tetrarsatricyclo [3.3.1.13,7] decane) ($C_3H_6As_4O_3$) (Fig. 2G), a natural product isolated from *Echinochalina*

bargibanti, a marine sponge belonging to the class Demospongiae (Mancini et al. 2006). Arsenicin A has both antibiotic and anti-APL leukemia activity. It has a cage-like structure similar to the carbon structure in the diamond backbone adamantane ($(CH)_4(CH_2)_6$), in which the four methanetriyl carbon bridgeheads are replaced by arsenic and three methylene bridges are replaced by oxygen (Lu et al. 2012, 2010). The anti-proliferative activity of arsenicin A was examined in the PML RARα-positive APL cell line NB4 (Lu et al. 2012). Arsenicin A exhibits a 21-fold greater anti-proliferative activity compared to ATO in NB4 cells. Using flow cytometry, arsenicin A was shown to induce cell death at a 27-fold lower concentration (IC_{50}=53 nM) compared with ATO (IC_{50} = 1440 nM), and proliferative arrest at 20 nM compared with 790 nM for ATO (Lu et al. 2012).

Five arsenicin A analogs were synthesized, and their activity was evaluated *in vitro* against a full panel of human cancer cell lines from the National Cancer Institute (NCI-USA) (Mancini et al. 2017). Three of these compounds, designated **compound 2** (9,10-dimethyl-2,4,6,8-tetraoxa-1,3,5,7,-tetraarsatricyclo[3.3.1.13,7]decane) ($C_4H_8As_4O_4$) (Fig. 2H), **compound 3** (2,4,6,8-tetraoxa-1,3,5,7-tetraarsa-adamantane) ($C_2H_4As_4O_4$) (Fig. 2I), and **compound 5** (an isomer of Arsenicin A) (Fig. 2J), showed significantly higher cytotoxicity against the various cancer cell lines than ATO. **Compound 2** was particularly effective in inhibiting growth of solid tumor cell lines of colon cancer, melanoma, ovarian cancer, renal cancer, prostate cancer, and breast cancer. Two sulfur containing derivatives, arsenicin B and arsenicin C, also possess antibiotic

activity against human pathogens. Although less potent than arsenicin A against leukemia cells, these sulfur-containing polyarsenicals have especially potent antimicrobial activity against *Staphylococcus aureus*, a major human pathogen with growing resistance to conventional antibiotics (Tähtinen et al. 2018). These findings lend new perspectives on the development and use of polyorganoarsenicals as therapeutics.

1.3.3 Arsenical antiparasitic agents

Tryparsamide (*p*-glycineamidophenylarsonate) (Fig. 2K), developed by Walter A. Jacobs and Michael Heidelberger at the Rockefeller University in 1919, is acknowledged as the first effective arsenical therapeutic agent against Gambian sleeping sickness. That disease is the slow-progressing form of human African trypanosomiasis (HAT) and is caused by *Trypanosoma brucei gambiense*, which is endemic in western and central Africa, especially in the late stage of the infection (e.g. neurological stage through central nervous system invasion) (Gibaud and Jaouen 2010). Although this drug was widely used from the early 1920's, its use waned in the 1940's due to the spread of resistant strains. In the 1940s, Ernst A. H. Friedheim improved the treatment of trypanosomiasis with the introduction of melaminophenyl arsenicals (Fig. 1), although toxicity was still reported (Gibaud and Jaouen 2010). Melarsen (4-(4,6-diamino-1,3,5-triazin-2-yl)amino]phenylarsenate) (Fig. 2L), the first melaminophenyl arsenical that Friedheim synthesized in 1939, was less active than tryparsamide. In contrast, melarsen oxide (Fig. 2M), the reduced form of melarsen and the first trivalent

organoarsenical used against trypanosomes, was very effective against both early (hemolymphatic) and late (neurologic) stages, yet it exhibited high toxicity (Friedheim 1948). Friedeim combined dimercaprol or BAL (British anti-Lewisite), the counteract compound for Lewisite, the trivalent organoarsenical-based chemical weapon first used in World War I (Peters et al. 1945), with melarsen oxide to produce the drug melarsoprol (MelB or arsobal) (Fig. 2N) (Friedheim 1949). Melarsoprol is 100-fold less cytotoxic and 2.5-fold less trypanocidal compared with melarsen oxide (Fairlamb and Horn 2018). It was introduced into clinical use in 1949 for use in African countries to treat Gambian sleeping sickness. Melarsoprol can cross the blood–brain barrier (Sekhon 2013). However, a serious side effect of melarsoprol is reactive encephalopathy, which occurs in about 10% of patients (Blum et al. 2001; Pepin and Milord 1991). Even so, its ability to cross the blood–brain barrier into the cerebrospinal fluid made it especially useful for treatment of second stage Gambian sleeping sickness, when the trypanosome enters the central nervous system (Colotti et al. 2018; Rodgers et al. 2011). Given the absence of effective alternatives, the World Health Organization (WHO) recommends its use as the only chemotherapeutic for the second stage of the faster-progressing form of human African trypanosomiasis caused by *Trypanosoma brucei rhodesiense,* which is more common in southern and eastern Africa (Büscher et al. 2017). Melarsoprol is a prodrug, and the active form of the drug is melarsen oxide (Fig. 2M). This trivalent form of melarsen (Fig. 2L) can be detected in cerebrospinal fluid 1 h after injection (Keiser et al. 2000). Melarsoprol is rapidly broken down mainly into

melarsen oxide, perhaps enzymatically (Fair lamb and Horn 2018). As a trivalent organoarsenical, melarsen oxide has high affinity for thiols and forms a stable adduct with the parasite's alternative to glutathione, trypanothione. Reduction of free cytosolic trypanothione inhibits trypanothione reductase, the parasite enzyme that contributes to cytosolic redox balance (Cunningham et al. 1994; Fairlamb et al. 1989). In addition, melarsen oxide causes rapid lysis of *Trypanosoma brucei in vitro* (Van Schaftingen et al. 1987). P2 adenosine transporter (TbAT1) (Carter and Fairlamb 1993; Mäser et al. 1999) and aquaglyceroporin 2 (TbAQP2) (Alsford et al. 2012; Baker et al. 2012) are shown to be involved in cellular uptake of melarsoprol in *T. brucei*. Beginning in the 1990s, resistance to melarsoprol became widespread (Brun et al. 2001). Melarsoprol resistance in clinical isolates (Graf et al. 2013; Pyana Pati et al. 2014) is predominantly related to mutations in the parasite *Tbaqp2* gene (Munday et al. 2015). Mutations in this aquaglyceroporin, which is involved in uptake of melarsoprol, include deletions (Baker et al. 2012) or rearrangements with *Tbaqp3* to form a chimeric *aqp2-3* gene (Munday et al. 2014). Resistance to melarsoprol in human African trypanosomiasis patients has led to a decrease in the use of this arsenical drug (Fairlamb and Horn 2018). With the development of newer drugs and antibiotics, interest in arsenic-based drugs gradually waned mainly due to their low therapeutic index.

1.3.4 Antiviral arsenic agents

In addition to the use of arsenicals for control of pathogens and as cancer chemotherapeutics, their potential as antiviral agents are also under investigation. ATO has been shown to inhibit Hepatitis C Virus (HCV) replication at sub micromolar concentrations (Hwang et al. 2004). The concentrations that gave 50% inhibition of replication (EC_{50}) without causing cellular cytotoxicity are 0.35 and <0.2 µM, when determined by a reporter-based HCV replication assay and by RT-qPCR analysis, respectively. The anti-HCV activity of ATO was also demonstrated using an engineered cell line-based assay system that constitutes all steps in the full cycle of HCV infection and replication, where ATO at 0.3 µM abolished the HCV signal, while high concentrations of interferon-α, an antiviral cytokine used for the treatment of chronic hepatitis C, only minimally suppressed the viral signal. In a follow-up study, treatment of HCV-infected cells with 1 µM ATO, which effectively inhibited the HCV RNA replication without exhibiting cytotoxicity, led to depletion of intracellular glutathione and an increase in superoxide anion radicals (Kuroki et al. 2009). The anti-HCV activity of ATO was inhibited in the presence of *N*-acetylcysteine, an antioxidant and glutathione precursor. These results suggest that ATO exerts its effect against HCV by modulating the intracellular glutathione redox system and oxidative stress. These findings demonstrate the potential of ATO for the development of potent antiviral agents against HCV and related viruses.

Viral latency has been recognized as the major source of viral rebound in human immunodeficiency virus-1 (HIV-1) infections after discontinuation of antiretroviral therapy (ART) (Siliciano and Siliciano 2000). There is, therefore, a need to render the latent HIV-1 susceptible to eradication. One way to provide drug access is by reactivation of viral replication. ATO has been reported to activate latent HIV-1 in the Jurkat T cell line in a process that involves the nuclear factor kappa B (NF-κB) signaling pathway (Wang et al. 2013). Similarly, inorganic sodium arsenite was shown to reactivate gene expression and viral replication of the latent genome of herpes simplex virus type 1 (HSV1) (Preston and Nicholl 2008). These results suggest that inorganic arsenicals may be able to enhance ART. Recently the ability of ATO in combination with ART to regulate viral reservoirs in primary CD4+T lymphocytes of HIV-1-infected patients and simian immunodeficiency virus (SIV)-infected Chinese rhesus macaques was examined (Yang et al. 2019). ATO significantly increased the levels of cell-associated RNAs in resting CD4+T cells from both HIV-1-infected patients and SIV-infected macaques in a dose-dependent manner. Using chronically SIV-infected macaques, ATO in combination with ART delayed viral rebound, decreased SIV integrated DNA in CD4+T cells and restored CD4+T cell counts *in vivo*. In contrast, there was a rebound in the control group treated with ART alone in an average interval of 22 days after discontinuation of therapy. Furthermore, SIV specific immune responses against the multiple SIV antigens increased after treatment with ATO. The use of ATO as a latency-reversing agent (LRA) in combination with combined ART (cART) is currently under

investigation in a clinical trial ("The Effect of ATO on Eliminating HIV-1 Reservoir Combined with cART" 2019). https://clinicaltrials.gov/ct2/show/NCT03980665

ATO has been reported to exhibit potent inhibition of human adenovirus infection *in vitro* (Hofmann et al. 2020). PML nuclear bodies, otherwise referred to as PML oncogenic domains, are interferon (IFN)-inducible nuclear structures that participate in cellular processes including apoptosis, senescence and antiviral defense. Infection with human adenovirus reorganizes the dot-like PML nuclear bodies into track-like structures, impairing their function. This aberrant PML nuclear body phenotype is observed in acute PML cells. *In vitro* treatment of APL cells with ATO at micromolar concentrations produced significant anti-adenovirus activity. This activity was partly due to the ability of ATO to induce oxidation of PML nuclear bodies before multimerization by the virus, reconstituting the usual dot-like structure and restoring the antiviral function of PML nuclear bodies in the cells of APL patients' cells (Hofmann et al. 2020).

The effectiveness of arsenic-based drugs in virus associated cancers has also been reported (Kchour et al. 2013). In patients with human T-cell leukemia virus type 1 (HTLV-1) associated adult T-cell leukemia/lymphoma (ATL), ATO in combination with IFN-α and zidovudine, an FDA-approved nucleoside reverse-transcriptase inhibitor (NRTI) class antiretroviral drug, improved the cytokine gene expression profile by a shift from an initial immunosuppressive-like state (T_{reg} (T regulatory)/(Th2 phenotype)) to an immunocompetent-like state (Th1 phenotype)

after 30 days of treatment. This shift is possibly the result of the enhanced immune response leading to eradication of ATL cells and control of infections caused by opportunistic pathogens. These results support suggestions on the use of ATO to treat immune disorders (Wang et al. 2019; An et al. 2020).

Epstein–Barr virus (EBV), the first identified human oncogenic virus, is associated with various malignancies, including carcinomas (e.g., nasopharyngeal carcinoma) and lymphomas (e.g., Burkitt's lymphoma). In a study of the role of PML nuclear bodies in EBV latency, treatment with low dose ATO disrupted PML nuclear bodies, leading to induction of EBV lytic proteins and increased susceptibility of the virus to ganciclovir, an approved FDA drug for the treatment of EBV-associated disorders (Sides et al. 2013). Low concentrations of ATO (0.5—2 nM) were shown to inhibit expression of EBV lytic genes Zta, Rta and BMRF1, promoting cell death in various EBV-positive latency cells (Mutu, Akata, BX-1, Cl13 and JY) in a dose-dependent manner. A synergistic effect was observed with ganciclovir, specifically in EBV-positive cells. These effects were reversed in the presence of a proteasome inhibitor, which suggests that ATO-mediated inhibition of EBV lytic genes occurs via the ubiquitin pathway, promoting ubiquitin conjugation and proteasomal degradation of EBV genes (Yin et al. 2017). Induction of cell death by ATO was also observed in P3HR1 cells, another EBV-positive latency cell line, yet it occurs via autophagy. With this cell line, treatment with sodium arsenite also leads to cell death but via a different mechanism, caspase-dependent apoptosis (Zebboudj

et al. 2014). These results demonstrate that ATO and sodium arsenite have the potential to be therapeutic agents for EBV-associated lymphoma.

A recent *in silico* study identified darinaparsin (Fig. 2E) as a potent inhibitor of the RNA-dependent RNA polymerases of SARS-CoV-2. The drug inhibited the 3C-like protease and papain-like protease that are necessary for formation of the viral replication complex (Chowdhury et al. 2020). These results suggest that, in addition to its anticancer activity (Bansal et al. 2015; Mann et al. 2009; Tian et al. 2012), darinaparsin has the potential to be repurposed against the novel coronavirus that is responsible for the current global pandemic.

1.3.5 Arsenical natural products as antibiotics

Selman Waksman, the Russian-Ukrainian-born American microbiologist, defined the term 'antibiotic' as "*a chemical substance, produced by microorganisms, which has the capacity to inhibit the growth of and even to destroy bacteria and other microorganisms*" (Waksman 1947). In 1952, Waksman was awarded the Nobel Prize in Physiology or Medicine for his discovery of the aminoglycoside antibiotic streptomycin, a natural product produced by the soil bacterium *Streptomyces griseus* that gave the organism a growth advantage over other soil bacteria. In this section two organoarsenicals with antimicrobial activity, methylarsenite (MAs(III)) and arsinothricin (AST), will be described. Both are natural products produced by

soil bacteria to kill other bacteria, meeting Waksman's definition of an antibiotic (Li et al. 2021).

1.3.5.1 *Methylarsenite (MAs(III)): a primordial antibiotic*

Highly toxic MAs(III) (Fig. 2S) is produced by methylation of inorganic arsenite (As(III)) by the enzyme As(III) *S*-adenosylmethionine (SAM) methyltransferase, which is termed ArsM in microbes and AS3MT in animals (Dheeman et al. 2014; Qin et al. 2006). The *arsM* gene is considered to be one of the most ancient *ars* genes according to molecular clock analyses, arising at least 3 billion years ago (Chen et al. 2017; Chen and Rosen 2020). Thus, environmental arsenic methylation was widespread nearly a billion years before the Great Oxidation Event (GOE), when oxygen accumulated in the atmosphere. In the original anoxic atmosphere, trivalent MAs(III) would be stable. Since the ArsM product MAs(III) is considerably more toxic than the substrate As(III), methylation has been proposed to be an activation process, generating the primordial antibiotic MAs(III), which gave producers a competitive growth advantage over sensitive microbes during the Archean era (Li et al. 2016). Further methylation generates nontoxic volatile trimethylarsine (TMAs(III)), which may have functioned as a primitive mechanism for self-protection by the MAs(III)-producing microbes. After the GOE, MAs(III) would have been unstable in air, oxidizing to relatively nontoxic methylarsenate, MAs(V). Filling an ecological niche, other aerobic bacteria evolved the ability to reduce pentavalent MAs(V), regenerating the MAs(III) antibiotic (Yan et al. 2019; Yoshinaga et al. 2011). The genes involved in MAs(V) reduction have not yet been

identified, but this reaction now gives extant reducing microorganisms an advantage over MAs(III)-sensitive bacteria in microbial communities (Chen et al. 2019). Trivalent arsenicals such as MAs(III) are toxic in part due to their affinity for thiols groups in proteins and other cellular metabolites (Shen et al. 2013). Since MAs(III) can react with a large number of molecules, no single target can be assigned for its mechanism of action that applies in every cell.

However, one target for the antibiotic action of MAs(III) was recently identified in *Shewanella putrefaciens* 200 (Garbinski et al. 2020). MAs(III), but not inorganic As(III), effectively inhibits the enzyme MurA (uridine diphosphate (UDP)-*N*-acetylglucosamine enol pyruvyl transferase), a cytoplasmic enzyme involved in the synthesis of the key precursor of the peptidoglycan, UDP-*N*-acetylmuramate (UNAM) (Barreteau et al. 2008). Only prokaryotes utilize peptidoglycan as an essential structural component of the cell wall, which makes it a singular target for antibacterial therapy in gram-negative and gram-positive pathogenic bacteria (Du et al. 2000; Raz 2012; Sonkar et al. 2017; Vollmer et al. 2008). Fosfomycin ($C_3H_7O_4P$), the only clinically approved antibiotic that acts against MurA, inhibits MurA by alkylation of the highly conserved catalytic cysteine residue in the active site (Baum et al. 2001). However, the conserved cysteine is often replaced by an aspartate in MurA orthologs from various pathogens such as *Mycobacterium tuberculosis*, contributing to their intrinsic fosfomycin resistance (De Smet et al. 1999). MurA from *S. putrefaciens* 200 has the conserved catalytic cysteine and is sensitive to fosfomycin, while its Cys-to-Asp mutant is resistant to fosfomycin

but remained sensitive to MAs(III), indicating that the two compounds have different mechanisms of action. MAs(III) represents a new area for the development of novel compounds for combating the threat of antibiotic resistance (Garbinski et al. 2020). For MAs(III) to exert its antibiotic action, it first must enter sensitive cells. How do arsenicals in general and MAs(III) in particular get into and out of cells? The aquaglyceroporin GlpF facilitates uptake As(III) and Sb(III) into cells of *Escherichia coli* (Meng et al. 2004; Sanders et al. 1997). The uptake of MAs(III) by GlpF has not been studied, but other AQPs facilitate its movement into and out of cells. The aquaglyceroporin AqpS from *Sinorhizobium meliloti* was recently demonstrated to conduct both MAs(III) and MAs(V) (Chen et al. 2021). The heterologous expression of the related mammalian aquaporin AQP9 in *Saccharomyces cerevisiae* resulted in three-fold more MAs(III) accumulation than inorganic As(III) (Liu et al. 2006a, b). In addition, inorganic As(III) is transported by sugar permeases, including yeast hexose (Hxt) transporters (Liu et al. 2006a, b) and plant inositol permeases (Duan et al. 2016). The mammalian glucose permease GLUT1 has been shown to transport MAs(III) as well as As(III) (Liu et al. 2006a, b). However, it is not clear if bacterial sugar transporters also transport arsenicals. In response to the high toxicity of MAs(III), bacteria adapted by developing resistance mechanisms (Chen and Rosen 2020). One of the most common mechanisms of bacterial resistance to antibiotics is to pump it out of the cells (Jia et al. 2019). Two MAs(III) efflux permeases are ArsP (Chen et al. 2015a, b) and ArsK (Jia et al. 2019; Shi et al. 2018). Other mechanisms that confer resistance to MAs(III) are the C–As

bond lyase ArsI, which demethylates MAs(III) to As(III) (Pawitwar et al. 2017; Yoshinaga and Rosen 2014), and methylarsenite oxidases such as ArsH, ArsV and ArsU that oxidize MAs(III) to MAs(V) (Chen et al. 2015a, b; Chen et al. 2021; Chen et al. 2022).

1.3.5.2 *Arsinothricin (AST), a pentavalent organoarsenical antibiotic*

Arsinothricin (2-amino-4-(hydroxymethylarsinoyl) butanoate, or AST) (Fig. 2T) is a newly identified broad-spectrum organoarsenical antibiotic (Nadar et al. 2019). AST was first discovered as a natural product synthesized by the rice rhizosphere bacterium *Burkholderia gladioli* strain GSRB05 (Kuramata et al. 2016). AST is a non-proteinogenic analog of both glutamate and the arsenic mimetic of phosphinothricin (2-amino-4-(hydroxymethylphosphinyl) butanoate or PT), the antibiotic moiety of a *Streptomyces* antibiotic prodrug phosphinothricin tripeptide (PTT) or bialaphos (Nadar et al. 2019; Kuramata et al. 2016). AST inhibits the growth of *M. bovis* BCG, the attenuated etiological agent of bovine tuberculosis, which is closely related to *M. tuberculosis,* the cause of human tuberculosis, and one of the WHO-designated priority pathogens carbapenem-resistant *Enterobacter cloacae*, whereas it exhibits low cytotoxicity on human monocytes. AST is chemically unrelated to other organoarsenicals and is a promising candidate to usher in a new class of antimicrobial agents (Nadar et al. 2019). MAs(III) and other trivalent arsenicals exert their toxicity through reaction with thiols. In contrast, AST is a pentavalent organoarsenical, and pentavalent arsenicals have low reactivity with thiols. Even though other pentavalent arsenicals

are relatively benign and less toxic, AST is as effective an antimicrobial as MAs(III) and is 15-fold more effective as an antimicrobial than PT. PT and AST act by inhibition of glutamine synthetase (GS), a central enzyme in nitrogen metabolism. The likely mechanism of action is by mimicking the γ-glutamyl phosphate intermediate in the glutamine synthetase catalytic pathway (Nadar et al. 2019; Suzol et al. 2020). Recently the biosynthetic gene cluster for biosynthesis of AST was identified (Galván et al. 2021). An *ars* operon consisting of three genes, *arsQML*, was identified in the draft genome sequence of *B. gladioli* GSRB05, the AST producer. These three genes were shown to encode genes for the synthesis of AST and for its efflux from the cells. The *arsL* gene is proposed to encode a non-canonical radical SAM enzyme that transfers the 3-amino-3-carboxypropyl (ACP) group from SAM to inorganic arsenite (As(III)), forming hydroxyarsinothricin (2-amino-4-(dihydroxyarsinoyl)butanoate, or AST-OH), the precursor of AST. The *arsM* gene product, an As(III) SAM methyltransferase, methylates AST-OH, producing AST. Finally, *arsQ* encodes an efflux permease that extrudes AST from the cells, both protecting the producing cells from its own product and releasing AST into the extracellular milieu, allowing it to exert its antibiotic action (Galván et al. 2021). For AST to be a useful antibiotic, it must be available in sufficient quantities for clinical trials and for further drug development. Recently, a semi-synthetic method was reported in which D,L-AST-OH is chemically synthesized and then enzymatically methylated by ArsM to produce D,L-AST (Suzol et al. 2020). Paul Ehrlich, the father of modern drug chemotherapy who synthesized the antimicrobial organoarsenical salvarsan, prophesied that drug resistance follows

the drug like a faithful shadow (Ebrahim 2010). This has proven true for nearly every antibiotic and antimicrobial, and resistance to AST has already arisen. AST is inactivated by acetylation of α-amino group by the enzyme ArsN1. The *arsN1* gene is found in *ars* operons, suggesting that resistance to AST probably arose soon after the evolution of its synthesis. ArsN1 is highly selective and has higher affinity for AST than structurally related PT (Nadar et al. 2019). The *arsN1* gene is widely distributed in bacteria, which implies that AST is also produced by many environmental bacteria. Even so, AST still has a future as an antibiotic. First, AST can be used in combination with ArsN1 inhibitors that can be predicted from the crystal structure of AST-bound ArsN1. Second, the chemical synthesis of AST can be used to produce modified derivatives with higher inhibition of GS or that evade ArsN1 acetylation. These inhibitors and derivatives will improve the clinical utility of this promising new class of antimicrobial drugs.

1.4 Synthetic aromatic arsenicals in animal husbandry

Although their medicinal uses waned after the advent of penicillin in the early 1940s, synthetic aromatic arsenicals have been repurposed for use in animal husbandry. Four pentavalent aromatic arsenicals were extensively used in the poultry and swine industry in the US since the mid-1940's and played significant roles as feed additives for improvement of weight gain, feed efficiencies and pigmentation, as well as prevention and treatment of parasitic infectious diseases until banned in the mid-2010's. Atoxyl (*p*-ASA) (Fig. 2U), the first organoarsenical drug for human trypanosomiasis, was repurposed for poultry and swine to promote

growth and prevent or treat dysentery (Sharma and Anand 1997). Carbarsone (4-carbamoylaminophenylarsenate or Car(V)) (Fig. 2V), the carbamoylated *p*-ASA(V) derivative originally introduced in 1931 for the treatment of human protozoal infectious diseases trichomoniasis and amebiasis, was later restricted to application with turkeys to improve weight and control blackhead disease, a protozoan disease caused by *Histomonas meleagridis* (Hoekenga 1951; McDougald 1979; Radke 1955; Sasaki et al. 1956; Worden and Wood 1973). The other two are nitroaromatic pentavalent arsenicals, roxarsone (4-hydroxy-3-nitrophenylarsenate or Rox(V)) (Fig. 2W) and nitarsone (4-nitrophenylarsenate or Nit(V)) (Fig. 2X) that were exclusively used for animal husbandry. Rox(V) was used for poultry to promote growth, treat coccidiosis, an intestinal protozoan parasitic disease caused by *Eimeria tenella*, as well as prevent gastrointestinal tract infections. Although mostly excreted unchanged from the animals, administered organoarsenical drugs were shown to increase the level of inorganic arsenic species in the chicken breasts (Liu et al. 2016). Rox(V) and Nit(V) have been banned for nearly two decades by the European Union, in 2014 and 2015, respectively, by the FDA (https://www.fda.gov/animal-veterinary/product-safety-information/arsenic-based-animal-drugs-and-poultry), and more recently banned in China (Hu et al. 2019), although compliance is difficult to enforce. Several countries including Malaysia, Canada and Australia followed this move, yet their use is still allowed in countries such as Argentina, Brazil, Chile, Mexico, and Vietnam (Hu et al. 2019). Nit(V) was the last drug in use in the United States to prevent and treat blackhead disease in poultry, and currently there are no

efficacious drugs for this serious avian disease, raising a concern in poultry industry (https://www.fda.gov/animal-veterinary/resources-you/blackhead-disease-poultry).

1.5 Future perspectives

The major drawback of the use of arsenic in medicine is its toxicity. Therefore, there is a need to employ current advances in science to develop new generation arsenicals that can make up for the shortcomings of currently used arsenic-based drugs. Development of future arsenical drugs will build on the chemistry and properties of arsenic-based drugs already proven to be effective. Before advancements in scientific research, most arsenic-based drugs throughout history were marketed and used without rigorous clinical trials or understanding of their mechanisms of action. This lack of scientific rigor may have been responsible for the disuse of arsenic-based drugs in the late 1900s. The re-emergence of arsenic as a frontline treatment for APL shows the potential for development of new arsenicals with higher therapeutic efficacy and lower toxicity.

1.6 Acknowledgements

This work was supported by NSF BIO/ MCB grant 1817962 to M.Y. and NIH grant R35GM136211 to B.P.R,

REFERENCES

Ahn RW, Chen F, Chen H, Stern ST, Clogston JD, Patri AK, Raja MR, Swindell EP, et al. A novel nanoparticulate formulation of arsenic trioxide with enhanced therapeutic efficacy in a murine model of breast cancer. *Clin Cancer Res.* 2010;16:3607–3617. doi: 10.1158/1078-0432.CCR-10-0068.

Alsford S, Eckert S, Baker N, Glover L, Sanchez-Flores A, Leung KF, Turner DJ, Field MC, et al. High-throughput decoding of antitrypanosomal drug efficacy and resistance. *Nature.* 2012;482:232–236. doi: 10.1038/nature10771.

An YL, Nie F, Wang ZY, Zhang DS. Preparation and characterization of realgar nanoparticles and their inhibitory effect on rat glioma cells. *Int J Nanomed.* 2011;6:3187–3194. doi: 10.2147/IJN.S26237

An K, Xue MJ, Zhong JY, Yu SN, Lan TS, Qi ZQ, Xia JJ. Arsenic trioxide ameliorates experimental autoimmune encephalomyelitis in C57BL/6 mice by inducing CD4(+) T cell apoptosis. *J Neuroinflamm.* 2020;17:147. doi: 10.1186/s12974-020-01829-x.

Ayala G, Wang D, Wulf G, Frolov A, Li R, Sowadski J, Wheeler TM, Lu KP, et al. The prolyl isomerase Pin1 is a novel prognostic marker in human prostate cancer. *Cancer Res.* 2003;63:6244–6251.

Baker N, Glover L, Munday JC, Aguinaga Andrés D, Barrett MP, de Koning HP, Horn D. Aquaglyceroporin 2 controls susceptibility to melarsoprol and pentamidine in African trypanosomes. *Proc Natl Acad Sci USA.* 2012;109:10996–11001. doi: 10.1073/pnas.1202885109.

Bansal N, Farley NJ, Wu L, Lewis J, Youssoufian H, Bertino JR. Darinaparsin inhibits prostate tumor-initiating cells and Du145 xenografts and is an inhibitor of hedgehog signaling. *Mol Cancer Ther.* 2015;14:23–30. doi: 10.1158/1535-7163.MCT-13-1040.

Bao L, Kimzey A, Sauter G, Sowadski JM, Lu KP, Wang DG. Prevalent overexpression of prolyl isomerase Pin1 in human cancers. *Am J Pathol.* 2004;164:1727–1737. doi: 10.1016/S0002-9440(10)63731-5.

Bao X, Ren T, Huang Y, Wang S, Zhang F, Liu K, Zheng B, Guo W. Induction of the mesenchymal to epithelial transition by demethylation-activated microRNA-125b is involved in the anti-migration/invasion effects of arsenic trioxide on human chondrosarcoma. *J Exp Clin Cancer Res.* 2016;35:129. doi: 10.1186/s13046-016-0407-y.

Barreteau H, Kovac A, Boniface A, Sova M, Gobec S, Blanot D. Cytoplasmic steps of peptidoglycan biosynthesis. *FEMS Microbiol Rev.* 2008;32:168–207. doi: 10.1111/j.1574-6976.2008.00104.x.

Baum EZ, Montenegro DA, Licata L, Turchi I, Webb GC, Foleno BD, Bush K. Identification and characterization of new inhibitors of the Escherichia coli MurA enzyme. *Antimicrob Agents Chemother.* 2001;45:3182–3188. doi: 10.1128/AAC.45.11.3182-3188.2001.

Bentley R, Chasteen TG. Arsenic curiosa and humanity. *Chem Educ.* 2002;7:51–60. doi: 10.1007/s00897020539a

Blum J, Nkunku S, Burri C. Clinical description of encephalopathic syndromes and risk factors for their occurrence and outcome during melarsoprol treatment of human African trypanosomiasis. *Trop Med Int Health.* 2001;6:390–400. doi: 10.1046/j.1365-3156.2001.00710.x

Borrow J, Goddard AD, Sheer D, Solomon E. Molecular analysis of acute promyelocytic leukemia breakpoint cluster region on chromosome 17. *Science.* 1990;249:1577–1580. doi: 10.1126/science.2218500.

Borzelleca JF. Paracelsus: herald of modern toxicology. *Toxicol Sci.* 2000;53:2–4. doi: 10.1093/toxsci/53.1.2.

Brun R, Schumacher R, Schmid C, Kunz C, Burri C. The phenomenon of treatment failures in Human African Trypanosomiasis. *Trop Med Int Health.* 2001;6:906–914. doi: 10.1046/j.1365-3156.2001.00775.x.

Büscher P, Cecchi G, Jamonneau V, Priotto G. Human African trypanosomiasis. *Lancet.* 2017;390:2397–2409. doi: 10.1016/S0140-6736(17)31510-6.

Carney DA. Arsenic trioxide mechanisms of action–looking beyond acute promyelocytic leukemia. *Leuk Lymphoma.* 2008;49:1846–1851. doi: 10.1080/10428190802464745.

Carter NS, Fairlamb AH. Arsenical-resistant trypanosomes lack an unusual adenosine transporter. *Nature.* 1993;361:173–176. doi: 10.1038/361173a0.

Chen Z, Chen SJ. Poisoning the devil. *Cell.* 2017;168:556–560. doi: 10.1016/j.cell.2017.01.029.

Chen J, Rosen BP (2020) The arsenic methylation cycle: how microbial communities adapted methylarsenicals for use as weapons in the continuing war for dominance. Front Environ Sci 8:43

Chen J, Zhang J, Wu YF, Zhao FJ, Rosen BP. ArsV and ArsW provide synergistic resistance to the antibiotic methylarsenite. Environ Microbiol. 2021 Dec;23(12):7550-7562. doi: 10.1111/1462-2920.15817. Epub 2021 Oct 21. PMID: 34676971; PMCID: PMC8865377.

Chen J, Zhang J, Rosen BP. Organoarsenical tolerance in Sphingobacterium wenxiniae, a bacterium isolated from activated sludge. Environ Microbiol. 2022 Feb;24(2):762-771. doi: 10.1111/1462-2920.15599. Epub 2021 May 27. PMID: 33998126; PMCID: PMC8890440.

Chen GQ, Shi XG, Tang W, Xiong SM, Zhu J, Cai X, Han ZG, Ni JH, et al. Use of arsenic trioxide (As_2O_3) in the treatment of acute promyelocytic leukemia (APL): I. As_2O_3 exerts dose-dependent dual effects on APL cells. *Blood.* 1997;89:3345–3353.

Chen H, MacDonald RC, Li S, Krett NL, Rosen ST, O'Halloran TV. Lipid encapsulation of arsenic trioxide attenuates cytotoxicity and allows for controlled anticancer drug release. *J Am Chem Soc.* 2006;128:13348–13349. doi: 10.1021/ja064864h.

Chen J, Bhattacharjee H, Rosen BP. ArsH is an organoarsenical oxidase that confers resistance to trivalent forms of the herbicide monosodium methylarsenate and the poultry growth promoter roxarsone. *Mol Microbiol.* 2015;96:1042–1052. doi: 10.1111/mmi.12988.

Chen J, Madegowda M, Bhattacharjee H, Rosen BP. ArsP: a methylarsenite efflux permease. *Mol Microbiol.* 2015;98:625–635. doi: 10.1111/mmi.13145

Chen SC, Sun GX, Rosen BP. Recurrent horizontal transfer of arsenite methyltransferase genes facilitated adaptation of life to arsenic. *Sci Rep.* 2017;7:7741:1–11.

Chen J, Yoshinaga M, Rosen BP. The antibiotic action of methylarsenite is an emergent property of microbial communities. *Mol Microbiol.* 2019;111:487–494. doi: 10.1111/mmi.14169.

Chen J, Nadar VS, Rosen BP. Aquaglyceroporin AqpS from Sinorhizobium meliloti conducts both trivalent and pentavalent methylarsenicals. *Chemosphere.* 2021;270:129379. doi: 10.1016/j.chemosphere.2020.129379.

Cholujova D, Bujnakova Z, Dutkova E, Hideshima T, Groen RW, Mitsiades CS, Richardson PG, Dorfman DM, et al. Realgar nanoparticles versus ATO arsenic compounds induce in vitro and in vivo activity against multiple myeloma. *Br J Haematol.* 2017;179:756–771. doi: 10.1111/bjh.14974

Chowdhury T, Roymahapatra G, Mandal SM (2020) In silico identification of a potent arsenic based approved drug darinaparsin against SARS-CoV-2: inhibitor of RNA dependent RNA polymerase (RdRp) and essential proteases. Infect Disord Drug Targets.

Colotti G, Fiorillo A, Ilari A. Metal- and metalloid-containing drugs for the treatment of trypanosomatid diseases. *Front Biosci (landmark Ed)* 2018;23:954–966. doi: 10.2741/4628.

Cunningham ML, Zvelebil MJ, Fairlamb AH. Mechanism of inhibition of trypanothione reductase and glutathione reductase by trivalent organic arsenicals. *Eur J Biochem.* 1994;221:285–295. doi: 10.1111/j.1432-1033.1994.tb18740.x.

Dawood M, Hamdoun S, Efferth T. Multifactorial modes of action of arsenic trioxide in cancer cells as analyzed by classical and network pharmacology. *Front Pharmacol.* 2018;9:143. doi: 10.3389/fphar.2018.00143.

De Smet KAL, Kempsell KE, Gallagher A, Duncan K, Young DB. Alteration of a single amino acid residue reverses fosfomycin resistance of recombinant MurA from Mycobacterium tuberculosis. *Microbiology (reading)* 1999;145(Pt 11):3177–3184. doi: 10.1099/00221287-145-11-3177.

de Thé H, Chomienne C, Lanotte M, Degos L, Dejean A. The t(15;17) translocation of acute promyelocytic leukaemia fuses the retinoic acid receptor alpha gene to a novel transcribed locus. *Nature.* 1990;347:558–561. doi: 10.1038/347558a0.

Dheeman DS, Packianathan C, Pillai JK, Rosen BP. Pathway of human AS3MT arsenic methylation. *Chem Res Toxicol.* 2014;27:1979–1989. doi: 10.1021/tx500313k.

Doyle D. Notoriety to respectability: a short history of arsenic prior to its present day use in haematology. *Br J Haematol.* 2009;145:309–317. doi: 10.1111/j.1365-2141.2009.07623.x.

Du W, Brown JR, Sylvester DR, Huang J, Chalker AF, So CY, Holmes DJ, Payne DJ, et al. Two active forms of UDP-N-acetylglucosamine enolpyruvyl transferase in gram-positive bacteria. *J Bacteriol.* 2000;182:4146–4152. doi: 10.1128/JB.182.15.4146-4152.2000.

Duan GL, Hu Y, Schneider S, McDermott J, Chen J, Sauer N, Rosen BP, Daus B, et al. Inositol transporters AtINT2 and AtINT4 regulate arsenic accumulation in Arabidopsis seeds. *Nat Plants.* 2016;2:15202. doi: 10.1038/nplants.2015.202

Ebrahim GJ. Bacterial resistance to antimicrobials. *J Trop Pediatr.* 2010;56:141–143. doi: 10.1093/tropej/fmq037.

Emadi A, Gore SD. Arsenic trioxide—an old drug rediscovered. *Blood Rev.* 2010;24:191–199. doi: 10.1016/j.blre.2010.04.001.

Emelyanov A, Bulavin DV. Wip1 phosphatase in breast cancer. *Oncogene.* 2015;34:4429–4438. doi: 10.1038/onc.2014.375.

Ernst E. Toxic heavy metals and undeclared drugs in Asian herbal medicines. *Trends Pharmacol Sci.* 2002;23:136–139. doi: 10.1016/S0165-6147(00)01972-6.

Fairlamb AH, Horn D. Melarsoprol resistance in african trypanosomiasis. *Trends Parasitol.* 2018;34:481–492. doi: 10.1016/j.pt.2018.04.002.

Fairlamb AH, Henderson GB, Cerami A. Trypanothione is the primary target for arsenical drugs against African trypanosomes. *Proc Natl Acad Sci USA.* 1989;86:2607–2611. doi: 10.1073/pnas.86.8.2607.

Fan XY, Chen XY, Liu YJ, Zhong HM, Jiang FL, Liu Y. Oxidative stress-mediated intrinsic apoptosis in human promyelocytic leukemia HL-60 cells induced by organic arsenicals. *Sci Rep.* 2016;6:29865. doi: 10.1038/srep29865.

Fang W, Peng ZL, Dai YJ, Wang DL, Huang P, Huang HP. (-)-Epigallocatechin-3-gallate encapsulated realgar nanoparticles exhibit enhanced anticancer therapeutic efficacy against acute promyelocytic leukemia. *Drug Delivery.* 2019;26:1058–1067. doi: 10.1080/10717544.2019.1672830.

Frampton JE. Darinaparsin: First Approval. Drugs. 2022;82(16):1603-9. Epub 2022/11/05. doi: 10.1007/s40265-022-01795-z. PubMed PMID: 36331780.

Friedheim EA. Melarsen oxide in the treatment of human trypanosomiasis. *Ann Trop Med Parasitol.* 1948;42:357–363. doi: 10.1080/00034983.1948.11685383.

Friedheim EA. Mel B in the treatment of human trypanosomiasis. *Am J Trop Med Hyg.* 1949;29:173–180. doi: 10.4269/ajtmh.1949.s1-29.173.

Galván AE, Paul NP, Chen J, Yoshinaga-Sakurai K, Utturkar SM, Rosen BP, Yoshinaga M. Identification of the biosynthetic gene cluster for the organoarsenical antibiotic arsinothricin. *Microbiol Spectr.* 2021;9:e0050221. doi: 10.1128/Spectrum.00502-21.

Garbinski LD, Rosen BP, Yoshinaga M. Organoarsenicals inhibit bacterial peptidoglycan biosynthesis by targeting the essential enzyme MurA. *Chemosphere.* 2020;254:126911. doi: 10.1016/j.chemosphere.2020.126911.

Giafis N, Katsoulidis E, Sassano A, Tallman MS, Higgins LS, Nebreda AR, Davis RJ, Platanias LC. Role of the p38 mitogen-activated protein kinase pathway in the generation of arsenic trioxide-dependent cellular responses. *Cancer Res.* 2006;66:6763–6771. doi: 10.1158/0008-5472.CAN-05-3699.

Gibaud S, Jaouen G. Arsenic-based drugs: from fowler's solution to modern anticancer chemotherapy. In: Jaouen GMNN, editor. *Medicinal organometallic chemistry.* Berlin: Springer; 2010.

Golomb HM, Rowley JD, Vardiman JW, Testa JR, Butler A. "Microgranular" acute promyelocytic leukemia: a distinct clinical, ultrastructural, and cytogenetic entity. *Blood.* 1980;55:253–259. doi: 10.1182/blood.V55.2.253.253.

Gorby MS. Arsenic poisoning. *West J Med.* 1988;149:308–315.

Graf FE, Ludin P, Wenzler T, Kaiser M, Brun R, Pyana PP, Büscher P, de Koning HP, et al. Aquaporin 2 mutations in Trypanosoma brucei gambiense field isolates correlate with decreased susceptibility to pentamidine and melarsoprol. *PLoS Negl Trop Dis.* 2013;7:e2475. doi: 10.1371/journal.pntd.0002475.

Grignani F, Ferrucci PF, Testa U, Talamo G, Fagioli M, Alcalay M, Mencarelli A, Grignani F, et al. The acute promyelocytic leukemia-specific PML-RAR alpha fusion protein inhibits differentiation and promotes survival of myeloid precursor cells. *Cell.* 1993;74:423–431. doi: 10.1016/0092-8674(93)80044-F.

Grisolano JL, Wesselschmidt RL, Pelicci PG, Ley TJ. Altered myeloid development and acute leukemia in transgenic mice expressing PML-RAR alpha under control of cathepsin G regulatory sequences. *Blood.* 1997;89:376–387. doi: 10.1182/blood.V89.2.376.

Hoekenga MT. A comparison of aureomycin and carbarsone in the treatment of intestinal amebiasis. *Am J Trop Med Hyg.* 1951;31:423–425. doi: 10.4269/ajtmh.1951.s1-31.423.

Hofmann S, Mai J, Masser S, Groitl P, Herrmann A, Sternsdorf T, Brack-Werner R, Schreiner S. ATO (arsenic trioxide) effects on promyelocytic leukemia nuclear bodies reveals antiviral intervention capacity. *Adv Sci (weinh)* 2020;7:1902130. doi: 10.1002/advs.201902130.

Hoonjan M, Jadhav V, Bhatt P. Arsenic trioxide: insights into its evolution to an anticancer agent. *J Biol Inorg Chem.* 2018;23:313–329. doi: 10.1007/s00775-018-1537-9.

Horsley L, Cummings J, Middleton M, Ward T, Backen A, Clamp A, Dawson M, Farmer H, et al. A phase 1 trial of intravenous 4-(N-(S-glutathionylacetyl)amino) phenylarsenoxide (GSAO) in patients with advanced solid tumours. *Cancer Chemother Pharmacol.* 2013;72:1343–1352. doi: 10.1007/s00280-013-2320-9.

Hu Y, Cheng H, Tao S, Schnoor JL. China's ban on phenylarsonic feed additives, a major step toward reducing the human and ecosystem health risk from arsenic. *Environ Sci Technol.* 2019;53:12177–12187. doi: 10.1021/acs.est.9b04296.

Hughes MF, Beck BD, Chen Y, Lewis AS, Thomas DJ. Arsenic exposure and toxicology: a historical perspective. *Toxicol Sci.* 2011;123:305–332. doi: 10.1093/toxsci/kfr184.

Huynh TT, Sultan M, Vidovic D, Dean CA, Cruickshank BM, Lee K, Loung CY, Holloway RW, et al. Retinoic acid and arsenic trioxide induce lasting differentiation and demethylation of target genes in APL cells. *Sci Rep.* 2019;9:9414. doi: 10.1038/s41598-019-45982-7.

Hwang DR, Tsai YC, Lee JC, Huang KK, Lin RK, Ho CH, Chiou JM, Lin YT, et al. Inhibition of hepatitis C virus replication by arsenic trioxide. *Antimicrob Agents Chemother.* 2004;48:2876–2882. doi: 10.1128/AAC.48.8.2876-2882.2004.

Jia MR, Tang N, Cao Y, Chen Y, Han YH, Ma LQ. Efficient arsenate reduction by As-resistant bacterium Bacillus sp. strain PVR-YHB1-1: characterization and genome analysis. *Chemosphere.* 2019;218:1061–1070. doi: 10.1016/j.chemosphere.2018.11.145.

Jolliffe DM. A history of the use of arsenicals in man. *J R Soc Med.* 1993;86:287–289. doi: 10.1177/014107689308600515.

Kaźmierczak-Barańska J, Boguszewska K, Adamus-Grabicka A, Karwowski BT (2020) Two faces of vitamin C-antioxidative and pro-oxidative agent. Nutrients 12.

Kchour G, Rezaee R, Farid R, Ghantous A, Rafatpanah H, Tarhini M, Kooshyar MM, El Hajj H, et al. The combination of arsenic, interferon-alpha, and zidovudine restores an "immunocompetent-like" cytokine expression profile in patients with adult T-cell leukemia lymphoma. *Retrovirology.* 2013;10:91. doi: 10.1186/1742-4690-10-91.

Keiser J, Ericsson O, Burri C. Investigations of the metabolites of the trypanocidal drug melarsoprol. *Clin Pharmacol Ther.* 2000;67:478–488. doi: 10.1067/mcp.2000.105990.

Koch I, Moriarty M, House K, Sui J, Cullen WR, Saper RB, Reimer KJ. Bioaccessibility of lead and arsenic in traditional Indian medicines. *Sci Total Environ.* 2011;409:4545–4552. doi: 10.1016/j.scitotenv.2011.07.059.

Kozono S, Lin YM, Seo HS, Pinch B, Lian X, Qiu C, Herbert MK, Chen CH, et al. Arsenic targets Pin1 and cooperates with retinoic acid to inhibit cancer-driving pathways and tumor-initiating cells. *Nat Commun.* 2018;9:3069. doi: 10.1038/s41467-018-05402-2.

Kuramata M, Sakakibara F, Kataoka R, Yamazaki K, Baba K, Ishizaka M, Hiradate S, Kamo T, et al. Arsinothricin, a novel organoarsenic species produced by a rice rhizosphere bacterium. *Environ Chem.* 2016;13:723–731. doi: 10.1071/EN14247.

Kuroki M, Ariumi Y, Ikeda M, Dansako H, Wakita T, Kato N. Arsenic trioxide inhibits hepatitis C virus RNA replication through modulation of the glutathione redox system and oxidative stress. *J Virol.* 2009;83:2338–2348. doi: 10.1128/JVI.01840-08.

Lalwani N, Chen YS, Brooke G, Cross NA, Allen DW, Reynolds A, Ojeda J, Tizzard GJ, et al. Triphenylarsonium-functionalised gold nanoparticles: potential nanocarriers for intracellular therapeutics. *Chem Commun (camb)* 2015;51:4109–4111. doi: 10.1039/C4CC09304F.

Li J, Yang Y, Peng Y, Austin RJ, van Eyndhoven WG, Nguyen KC, Gabriele T, McCurrach ME, et al. Oncogenic properties of PPM1D located within a breast cancer amplification epicenter at 17q23. *Nat Genet.* 2002;31:133–134. doi: 10.1038/ng888.

Li J, Pawitwar SS, Rosen BP. The organoarsenical biocycle and the primordial antibiotic methylarsenite. *Metallomics.* 2016;8:1047–1055. doi: 10.1039/C6MT00168H.

Li YP, Fekih IB, Fru EC, Moraleda-Munoz A, Li X, Rosen BP, Yoshinaga M, Rensing C (2021) Antimicrobial Activity of Metals and Metalloids. Annu Rev Microbiol.

Liu Z, Sanchez MA, Jiang X, Boles E, Landfear SM, Rosen BP. Mammalian glucose permease GLUT1 facilitates transport of arsenic trioxide and methylarsonous acid. *Biochem Biophys Res Commun.* 2006;351:424–430. doi: 10.1016/j.bbrc.2006.10.054.

Liu Z, Styblo M, Rosen BP. Methylarsonous acid transport by aquaglyceroporins. *Environ Health Perspect.* 2006;114:527–531. doi: 10.1289/ehp.8600.

Liu J, Lu Y, Wu Q, Goyer RA, Waalkes MP. Mineral arsenicals in traditional medicines: orpiment, realgar, and arsenolite. *J Pharmacol Exp Ther.* 2008;326:363–368. doi: 10.1124/jpet.108.139543.

Liu Q, Peng H, Lu X, Zuidhof MJ, Li XF, Le XC. Arsenic species in chicken breast: temporal variations of metabolites, elimination kinetics, and residual concentrations. *Environ Health Perspect.* 2016;124:1174–1181. doi: 10.1289/ehp.1510530.

Liu L, Zhang Y, Yun Z, He B, Zhang Q, Hu L, Jiang G. Speciation and bioaccessibility of arsenic in traditional Chinese medicines and assessment of its potential health risk. *Sci Total Environ.* 2018;619–620:1088–1097.

Lloyd NC, Morgan HW, Nicholson BK, Ronimus RS. The composition of Ehrlich's salvarsan: resolution of a century-old debate. *Angew Chem Int Ed Engl.* 2005;44:941–944. doi: 10.1002/anie.200461471

Lu Z, Hunter T. Prolyl isomerase Pin1 in cancer. *Cell Res.* 2014;24:1033–1049. doi: 10.1038/cr.2014.109.

Lu D, Rae AD, Salem G, Weir ML, Willis AC, Wild SB. Arsenicin A, a natural polyarsenical: synthesis and crystal structure. *Organometallics.* 2010;29:32–33. doi: 10.1021/om900998q.

Lu D, Coote ML, Ho J, Kilah NL, Lin C-Y, Salem G, Weir ML, Willis AC, et al. Resolution and improved synthesis of (±)-arsenicin a: a natural adamantane-type tetraarsenical possessing strong anti-acute promelocytic leukemia cell line activity. *Organometallics.* 2012;31:1808–1816. doi: 10.1021/om201180d.

Luo ML, Gong C, Chen CH, Hu H, Huang P, Zheng M, Yao Y, Wei S, et al. The Rab2A GTPase promotes breast cancer stem cells and tumorigenesis via Erk signaling activation. *Cell Rep.* 2015;11:111–124. doi: 10.1016/j.celrep.2015.03.002.

Mancini I, Guella G, Frostin M, Hnawia E, Laurent D, Debitus C, Pietra F. On the first polyarsenic organic compound from nature: arsenicin A from the New Caledonian marine sponge Echinochalina bargibanti. *Chemistry.* 2006;12:8989–8994. doi: 10.1002/chem.200600783.

Mancini I, Planchestainer M, Defant A. Synthesis, and in-vitro anticancer evaluation of polyarsenicals related to the marine sponge derived Arsenicin A. *Sci Rep.* 2017;7:11548. doi: 10.1038/s41598-017-11566-6.

Mann KK, Wallner B, Lossos IS, Miller WH., Jr Darinaparsin: a novel organic arsenical with promising anticancer activity. *Expert Opin Investig Drugs.* 2009;18:1727–1734. doi: 10.1517/13543780903282759.

Mäser P, Sütterlin C, Kralli A, Kaminsky R. A nucleoside transporter from Trypanosoma brucei involved in drug resistance. *Science.* 1999;285:242–244. doi: 10.1126/science.285.5425.242.

Matteson AR, Gannon TW, Jeffries MD, Haines S, Lewis DF, Polizzotto ML. Arsenic retention in foliage and soil after monosodium methyl arsenate (MSMA) application to turfgrass. *J Environ Qual.* 2014;43:379–388. doi: 10.2134/jeq2013.07.0268.

McDougald LR. Efficacy and compatibility of amprolium and carbarsone against Coccidiosis and blackhead in turkeys. *Poult Sci.* 1979;58:76–80. doi: 10.3382/ps.0580076.

Meng YL, Liu Z, Rosen BP. As(III) and Sb(III) uptake by GlpF and efflux by ArsB in Escherichia coli. *J Biol Chem.* 2004;279:18334–18341. doi: 10.1074/jbc.M400037200.

Miller WH, Jr, Schipper HM, Lee JS, Singer J, Waxman S. Mechanisms of action of arsenic trioxide. *Cancer Res.* 2002;62:3893–3903.

Miodragović ĐU, Quentzel JA, Kurutz JW, Stern CL, Ahn RW, Kandela I, Mazar A, O'Halloran TV. Robust structure and reactivity of aqueous arsenous acid-platinum(II) anticancer complexes. *Angew Chem Int Ed Engl.* 2013;52:10749–10752. doi: 10.1002/anie.201303251.

Miodragović Đ, Merlino A, Swindell EP, Bogachkov A, Ahn RW, Abuhadba S, Ferraro G, Marzo T, et al. Arsenoplatin-1 Is a dual pharmacophore anticancer agent. *J Am Chem Soc.* 2019;141:6453–6457. doi: 10.1021/jacs.8b13681.

Munday JC, Eze AA, Baker N, Glover L, Clucas C, Aguinaga Andrés D, Natto MJ, Teka IA, et al. Trypanosoma brucei aquaglyceroporin 2 is a high-affinity transporter for pentamidine and melaminophenyl arsenic drugs and the main genetic determinant of resistance to these drugs. *J Antimicrob Chemother.* 2014;69:651–663. doi: 10.1093/jac/dkt442.

Munday JC, Settimo L, de Koning HP. Transport proteins determine drug sensitivity and resistance in a protozoan parasite. *Trypanosoma Brucei Front Pharmacol.* 2015;6:32.

Nadar VS, Chen J, Dheeman DS, Galván AE, Yoshinaga-Sakurai K, Kandavelu P, Sankaran B, Kuramata M, et al. Arsinothricin, an arsenic-containing non-

proteinogenic amino acid analog of glutamate, is a broad-spectrum antibiotic. *Commun Biol.* 2019;2:131. doi: 10.1038/s42003-019-0365-y.

Natrajan R, Lambros MB, Rodríguez-Pinilla SM, Moreno-Bueno G, Tan DS, Marchió C, Vatcheva R, Rayter S, et al. Tiling path genomic profiling of grade 3 invasive ductal breast cancers. *Clin Cancer Res.* 2009;15:2711–2722. doi: 10.1158/1078-0432.CCR-08-1878.

Noguera NI, Pelosi E, Angelini DF, Piredda ML, Guerrera G, Piras E, Battistini L, Massai L, et al. High-dose ascorbate and arsenic trioxide selectively kill acute myeloid leukemia and acute promyelocytic leukemia blasts in vitro. *Oncotarget.* 2017;8:32550–32565. doi: 10.18632/oncotarget.15925.

Ogura M, Kim WS, Uchida T, Uike N, Suehiro Y, Ishizawa K, Nagai H, Nagahama F, et al. Phase I studies of darinaparsin in patients with relapsed or refractory peripheral T-cell lymphoma: a pooled analysis of two phase I studies conducted in Japan and Korea. *Jpn J Clin Oncol.* 2021;51:218–227. doi: 10.1093/jjco/hyaa177.

Panda A, Hazra J. Arsenical compounds in ayurveda medicine: a prospective analysis. *Int J Res Ayurveda Pharmacy.* 2012;3:772–776. doi: 10.7897/2277-4343.03614.

Pandolfi PP. Oncogenes and tumor suppressors in the molecular pathogenesis of acute promyelocytic leukemia. *Hum Mol Genet.* 2001;10:769–775. doi: 10.1093/hmg/10.7.769.

Pawitwar SS, Nadar VS, Kandegedara A, Stemmler TL, Rosen BP, Yoshinaga M. Biochemical characterization of ArsI: a novel C-as lyase for degradation of environmental organoarsenicals. *Environ Sci Technol.* 2017;51:11115–11125. doi: 10.1021/acs.est.7b03180.

Pepin J, Milord F. African trypanosomiasis, and drug-induced encephalopathy: risk factors and pathogenesis. *Trans R Soc Trop Med Hyg.* 1991;85:222–224. doi: 10.1016/0035-9203(91)90032-T.

Peters RA, Stocken LA, Thompson RH. British anti-lewisite (BAL) *Nature.* 1945;156:616–619. doi: 10.1038/156616a0.

Preston CM, Nicholl MJ. Induction of cellular stress overcomes the requirement of herpes simplex virus type 1 for immediate-early protein ICP0 and reactivates expression from quiescent viral genomes. *J Virol.* 2008;82:11775–11783. doi: 10.1128/JVI.01273-08.

Puccetti E, Ruthardt M. Acute promyelocytic leukemia: PML/RARalpha and the leukemic stem cell. *Leukemia.* 2004;18:1169–1175. doi: 10.1038/sj.leu.2403367.

Pyana Pati P, Van Reet N, Mumba Ngoyi D, Ngay Lukusa I, Karhemere Bin Shamamba S, Büscher P. Melarsoprol sensitivity profile of Trypanosoma brucei gambiense isolates from cured and relapsed sleeping sickness patients from the Democratic Republic of the Congo. *PLoS Negl Trop Dis.* 2014;8:e3212. doi: 10.1371/journal.pntd.0003212.

Qin J, Rosen BP, Zhang Y, Wang G, Franke S, Rensing C. Arsenic detoxification and evolution of trimethylarsine gas by a microbial arsenite S-adenosylmethionine methyltransferase. *Proc Natl Acad Sci USA.* 2006;103:2075–2080. doi: 10.1073/pnas.0506836103.

Radke RA. Ameboma of the intestine: an analysis of the disease as presented in 78 collected and 41 previously unreported cases. *Ann Intern Med.* 1955;43:1048–1066. doi: 10.7326/0003-4819-43-5-1048.

Raz R. Fosfomycin: an old–new antibiotic. *Clin Microbiol Infect.* 2012;18:4–7. doi: 10.1111/j.1469-0691.2011.03636.x.

Riethmiller S. From Atoxyl to Salvarsan: searching for the magic bullet. *Chemotherapy.* 2005;51:234–242. doi: 10.1159/000087453.

Rodgers J, Jones A, Gibaud S, Bradley B, McCabe C, Barrett MP, Gettinby G, Kennedy PG. Melarsoprol cyclodextrin inclusion complexes as promising oral candidates for the treatment of human African trypanosomiasis. *PLoS Negl Trop Dis.* 2011;5:e1308. doi: 10.1371/journal.pntd.0001308.

Rojewski MT, Baldus C, Knauf W, Thiel E, Schrezenmeier H. Dual effects of arsenic trioxide (As_2O_3) on non-acute promyelocytic leukaemia myeloid cell lines: induction of apoptosis and inhibition of proliferation. *Br J Haematol.* 2002;116:555–563. doi: 10.1046/j.0007-1048.2001.03298.x.

Rustighi A, Zannini A, Tiberi L, Sommaggio R, Piazza S, Sorrentino G, Nuzzo S, Tuscano A, et al. Prolyl-isomerase Pin1 controls normal and cancer stem cells of the breast. *EMBO Mol Med.* 2014;6:99–119. doi: 10.1002/emmm.201302909.

Sanders OI, Rensing C, Kuroda M, Mitra B, Rosen BP. Antimonite is accumulated by the glycerol facilitator GlpF in Escherichia coli. *J Bacteriol.* 1997;179:3365–3367. doi: 10.1128/jb.179.10.3365-3367.1997.

Sasaki T, Yokagawa M, Wykoff DE, Ritichie LS. Asymptomatic amebiasis; treatment with atabrine in combination with carbarsone or chiniofon. *U S Armed Forces Med J.* 1956;7:363–368.

Sekhon BS. Metalloid compounds as drugs. *Res Pharm Sci.* 2013;8:145–158.

Shao W, Fanelli M, Ferrara FF, Riccioni R, Rosenauer A, Davison K, Lamph WW, Waxman S, et al. Arsenic trioxide as an inducer of apoptosis and loss of PML/RAR alpha protein in acute promyelocytic leukemia cells. *J Natl Cancer Inst.* 1998;90:124–133. doi: 10.1093/jnci/90.2.124.

Sharma S, Anand N. Chapter 4—organometaliics. In: Sharma S, Anand N, editors. *Pharmacochemistry library.* New York: Elsevier; 1997. pp. 124–147.

Shen S, Li XF, Cullen WR, Weinfeld M, Le XC. Arsenic binding to proteins. *Chem Rev.* 2013;113:7769–7792. doi: 10.1021/cr300015c.

Shi D, Liu Y, Xi R, Zou W, Wu L, Zhang Z, Liu Z, Qu C, et al. Caveolin-1 contributes to realgar nanoparticle therapy in human chronic myelogenous leukemia K562 cells. *Int J Nanomedicine.* 2016;11:5823–5835. doi: 10.2147/IJN.S115158.

Shi K, Li C, Rensing C, Dai X, Fan X, Wang G (2018) Efflux transporter ArsK Is responsible for bacterial resistance to arsenite, antimonite, trivalent roxarsone, and methylarsenite. Appl Environ Microbiol 84

Shim MJ, Kim HJ, Yang SJ, Lee IS, Choi HI, Kim T. Arsenic trioxide induces apoptosis in chronic myelogenous leukemia K562 cells: possible involvement of p38 MAP kinase. *J Biochem Mol Biol.* 2002;35:377–383.

Sides MD, Sosulski ML, Luo F, Lin Z, Flemington EK, Lasky JA. Co-treatment with arsenic trioxide and ganciclovir reduces tumor volume in a murine xenograft model of nasopharyngeal carcinoma. *Virol J.* 2013;10:152. doi: 10.1186/1743-422X-10-152.

Siliciano JD, Siliciano RF. Latency and viral persistence in HIV-1 infection. *J Clin Invest.* 2000;106:823–825. doi: 10.1172/JCI11246

Sonkar A, Shukla H, Shukla R, Kalita J, Pandey T, Tripathi T. UDP-N-acetylglucosamine enolpyruvyl transferase (MurA) of acinetobacter baumannii (AbMurA): structural and functional properties. *Int J Biol Macromol.* 2017;97:106–114. doi: 10.1016/j.ijbiomac.2016.12.082.

Suzol SH, Hasan Howlader A, Galván AE, Radhakrishnan M, Wnuk SF, Rosen BP, Yoshinaga M. Semisynthesis of the organoarsenical antibiotic arsinothricin. *J Nat Prod.* 2020;83:2809–2813. doi: 10.1021/acs.jnatprod.0c00522.

Tähtinen P, Guella G, Saielli G, Debitus C, Hnawia E, Mancini I (2018), New sulfur-containing polyarsenicals from the new caledonian sponge Echinochalina bargibanti. Mar Drugs 16.

Testa U, Lo-Coco F. Targeting of leukemia-initiating cells in acute promyelocytic leukemia. *Stem Cell Investig.* 2015;2:8.

Thomas X, Troncy J. Arsenic: a beneficial therapeutic poison - a historical overview. *Adler Mus Bull.* 2009;35:3–13.

Tian J, Zhao H, Nolley R, Reese SW, Young SR, Li X, Peehl DM, Knox SJ. Darinaparsin: solid tumor hypoxic cytotoxin and radiosensitizer. *Clin Cancer Res.* 2012;18:3366–3376. doi: 10.1158/1078-0432.CCR-11-3179.

Van Schaftingen E, Opperdoes FR, Hers HG. Effects of various metabolic conditions and of the trivalent arsenical melarsen oxide on the intracellular levels of fructose 2,6-bisphosphate and of glycolytic intermediates in Trypanosoma brucei. *Eur J Biochem.* 1987;166:653–661. doi: 10.1111/j.1432-1033.1987.tb13563.x.

Verma A, Mohindru M, Deb DK, Sassano A, Kambhampati S, Ravandi F, Minucci S, Kalvakolanu DV, et al. Activation of Rac1 and the p38 mitogen-activated protein kinase pathway in response to arsenic trioxide. *J Biol Chem.* 2002;277:44988–44995. doi: 10.1074/jbc.M207176200.

Vollmer W, Blanot D, de Pedro MA. Peptidoglycan structure and architecture. *FEMS Microbiol Rev.* 2008;32:149–167. doi: 10.1111/j.1574-6976.2007.00094.x.

Waksman SA. What is an antibiotic or an antibiotic substance? *Mycologia.* 1947;39:565–569.
doi: 10.1080/00275514.1947.12017635.

Wang P, Qu X, Wang X, Liu L, Zhu X, Zeng H, Zhu H. As2O3 synergistically reactivate latent HIV-1 by induction of NF-κB. *Antiviral Res.* 2013;100:688–697. doi: 10.1016/j.antiviral.2013.10.010.

Wang X, Li D, Ghali L, Xia R, Munoz LP, Garelick H, Bell C, Wen X. Therapeutic potential of delivering arsenic trioxide into HPV-infected cervical cancer cells using liposomal nanotechnology. *Nanoscale Res Lett.* 2016;11:94. doi: 10.1186/s11671-016-1307-y.

Wang W, Li C, Zhang Z, Zhang Y. Arsenic trioxide in synergy with vitamin D rescues the defective VDR-PPAR-γ functional module of autophagy in rheumatoid arthritis. *PPAR Res.* 2019;2019:6403504. doi: 10.1155/2019/6403504.

Waxman S, Anderson KC. History of the development of arsenic derivatives in cancer therapy. *Oncologist.* 2001;6(Suppl 2):3–10. doi: 10.1634/theoncologist.6-suppl_2-3.

Worden AN, Wood EC. The effect of Carbarsone (33.6 per cent w-v p-ureidobenzene arsonic acid) on bodyweight gain, food conversion and tissue arsenic levels of turkey poults. *J Sci Food Agric.* 1973;24:35–41. doi: 10.1002/jsfa.2740240107.

Wu J, Shao Y, Liu J, Chen G, Ho PC. The medicinal use of realgar (As_4S_4) and its recent development as an anticancer agent. *J Ethnopharmacol.* 2011;135:595–602. doi: 10.1016/j.jep.2011.03.071.

Wulf G, Garg P, Liou YC, Iglehart D, Lu KP. Modeling breast cancer in vivo and ex vivo reveals an essential role of Pin1 in tumorigenesis. *Embo J.* 2004;23:3397–3407. doi: 10.1038/sj.emboj.7600323.

Yan Y, Chen J, Galván AE, Garbinski LD, Zhu YG, Rosen BP, Yoshinaga M. Reduction of organoarsenical herbicides and antimicrobial growth promoters by the legume symbiont *Sinorhizobium meliloti*. *Environ Sci Technol.* 2019;53:13648–13656. doi: 10.1021/acs.est.9b04026.

Yang Q, Feng F, Li P, Pan E, Wu C, He Y, Zhang F, Zhao J, et al. Arsenic trioxide impacts viral latency and delays viral rebound after termination of ART in chronically SIV-infected macaques. *Adv Sci (weinh)* 2019;6:1900319. doi: 10.1002/advs.201900319.

Yang FR, Zhao YF, Hu XW, Liu ZK, Yu XD, Li CY, Li XR, Li HJ. Nano-realgar suppresses lung cancer stem cell growth by repressing metabolic reprogramming. *Gene.* 2021;788:145666. doi: 10.1016/j.gene.2021.145666.

Yin Q, Sides M, Parsons CH, Flemington EK, Lasky JA. Arsenic trioxide inhibits EBV reactivation and promotes cell death in EBV-positive lymphoma cells. *Virol J.* 2017;14:121. doi: 10.1186/s12985-017-0784-7.

Yoda A, Toyoshima K, Watanabe Y, Onishi N, Hazaka Y, Tsukuda Y, Tsukada J, Kondo T, et al. Arsenic trioxide augments Chk2/p53-mediated apoptosis by inhibiting oncogenic Wip1 phosphatase. *J Biol Chem.* 2008;283:18969–18979. doi: 10.1074/jbc.M800560200.

Yoshinaga M, Rosen BP. A C·As lyase for degradation of environmental organoarsenical herbicides and animal husbandry growth promoters. *Proc Natl Acad Sci USA.* 2014;111:7701–7706. doi: 10.1073/pnas.1403057111.

Yoshinaga M, Cai Y, Rosen BP. Demethylation of methylarsonic acid by a microbial community. *Environ Microbiol.* 2011;13:1205–1215. doi: 10.1111/j.1462-2920.2010.02420.x.

Zebboudj A, Maroui MA, Dutrieux J, Touil-Boukoffa C, Bourouba M, Chelbi-Alix MK, Nisole S. Sodium arsenite induces apoptosis and Epstein–Barr virus reactivation in lymphoblastoid cells. *Biochimie.* 2014;107(Pt B):247–256. doi: 10.1016/j.biochi.2014.09.002.

Zhang XW, Yan XJ, Zhou ZR, Yang FF, Wu ZY, Sun HB, Liang WX, Song AX, et al. Arsenic trioxide controls the fate of the PML-RARalpha oncoprotein by directly binding PML. *Science.* 2010;328:240–243. doi: 10.1126/science.1183424.

Zhao QH, Zhang Y, Liu Y, Wang HL, Shen YY, Yang WJ, Wen LP. Anticancer effect of realgar nanoparticles on mouse melanoma skin cancer in vivo via transdermal drug delivery. *Med Oncol.* 2010;27:203–212. doi: 10.1007/s12032-009-9192-1.

Zhou XZ, Lu KP. The isomerase PIN1 controls numerous cancer-driving pathways and is a unique drug target. *Nat Rev Cancer.* 2016;16:463–478. doi: 10.1038/nrc.2016.49.

Zhu J, Chen Z, Lallemand-Breitenbach V, de Thé H. How acute promyelocytic leukaemia revived arsenic. *Nat Rev Cancer.* 2002;2:705–713. doi: 10.1038/nrc887.

CHAPTER 2: IDENTIFICATION OF THE BIOSYNTHETIC GENE CLUSTER FOR THE ORGANOARSENICAL ANTIBIOTIC ARSINOTHRICIN

2.1 Abstract

The soil bacterium *Burkholderia gladioli* GSRB05 produces the natural compound arsinothricin [2-amino-4-(hydroxymethylarsinoyl) butanoate] (AST), which has been demonstrated to be a broad-spectrum antibiotic. To identify the genes responsible for AST biosynthesis, a draft genome sequence of *B. gladioli* GSRB05 was constructed. Three genes, *arsQML*, in an arsenic resistance operon were found to be a biosynthetic gene cluster responsible for synthesis of AST and its precursor, hydroxyarsinothricin [2-amino-4-(dihydroxyarsinoyl) butanoate] (AST-OH). The *arsL* gene product is proposed to be a noncanonical radical *S*-adenosylmethionine (SAM) enzyme that is predicted to transfer the 3-amino-3-carboxypropyl (ACP) group from SAM to the arsenic atom in inorganic arsenite, forming AST-OH, which is methylated by the *arsM* gene product, a SAM methyltransferase, to produce AST. Finally, the *arsQ* gene product is an efflux permease that extrudes AST from the cells, a common final step in antibiotic-producing bacteria. Elucidation of the biosynthetic gene cluster for this novel arsenic-containing antibiotic adds an important new tool for continuation of the antibiotic era.

IMPORTANCE: Antimicrobial resistance is an emerging global public health crisis, calling for urgent development of novel potent antibiotics. We propose that arsinothricin and related arsenic-containing compounds may be the progenitors of a new class of antibiotics to extend our antibiotic era. Here, we report identification

of the biosynthetic gene cluster for arsinothricin and demonstrate that only three genes, two of which are novel, are required for the biosynthesis and transport of arsinothricin, in contrast to the phosphonate counterpart, phosphinothricin, which requires over 20 genes. Our discoveries will provide insight for the development of more effective organoarsenical antibiotics and illustrate the previously unknown complexity of the arsenic biogeochemical cycle, as well as bring new perspective to environmental arsenic biochemistry.

KEYWORDS: arsinothricin, organoarsenical antibiotic, biosynthetic gene cluster, *Burkholderia gladioli* GSRB05

2.2 Introduction

Arsenic is one of the most ubiquitous environmental toxic substances. Bacteria have taken advantage of its prevalence to evolve mechanisms that give them competitive advantages over bacterial competitors. These include pathways for arsenic respiration for energy generation (1–3), methylation of inorganic arsenic to increase its potency as an antimicrobial (4, 5), and even incorporation into arsenolipids for sparing phosphate under nutrient-limiting conditions (6, 7). A newly recognized adaptation is synthesis of a novel arsenic-containing antibiotic.

Antibiotic resistance is a global health challenge, and new antibiotics are urgently needed. Recently the rice rhizosphere bacterium *Burkholderia gladioli* GSRB05 was shown to produce the broad-spectrum arsenic-containing antibiotic arsinothricin ((2-amino-4-hydroxymethylarsinoyl) butanoate (AST) (8). AST

effectively inhibits growth of the World Health Organization (WHO) priority pathogens such as carbapenem-resistant *Enterobacter cloacae* (CRE) but has low cytotoxicity in human monocytes (9). It also inhibits growth of *Mycobacterium bovis* BCG, which causes tuberculosis (TB) in animals and humans and is closely related to *Mycobacterium tuberculosis*, the major causative agent of human TB. TB is classified by the WHO as a global health emergency (10), and the WHO has called for the development of new and innovative antibiotics against *M. tuberculosis* (https://www.who.int/activities/tackling-the-drug-resistant-tb-crisis). AST is a pentavalent organoarsenical and a nonproteinogenic amino acid analog of glutamate. It inhibits glutamine synthetase (GS), most likely because of its chemical similarity to the acyl-phosphate intermediate γ-glutamyl phosphate, in the GS catalytic cycle (9). GS is essential for nitrogen metabolism in *M. tuberculosis*, and inhibitors of *M. tuberculosis* GS are actively sought after as drugs against TB (11).

B. gladioli GSRB05 is the only known AST producer that has been shown to produce both pentavalent hydroxyarsinothricin [2-amino-4-(dihydroxyarsinoyl) butanoate] (AST-OH) and AST from As(III), with a possible precursor-product relationship (8). Here, we identified the biosynthetic gene cluster (BGC) for AST production from the genome of *B. gladioli* GSRB05. Three genes, *arsQ*, *arsM*, and *arsL*, are organized in an arsenic resistance (*ars*) operon. By way of comparison, the phosphonate analog of AST is the *Streptomyces* antibiotic phosphinothricin, which is used commercially as the herbicide glufosinate and has a very

complicated biosynthetic pathway (12). The BGC from *Streptomyces viridochromogenes* consists of 24 genes (accession no. X65195) (13), so a three-gene BGC for arsinothricin production is surprisingly small.

Identification of the AST BGC makes substantial contributions in two important areas – treatment of infectious diseases and radical *S*-adenosylmethionine (SAM) chemistry. First, the BGC is an uncomplicated pathway with only three steps required for the synthesis of AST. This arsenic-containing compound may be the founding member of a new class of antibiotics, adding to our arsenal of weapons against multidrug-resistant pathogens. Second, the radical SAM enzyme BgArsL (i.e., *B. gladioli* ArsL) catalyzes the key enzymatic reaction in AST biosynthesis. Radical SAM enzymes form the largest enzyme superfamily (14). Most members catalyze the transfer of a 5'-deoxyadenosyl radical to the substrate or function as methyltransferases using a methylene fragment from SAM (15). In contrast, BgArsL is proposed to be a noncanonical radical SAM enzyme that transfers the ACP moiety to As(III), forming AST-OH, a unique radical SAM reaction.

2.3 Results

Identification of the AST biosynthetic gene cluster. In this study, a time course of AST biosynthesis by *B. gladioli* GSRB05 was conducted in cells grown in ST 10^{-1} medium (Fig. 1). After a lag period of approximately 10 h, both trivalent and pentavalent AST-OH and pentavalent AST were produced. After approximately 15 h, all of the As(III) was consumed, the trivalent AST-OH peak decreased, and both

the AST and the pentavalent AST-OH peaks increased correspondingly. We interpret this result as As(III) conversion into trivalent AST-OH in the first step, which is then either methylated to AST in a second step or oxidized to pentavalent AST-OH. After 24 h, both the pentavalent and trivalent AST-OH peaks decreased, and the AST peak increased reciprocally, suggesting that the strain is able to reduce pentavalent AST-OH to the trivalent form to produce more AST. It is not clear if the product is trivalent or pentavalent AST because in our hands trivalent AST oxidizes in air too rapidly to be isolated. Trivalent AST-OH also oxidizes in air, but less rapidly than AST.

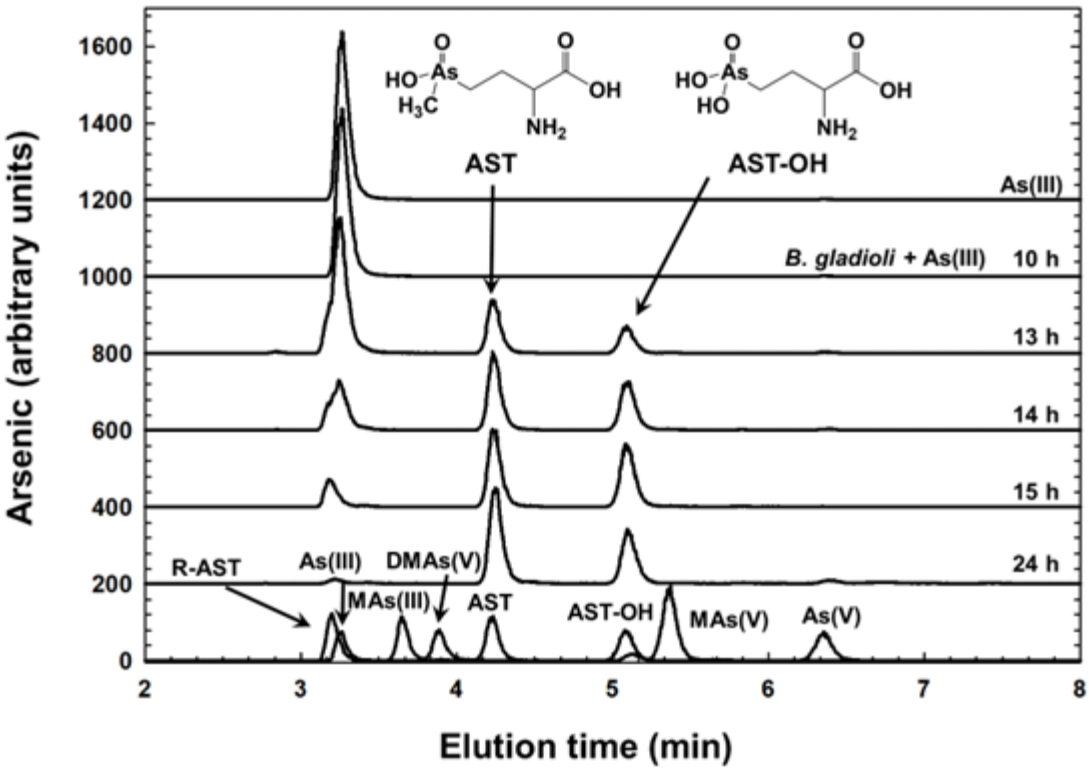

Fig 1. Time course of AST biosynthesis by *B. gladioli* GSRB05. Production of AST-OH and AST by cells of *B. gladioli* GSRB05 was assayed over a 24-h period. Cells were grown in LB medium until late log phase and transferred to ST 10^{-1} for up to 24 h in the presence of 3 μM As(III). Samples were speciated by C_{18} reverse-phase HPLC, and arsenic was determined by ICP-MS at the indicated times. After a lag period of approximately 10 h, AST-OH and AST synthesis was observed. During the remaining time, the amount of AST increased, and As(III) decreased correspondingly. Production of AST-OH leveled off after approximately 14 to 15 h, indicating that it is an intermediate in the pathway of AST biosynthesis from As(III). (Bottom line) Standards of arsenic compounds. R-AST-OH, trivalent hydroxyarsinothricin; As(III), arsenite; MAs(III), methylarsenite; DMAs(V), dimethylarsenate; AST, arsinothricin; AST-OH, hydroxyarsinothricin; MAs(V), methylarsenate; As(V), arsenate.

To identify the AST BGC knowing that methylation is involved, we made the assumption that a *B. gladioli* GSRB05 enzyme would be related to other known methylating enzymes. Arsenic methylation catalyzed by the ArsM As(III) S-adenosylmethionine methyltransferase is a common reaction in arsenic metabolism (16). Bacterial and algal ArsM enzymes methylate inorganic As(III) up to three times to produce methylarsenite [MAs(III)], dimethylarsenite [DMAs(III)], and trimethylarsenite [TMAs(III)]. These are rapidly oxidized nonenzymatically in air to the pentavalent species, which are neither substrates nor products of the enzyme-catalyzed reaction. We predicted that a *B. gladioli* GSRB05 ArsM ortholog is involved in the methylation of trivalent AST-OH and that its gene would be in the AST BGC. For that reason, a draft sequence of the *B. gladioli* GSRB05 genome was constructed (see Fig. S2 in the supplemental material). As anticipated, an *arsM* sequence was identified next to a cluster of genes related to arsenic metabolism but divergently oriented (Fig. 2A). These genes located on the opposite DNA strand are *arsR* (17), *pitA* (18), *aioAB* (2), encoding a putative ArsR As(III)-responsive transcriptional repressor, PitA, a low-affinity inorganic phosphate/arsenate (As(V)) transporter, and the AioAB arsenite oxidase that oxidizes As(III) to As(V), respectively. The predicted products of the genes upstream and downstream of *arsM* were searched against the basic local alignment search tool (BLAST; http://blast.ncbi.nlm.nih.gov). The gene immediately upstream of *arsM* is termed *arsQ* and encodes a putative membrane transporter annotated as related to the GntP family of gluconate permeases (19). The gene immediately downstream of *arsM* encodes a putative radical SAM

protein and is termed *arsL*. The *arsQML* gene cluster is found in the genomes of other proteobacterial genomes but is not widespread in the bacterial kingdom (Fig. 2B). Their association suggests that these three genes have a related function. The next four genes were termed *orf1–4* and are annotated as encoding two class I SAM-dependent methyltransferases, a cytochrome P450-like protein, and an α/β-hydrolase. The four genes are not adjacent to *arsQML* in other bacterial genomes, and as described below, these four genes appear to be unrelated to AST biosynthesis.

The *B. gladioli arsM* gene product (BgArsM) is a 378-amino-acid-residue protein with a predicted mass of 41.71 kDa (accession no. MBW5287222). Most ArsM and related animal AS3MT enzymes have four conserved cysteine residues that are required for catalysis (20, 21). Multiple-sequence alignment of BgArsM and orthologs shows that BgArsM has four cysteine residues at positions 30, 54, 181, and 233. The N-terminus of BgArsM does not align well with those of other ArsMs, but Cys30 is in approximately the position expected for the first conserved cysteine, and the other three align with the remaining three conserved cysteine residues. The *arsL* gene product (BgArsL) is a 428-amino-acid-residue protein with a predicted mass of 47.5 kDa (accession no. MBW5287221). Multiple sequence alignment with other putative ArsL orthologs shows that BgArsL has three conserved cysteine residues at positions 194, 198, and 201. It is annotated as a radical SAM enzyme, with these three cysteine residues forming a CX_3CX_2C motif that is found in more than 90% of members of the radical SAM superfamily. In the

cyanobacterium *Synechocystis* sp. strain PCC 6803, a radical SAM enzyme, SsArsS, has been shown to function with SsArsM to catalyze the initial steps in arsenosugar biosynthesis (22). It was therefore reasonable to consider that BgArsM and BgArsL might function together in AST biosynthesis. The *arsQML* genes plus the four downstream *orf* genes were cloned and transformed into *E. coli* Top10. However, the transformants grew poorly. Considering that the heterologous expression of membrane proteins, in general, might be toxic for the host cells, *arsQ* was eliminated from the construct, leaving *arsML* and the four *orf* genes. Cells of *E. coli* Top10 with the remaining six genes grew well, indicating that *arsQ* was responsible for growth retardation. With the addition of 1 μM As(III), cells expressing the six genes produced AST and smaller amounts of AST-OH (Fig. 3A). Cells expressing an *arsL–orf1–4* construct lacking *arsM* produced only AST-OH and not AST. These results indicate that one or more of the five genes downstream of *arsM* are involved in AST-OH biosynthesis, followed by methylation to AST by BgArsM.

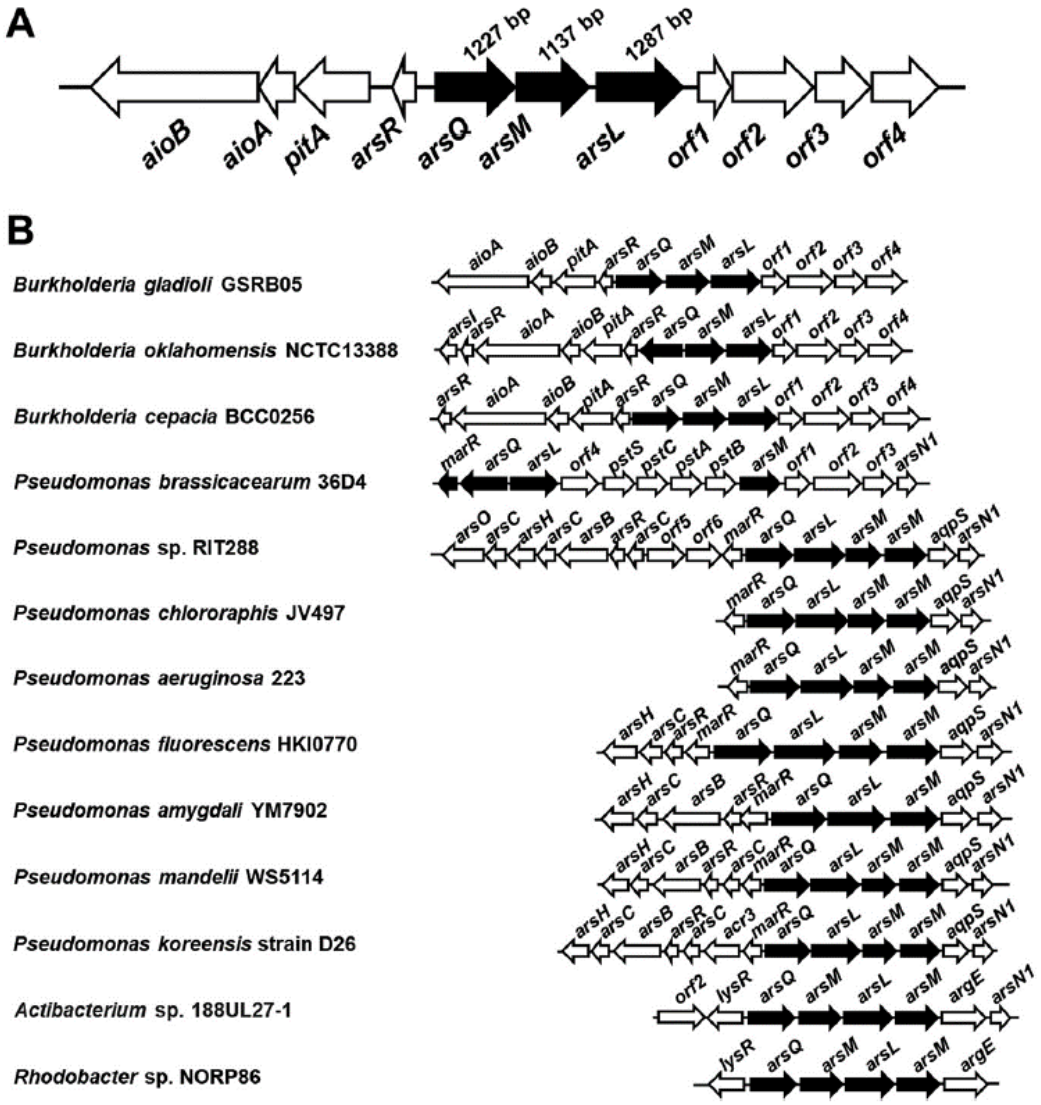

Fig. 2 The *B. gladioli* GSRB05 AST biosynthetic gene cluster. (A) The *B. gladioli* GSRB05 genome (accession no. JAGSIB000000000) contains a cluster of *ars* genes, including *arsQML*. (B) Phylogenetic distribution of the genes of the AST BGC. GenBank accession numbers are given in Materials and Methods.

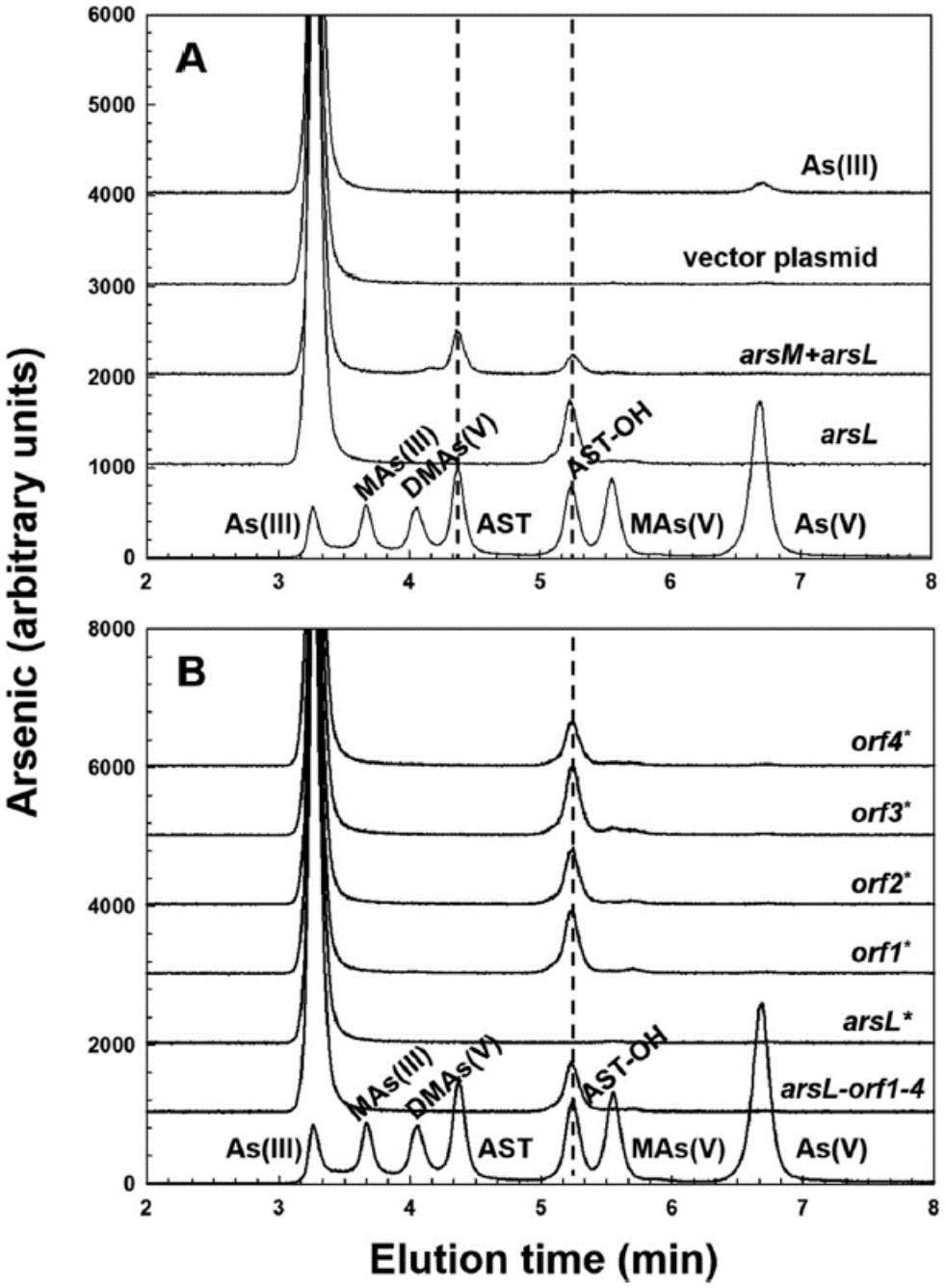
A
B
As(III)
vector plasmid
arsM+arsL
arsL
orf4*
orf3*
orf2*
orf1*
arsL*
arsL-orf1-4
MAs(III)
DMAs(V)
AST
AST-OH
MAs(V)
As(V)
Arsenic (arbitrary units)
Elution time (min)

Fig.3 AST-OH and AST biosynthesis in cells bearing *arsML–orf1–4*. As(III) biotransformation was assayed with selected genes from the AST BGC from *B. gladioli* GSRB05. (A) Cultures of *E*. *coli* Top10 expressing *arsML–orf1–4* and/or *arsL–orf1–4* in plasmid pUC118. From the bottom the lanes are arsenic standards, cells with 1 μM As(III) bearing pUC*arsL–orf1–4*, pUC*arsML–orf1–4*, vector plasmid pUC118, and medium with only 1 μM As(III). (B) Stop codons (*) were individually introduced into the genes in plasmid pUC*arsL–orf1–4*. From the bottom, the lanes are arsenic standards, cells expressing wild type *arsL–orf1–4* genes and stop codons in each gene. Cultures were grown in LB medium to late log phase, transferred to ST 10^{-1} medium with 1 μM As(III), and incubated for 36 h. Arsenic-containing species were determined by HPLC-ICP-MS.

BgArsM and BgArsL are both required for AST biosynthesis. To determine which gene or genes are required for AST-OH production, a mutation producing a stop codon was introduced into *arsL* and each of the other four genes in the *arsL–orf1–4* construct. Cells expressing each mutant were incubated with As(III), and the culture medium was analyzed by high-performance liquid chromatography-inductively coupled plasma mass spectrometry (HPLC-ICP-MS). Stop codons in the downstream *orf1–4* genes had no effect, and only the strain with the point mutation in the *arsL* gene lost the ability to produce AST-OH (Fig. 3B). Thus, only *arsL* is required for AST-OH production. These results strongly suggest that the biosynthetic pathway of AST is composed of only two reactions catalyzed by BgArsM and BgArsL. To confirm this hypothesis, we expressed *arsL* alone and the *arsML* genes together in the pETDuet-1 system (Fig. 4). Cells of *E. coli* BL21 expressing *arsL* alone produced AST-OH but not AST, while AST production was observed when *arsL* and *arsM* were coexpressed.

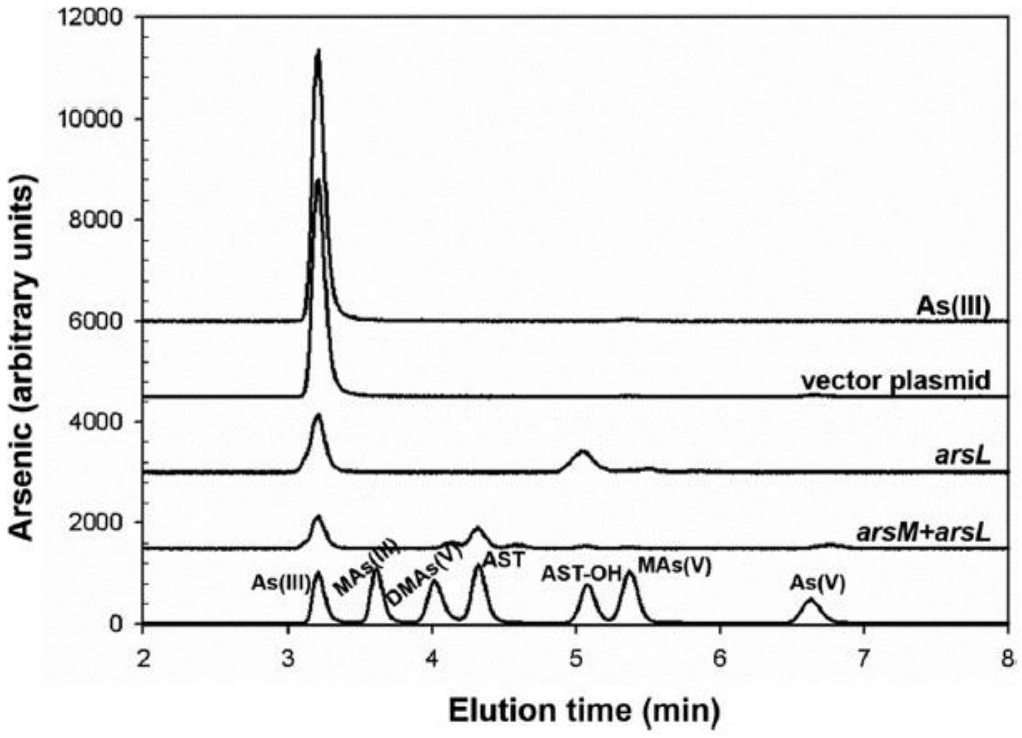

Fig.4 The *arsL* and *arsM* gene products are sufficient to catalyze sequential steps in the biosynthesis of AST. Production of AST-OH or AST was assayed in cultures of *E. coli* BL21 with 1 μM As(III), as described in the legend to Fig. 3. From the bottom, the lanes are arsenic standards, cells bearing pETDuet-1*arsLM*, pETDuet-1*arsL*, vector plasmid pETDuet-1, and medium with only 1 mM As(III).

The *arsQML* genes comprise an As(III)-inducible *ars* operon. To examine whether the *arsQ*, *arsL* and *arsM* genes comprise an As(III)-responsive *ars* operon, total RNA was obtained from cells of *B. gladioli* GSRB05 with or without As(III), and cDNA was subsequently synthesized by reverse transcription-PCR (RT-PCR). From the amount of RNA detected in quantitative real-time PCR (RT-qPCR) analysis, expression of *arsQ*, *arsM* and *arsL* increased approximately 8.5-, 7.2-, and 11.9-fold, respectively, following induction with 3 μM As(III) compared with RNA from uninduced cells (Fig. 5). The results demonstrate that the *arsQML*

genes comprise an *ars* operon. As(III) responsiveness suggests that the operon is controlled by an ArsR repressor, likely the product of the upstream *arsR* gene. When the reverse primers were designed to anneal a cDNA region including either *orf1* or *orf2*, almost no amplification was observed, indicating that the downstream four *orf* genes are not part of the *arsQML* operon.

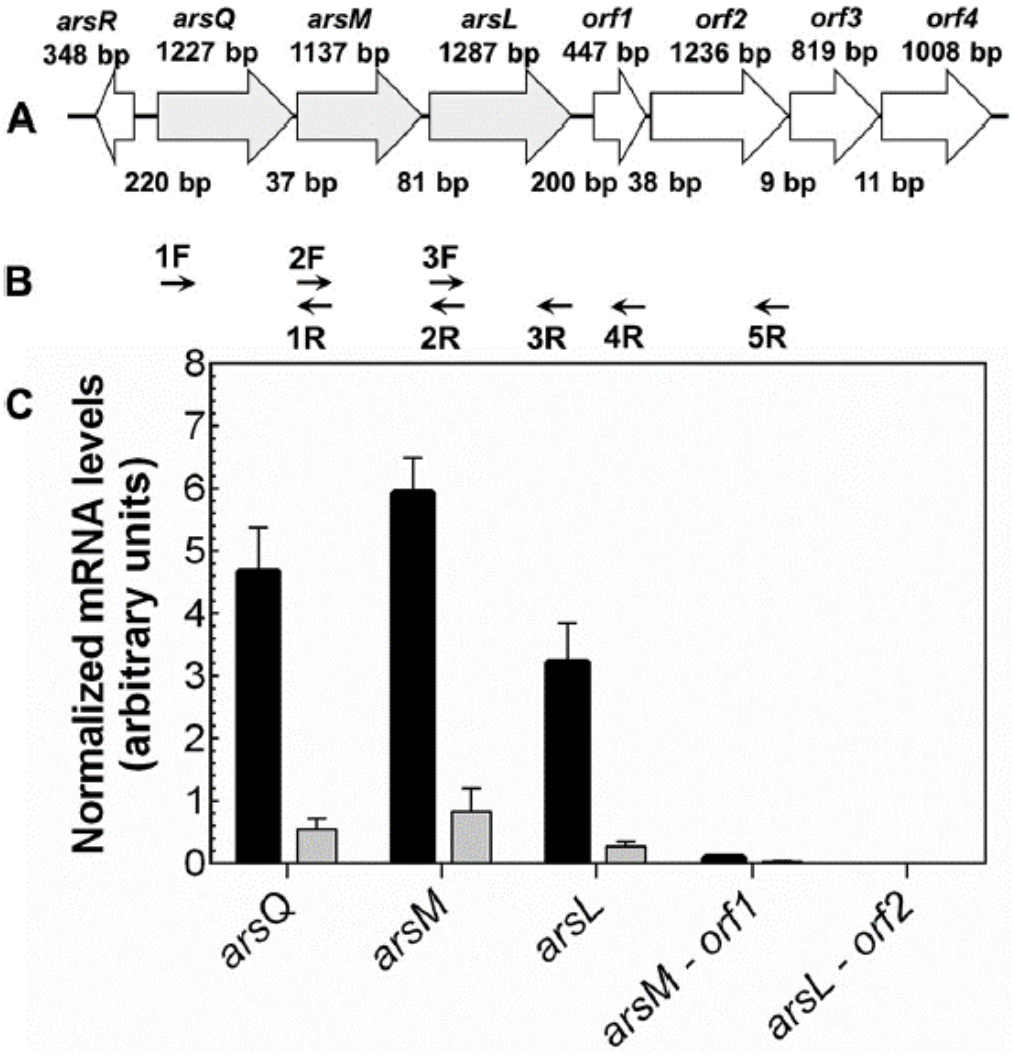

Fig. 5 The BGC is the *arsQML* operon. (A) The BGC and upstream and downstream genes are illustrated, with the size of each gene and intergenic regions given in nucleotide base pairs. (B) The indicated forward (F) and reverse I primers were used to amplify transcriptional products by RT PCR. (C) Analysis of transcription of the *arsQ* (primers 1F-1R), *arsM* (primers 2F-2R) or *arsL* (primers 3F-3R) genes individually and cotranscription of *arsM–orf1* (primers 2F-4R) and *arsL–orf2* (primers 3F 5R) genes. *B. gladioli* GSRB05 was grown in LB medium until late log phase and then transferred to ST 10^{-1} medium. Cultures were incubated for 13 h in the presence (black bars) or absence (shaded bars) of 3 µM As(III). cDNA was synthesized by RT-PCR from total RNA obtained from cultures of *B. gladioli* GSRB05. Data are the mean ± SE (n = 4).

ArsQ confers moderate resistance to AST. Antibiotic BGCs frequently have genes for efflux of the antibiotic. This serves dual purposes of removing the active antibiotic from the cytosol, thus protecting the producing organism, and exporting the compound into the medium, where it can exert its antibiotic action against other bacteria. The *arsQ* gene encodes a putative membrane protein of 408 amino acid residues with a predicted mass of 42.9 kDa (accession no. MBW5287223). ArsQ orthologs are found primarily in Proteobacteria and are annotated as gluconate permeases. AST and gluconate are similar in size and charge, so a reasonable inference is that the BgArsQ functions as an AST efflux permease. A multiple-sequence alignment with the 100 most closely related proteins shows variation in the N-terminal 90 residues, but the remaining 318 residues are highly conserved (see Fig. S5 in the supplemental materials). The *arsQ* gene was cloned into vector pTrcHisA and transformed into the As(III)-hypersensitive strain *E. coli* AW3110 (23). Addition of the inducer IPTG (isopropyl-β-D-1-thiogalactopyranoside) produced growth inhibition, so the cells were grown without inducer, and the effect of leaky expression of *arsQ* on AST inhibition was assayed (Fig. 6A). Cells expressing *arsQ* were clearly more resistant to AST than those with vector only, supporting my hypothesis that BgArsQ is an AST efflux permease. The resistance was not dramatic—probably due to low levels of expression of BgArsQ.

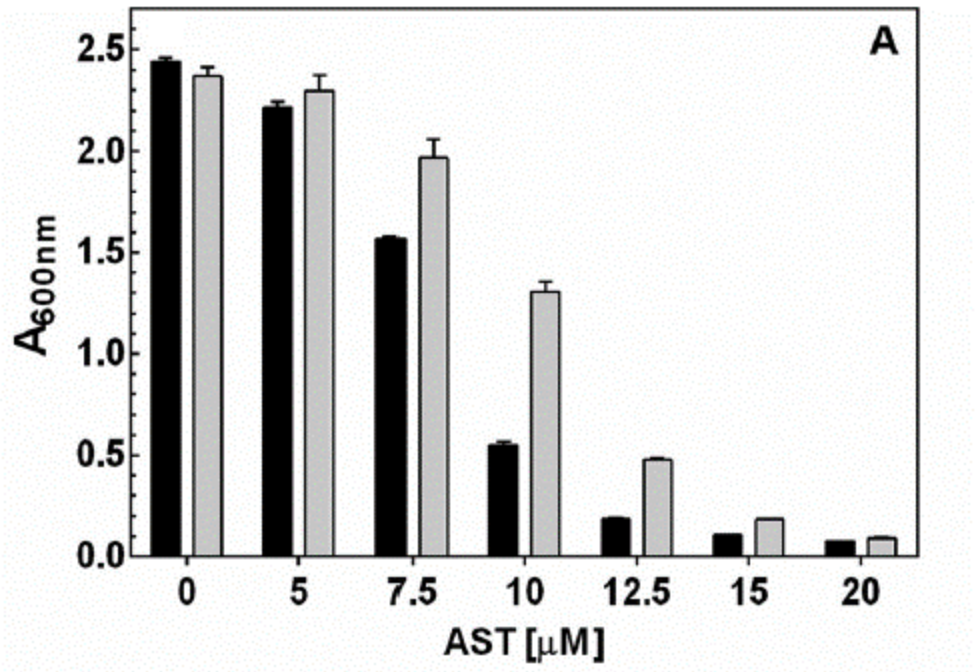

Fig. 6 BgArsQ is an AST efflux permease. Expression of *arsQ* confers resistance to AST. Overnight cultures of *E. coli* AW3110 bearing either pTrcHisA*arsQ* (shaded bars) or vector plasmid pTrcHisA (black bars) were diluted 100-fold into fresh M9 medium containing the indicated concentrations of AST. A_{600} was measured after 24 h of growth at 37 °C.

2.4 Discussion

Identification of the biosynthetic gene cluster for arsinothricin is an essential step in elucidation of the antimicrobial action of this novel arsenic-containing antibiotic. With only three genes, the BGC is surprisingly small, especially compared with the BGC for the phosphonate counterpart, phosphinothricin, which includes 24 genes. The AST BGC has a rather narrow phylogenetic distribution. The *arsQML* gene cluster is found primarily in members of the Proteobacteria phylum, such as the classes Alpha proteobacteria (*Rhodobacter*), Betaproteobacteria (*Burkholderia*), and Gamma proteobacteria (*Pseudomonas*). Most BgArsQ orthologs are found in

Proteobacteria, while orthologs of BgArsM and BgArsL are more widely distributed. However, it is not clear if those are involved in AST biosynthesis. Near other *arsL* genes are also genes for other putative permeases that are unrelated to ArsQ. It is not known if their substrates include AST, but alternate AST transporters would not be surprising. This is reminiscent of the existence of multiple permeases for inorganic and organic arsenicals, such as ArsB, Acr3, ArsP, ArsK, and ArsJ (26). We propose that AST is synthesized in a three-step pathway: (i) AST-OH synthesis by BgArsL, (ii) methylation of AST-OH to AST by BgArsM, and (iii) export of AST or related compounds by BgArsQ (Fig. 7).

BgArsL can be predicted to be a radical SAM enzyme, a member of the largest enzyme superfamily. It has three cysteine residues (Cys194, Cys198, and Cys201) that are highly conserved in radical SAM enzymes and form a [4Fe-4S]+ cluster for reductive cleavage of SAM. Since BgArsL has only three conserved cysteine residues, it likely has a single $[4Fe\text{-}4S]^{+}$ cluster. The majority of radical SAM enzymes produce a 5’-deoxyadenosyl radical that performs a wide variety of organic chemical biotransformations (15). AST-OH is an amino acid with arsenate replacing the γ-carboxyl group of glutamic acid, so it is reasonable to propose that BgArsL catalyzes addition of the 3-amino-3-carboxypropyl (ACP) group of SAM to As(III), forming trivalent AST-OH, as shown in Fig. 7. In this respect, I propose that BgArsL is a novel noncanonical radical SAM enzyme that forms an ACP radical rather than the more common 5'-deoxyadenosyl radical. This reaction would produce trivalent AST-OH. The only other noncanonical radical SAM enzyme that

transfers ACP is the diphthamide biosynthetic enzyme Dph2, which adds ACP to a histidine residue in translation elongation factor 2 (27). Rather than catalyzing protein modification like Dph2, ArsL catalyzes the unique chemistry of C-As bond formation. Enzymes with $[4Fe\text{-}4S]^{+}$ clusters are typically very oxygen sensitive, usually requiring anaerobic purification and/or reconstitution of the iron-sulfur cofactor (28). Future directions of study with BgArsL will be designed for the challenging characterization of the enzyme *in vitro*. BgArsM is a typical As(III) SAM methyltransferase. ArsM substrates include inorganic arsenite, methylarsenicals, and aromatic arsenicals. A mechanistic feature of this group of arsenic methyltransferases is that both the substrates and products are trivalent, and the pentavalent species are produced nonenzymatically by oxidation, usually with atmospheric O_2 (16). Cells of *E. coli* heterologously expressing the *arsL* gene transform As(III) into AST-OH, and cells expressing both *arsL* and *arsM* genes produce AST. Thus, we propose that in the second step, trivalent AST-OH is methylated by BgArsM to form the reduced form of AST, which would rapidly oxidize, yielding the pentavalent antibiotic AST. Future tests of this proposal will involve purification of BgArsM for enzymatic assays and development of analytical methods to detect the trivalent form of AST. Antibiotic producers frequently have transporters that transport the active antibiotic from the cells, both for self-protection and to inhibit growth of competitors (29). In the third and final step, AST or a related compound is exported from the cells by the efflux permease BgArsQ. It is not known whether BgArsQ substrates are trivalent, pentavalent, or both, whether AST-OH and AST are both substrates, or even if gluconate is a substrate,

due to apparent toxicity caused by *arsQ* expression. Future experiments will be designed to produce sufficient BgArsQ for biochemical characterization.

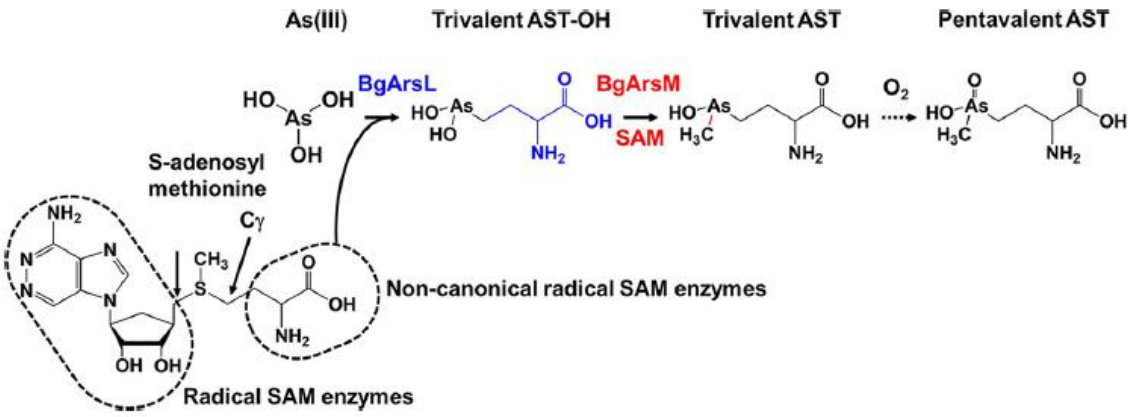

Fig. 7 Proposed pathway of AST biosynthesis. AST biosynthesis by *B. gladioli* GSRB05 is composed of two steps. In the first step, the noncanonical radical SAM enzyme BgArsL cleaves the Cγ bond of SAM, forming a 3-amino-3-carboxypropyl (ACP) radical that creates a C-As bond with As(III), producing trivalent AST-OH. This is different from most radical SAM enzymes that form 5'-deoxyadenosyl radical by reductive cleavage of SAM at the 5' position of the adenosine moiety. In the second step, BgArsM uses a second molecule of SAM to methylate trivalent AST-OH, generating trivalent AST, which spontaneously oxidizes nonenzymatically to the antibiotic pentavalent AST.

2.5 materials and methods

Strains, plasmid, media, and growth conditions. Strains and plasmids used in this study are described in Table S1 in the supplemental material. *B. gladioli* GSRB05 and *E. coli* cultures were grown aerobically overnight with shaking in lysogeny broth (LB) medium (30) at 30 or 37 °C, respectively. M9 medium (30) was supplemented with 0.2% glucose, 0.1 mM $CaCl_2$, and 1 mM $MgSO_4$. For resistance assays, antibiotics were supplemented at the following final

concentrations, as indicated: 50 μg/ml streptomycin (Sm), 25 μg/ml chloramphenicol (Cm), and 100 μg/ml ampicillin (Ap).

AST production. The protocol for AST production was modified from the original method (8). A single colony of *B. gladioli* GSRB05 was inoculated into 10 ml of LB medium and grown overnight. The culture was 100-fold diluted into 1 liter of fresh LB and grown again to an A_{600} of 1. Next, the cells were harvested and transferred into the same volume of ST 10^{-1} medium (31) supplemented with 20 μM As(III) and 0.2% glucose. The culture was incubated until As(III) was completely transformed into AST. AST was chromatographically purified as described previously (8) with a yield of approximately 5 mg AST/liter of culture medium and was free of AST-OH.

The time course of As(III) conversion into AST-OH and AST by *B. gladioli* GSRB05 was performed in a 50-ml culture of ST 10^{-1} medium containing 3 μM As(III). The same procedure was used to determine As(III) transformation by *E. coli* Top10 bearing the vector plasmid pUC118, pUC*arsL–orf1–4*, or pUC*arsML–orf1–4* as for *B. gladioli* GSRB05, but for *E. coli* BL21 bearing the plasmid pETDuet-1, pETDuet-1*arsL*, pETDuet-1*arsM*, or pETDuet-1*arsLM*, the pellet was directly transferred from the overnight LB culture into ST 10^{-1} medium supplemented with 1 μM As(III) and 0.4% glycerol, following which cultures were incubated for 36 h. For both *E. coli* Top10 and BL21, basal expression of genes in plasmids pUC118 and pETDuet-1 was sufficient to observe the activity of the genes.

Analysis of arsenic species. Arsenic species in the supernatant were analyzed by high-performance liquid chromatography-inductively coupled plasma mass spectrometry (HPLC-ICP-MS). For sample preparation, 0.5 ml of culture was collected and centrifuged at 13,000 rpm for 2 min at 4 °C. Supernatants were filtered with 3-kDa Amicon Ultra Centrifugal filters (MilliporeSigma, St. Louis, MO, USA) for 10 min. A mobile phase of 3 mM malonic acid, 5% methanol, and tetrabutylammonium hydroxide to reach a pH of 5.9 was used to elute a C_{18} reverse-phase column at a flow rate of 1.0 ml min^{-1}.

Construction of the draft genome sequence of *B. gladioli* GSRB05. Genome sequencing of *B. gladioli* GSRB05 was performed using the Illumina NextSeq platform at Center for Genome Technology, University of Miami, Miller School of Medicine (Miami, FL, USA). Sequence data were comprised of 7.8 million paired-end (2 x 150) reads. Quality trimming and filtering were performed using the TrimGalore (version 0.6.4) (https://www.bioinformatics.babraham.ac.uk/projects/trim_galore/) tool to remove adapter sequences, base pairs with a quality score of <30, and reads shorter than 50 bp. Quality-trimmed reads were assembled using SPAdes (version 3.13.0) (32) and ABySS (version 2.1.5) (33) at different kmers, and optimal assembly was selected as described previously (34). Genome annotation was accomplished using the NCBI Prokaryotic Genome Annotation Pipeline (35), and predictions of *arsM* orthologous genes were performed via BLAST (36) and OrthoMCL (37) sequence analysis against the predicted proteins.

Cloning and expression. Genomic DNA was extracted from 3 ml of a fresh overnight culture of *B. gladioli* GSRB05 using the E.Z.N.A. Bacterial DNA kit (Omega Bio-tek, Inc., Norcross, GA, USA). The gene cluster was sequentially amplified by PCR with Pfu Turbo high-fidelity DNA polymerase (Agilent Technologies, Inc., Santa Clara, CA, USA), and the entire cluster or groups of genes were cloned into plasmid pUC118 between the KpnI and XbaI restriction sites. To construct pUC*arsL–orf1–4*, the cloning was carried out in two steps, while for pUC*arsML–orf1–4*, an additional step was necessary (see Fig. S1 in the supplemental material) to amplify fragments of no more than 3.2 kb to avoid incorrect base insertion. Primers were designed with unique restriction sites to serially construct the final plasmids. The amplified products were gel purified, digested with the appropriate restriction enzymes, and inserted into vector plasmid pUC118 with the first gene in frame with the *lacZ* gene of the vector. The *arsL* and *arsML* genes were ordered from GenScript (Piscataway, NJ, USA) and cloned into pETDuet-1 (Millipore Sigma) and arsQ in pTrcHisA (Thermo Fisher Scientific, Inc., Waltham, MA, USA) to construct pETDuet-1*arsL*, pETDuet-1*arsML*, and pTrc*arsQ*, respectively. Each step of cloning was verified by sequencing the fragments. The complete list of the oligonucleotides used in this study is given in Table S1.

Site-directed mutagenesis. The primers for site-directed mutagenesis (see Table S2 in the supplemental material) were designed using the online QuikChange

Primer Design program (https://www.agilent.com/store/primerDesignProgram.jsp). A stop codon was individually inserted into each of the five genes in plasmid pUC*arsL–orf1–4* by substitution of one nucleotide at the beginning of the sequence. Unmutated plasmid pUC*arsL–orf1–4* was removed from the reaction mixture by digesting the methylated DNA with restriction enzyme DpnI (New England Biolabs, Ipswich, MA, USA). Each mutated plasmid was transformed into competent cells of *E. coli* TOP10 and purified, and the presence of the mutation was verified by sequencing.

mRNA extraction, reverse transcription, and quantitative real-time PCR. An RNeasy minikit (Qiagen, Valencia, CA, USA) was used to isolate total RNA from a 3-ml culture of *B. gladioli* GSRB05 that had been cultured with or without exposure to 3 μM As(III) in ST 10^{-1} medium for 13 h. The purity and concentrations of RNA were determined from the A_{260} using a Synergy H4 Hybrid microplate reader (BioTek Instruments, Inc., Winooski, VT, USA). RNA integrity was verified by electrophoresis (data not shown). Reverse transcription-PCR (RT-PCR) was performed to synthesize complementary DNA (cDNA) using a Verso cDNA synthesis kit (Thermo Fisher Scientific, Inc.) according to the manufacturer's instructions. Primer sets for real-time qPCR of target genes are listed in Table S2. One microliter of each of the purified RT-PCR products corresponding to 50 ng of total RNA was amplified in a 10-μl reaction mixture containing 0.5 μM each primer set and 5 μl of iQSYBR green supermix (Bio-Rad Laboratories, Inc., Hercules, CA, USA). Real-time qPCR assays were carried out using a Realplex2 PCR instrument

(Eppendorf, Hamburg, Germany) with the following cycle steps: initial denaturation for 2 min at 94 °C, followed by 40 cycles of 15 s at 94 °C for denaturation, and then 30 s at 50°C for annealing, and 1 min 30 s at 72 °C for extension of *arsQ*, *arsM*, and *arsL*. For fragments containing sequences from *arsM* to *orf1* (*arsM–orf1*) or from *arsL* to *orf2* (*arsL–orf2*), the reaction condition was changed to 30 s at 58 °C for annealing and 3 min 10 s at 72 °C for extension. All data were normalized to the amount of 16S rRNA. The threshold cycle ($2^{-\Delta CT}$) was calculated to compare the expression level of each gene.

Assays of *arsQ* function. To examine whether the *arsQ* gene could confer AST resistance, cells of *E. coli* AW3110 harboring plasmid pTrcHis2*AarsQ* were grown overnight in LB medium and washed and suspended in 0.9% NaCl. The washed cells were then inoculated into M9 medium at an A_{600} of 0.03 and incubated for 24 h in the presence of the indicated concentrations of AST.

AST BGC distribution. The prevalence of AST BGC was analyzed in representative organisms. GenBank accession numbers of the following bacterial genomes are given in parentheses: *B. gladioli* GSBR05 (JAGSIB000000000) is compared with putative orthologs from *Burkholderia oklahomensis* (NZ_UFUH01000001), *Burkholderia cepacia* (NZ_CADEUO010000007), *Pseudomonas aeruginosa* (NZ _CACPET010000007), *Pseudomonas fluorescens* (NZ_LVEJ01000018), *Pseudomonas amygdali* (NZ_LGLI01000031), *Actibacterium* sp. (NZ_JAFEUL010000009), and *Rhodobacter* sp.

(NVUP01000011). Multiple alignments of the sequences of ArsM (Fig. S3), ArsL (Fig. S4), and ArsQ (Fig. S5) orthologs were performed using T-Coffee (39) and the BoxShade version 3.21 server (https://embnet.vital-it.ch/software/BOX_form.html).

Data availability

The draft genome sequence for *B. gladioli* GSRB05 has been deposited in NCBI under accession no. JAGSIB000000000. Raw sequence reads have been deposited in NCBI under BioProject accession no. PRJNA722678.

2.6 Acknowledgement

This work was supported by NSF BIO/MCB grant 1817962 to M.Y. and NIH grant R35GM136211 to B.P.R.

REFERENCES

1. Krafft T, Macy JM. 1998. Purification and characterization of the respiratory arsenate reductase of Chrysiogenes arsenatis. Eur J Biochem 255:647–653. https://doi.org/10.1046/j.1432-1327.1998.2550647.x.

2. Ellis PJ, Conrads T, Hille R, Kuhn P. 2001. Crystal structure of the 100 kDa arsenite oxidase from Alcaligenes faecalis in two crystal forms at 1.64 Å and 2.03 Å. Structure 9:125–132. https://doi.org/10.1016/S0969-2126(01)00566-4.

3. Zargar K, Hoeft S, Oremland R, Saltikov CW. 2010. Identification of a novel arsenite oxidase gene, arxA, in the haloalkaliphilic, arsenite-oxidizing bac terium Alkalilimnicola ehrlichii strain MLHE-1. J Bacteriol 192:3755–3762. https://doi.org/10.1128/JB.00244-10.

4. Qin J, Rosen BP, Zhang Y, Wang G, Franke S, Rensing C. 2006. Arsenic detoxi fication and evolution of trimethylarsine gas by a microbial arsenite S-adeno sylmethionine methyltransferase. Proc Natl Acad Sci U S A 103:2075–2080. https://doi.org/10.1073/pnas.0506836103.

5. Chen J, Yoshinaga M, Rosen BP. 2019. The antibiotic action of methylar senite is an emergent property of microbial communities. Mol Microbiol 111:487–494. https://doi.org/10.1111/mmi.14169.

6. Devalla S, Feldmann J. 2003. Determination of lipid-soluble arsenic species in seaweed-eating sheep from Orkney. Appl Organometal Chem 17:906–912. https://doi.org/10.1002/aoc.550.

7. Amayo KO, Petursdottir A, Newcombe C, Gunnlaugsdottir H, Raab A, Krupp EM, Feldmann JR. 2011. Identification and quantification of arseno lipids using reversed-phase HPLC coupled simultaneously to high-resolution ICPMS and high-resolution electrospray MS without species-specific standards. Anal Chem 83:3589–3595. https://doi.org/10.1021/ac2005873.

8. Kuramata M, Sakakibara F, Kataoka R, Yamazaki K, Baba K, Ishizaka M, Hiradate S, Kamo T, Ishikawa S. 2016. Arsinothricin, a novel organoarsenic species produced by a rice rhizosphere bacterium. Environ Chem 13:723–731. https://doi .org/10.1071/EN14247.

9. Nadar VS, Chen J, Dheeman DS, Galván AE, Yoshinaga-Sakurai K, Kandavelu P, Sankaran B, Kuramata M, Ishikawa S, Rosen BP, Yoshinaga M. 2019. Arsino thricin, an arsenic-containing non-proteinogenic amino acid analog of gluta mate, is a broad-spectrum antibiotic. Commun Biol 2:131. https://doi.org/10 .1038/s42003-019-0365-y.

10. Gygli SM, Borrell S, Trauner A, Gagneux S. 2017. Antimicrobial resistance in Mycobacterium tuberculosis: mechanistic and evolutionary perspectives. FEMS Microbiol Rev 41:354–373. https://doi.org/10.1093/femsre/fux011.

11. Berlicki Ł, Obojska A, Forlani G, Kafarski P. 2005. Design, synthesis, and activity of analogues of phosphinothricin as inhibitors of glutamine synthe tase. J Med Chem 48:6340–6349. https://doi.org/10.1021/jm050474e.

12. Schinko E, Schad K, Eys S, Keller U, Wohlleben W. 2009. Phosphinothricin-tri peptide biosynthesis: an original version of bacterial secondary metabolism?Phytochemistry 70:1787–1800. https://doi.org/10.1016/j.phytochem.2009.09 .002.

13. Blodgett JA, Zhang JK, Yu X, Metcalf WW. 2016. Conserved biosynthetic pathways for phosalacine, bialaphos and newly discovered phosphonic acid natural products. J Antibiot (Tokyo) 69:15–25. https://doi.org/10.1038/ja .2015.77.

14. Wang SC, Frey PA. 2007. S-adenosylmethionine as an oxidant: the radical SAM superfamily. Trends Biochem Sci 32:101–110. https://doi.org/10.1016/j .tibs.2007.01.002.

15. Roach PL. 2011. Radicals from S-adenosylmethionine and their application to biosynthesis. Curr Opin Chem Biol 15:267–275. https://doi.org/10 .1016/j.cbpa.2010.11.015.

16. Chen J, Rosen BP. 2020. The arsenic methylation cycle: how microbial communities adapted methylarsenicals for use as weapons in the con tinuing war for dominance. Front Environ Sci 8. https://doi.org/10.3389/ fenvs.2020.00043.

17. Wu J, Rosen BP. 1991. The ArsR protein is a trans-acting regulatory pro tein. Mol Microbiol 5:1331–1336. https://doi.org/10.1111/j.1365-2958 .1991.tb00779.x.

18. Willsky GR, Malamy MH. 1980. Characterization of two genetically separa ble inorganic phosphate transport systems in Escherichia coli. J Bacteriol 144:356–365. https://doi.org/10.1128/jb.144.1.356-365.1980.

19. Klemm P, Tong S, Nielsen H, Conway T. 1996. The gntP gene of Escherichia coli is involved in gluconate uptake. J Bacteriol 178:61–67. https://doi.org/ 10.1128/jb.178.1.61-67.1996.

20. Dheeman DS, Packianathan C, Pillai JK, Rosen BP. 2014. Pathway of human AS3MT arsenic methylation. Chem Res Toxicol 27:1979–1989. https://doi .org/10.1021/tx500313k.

21. Marapakala K, Packianathan C, Ajees AA, Dheeman DS, Sankaran B, Kandavelu P, Rosen BP. 2015. A disulfide-bond cascade mechanism for As (III)

S-adenosylmethionine methyltransferase. Acta Crystallogr D Biol Crys tallogr 71:505–515. https://doi.org/10.1107/S1399004714027552.

22. Xue XM, Ye J, Raber G, Rosen BP, Francesconi K, Xiong C, Zhu Z, Rensing C, Zhu YG. 2019. Identification of steps in the pathway of arsenosugar biosynthesis. Environ Sci Technol 53:634–641. https://doi.org/10.1021/acs .est.8b04389.

23. Carlin A, Shi W, Dey S, Rosen BP. 1995. The ars operon of Escherichia coli con fers arsenical and antimonial resistance. J Bacteriol 177:981–986. https://doi .org/10.1128/jb.177.4.981-986.1995.

24. Rosen BP, Tsuchiya T. 1979. Preparation of everted membrane vesicles from Escherichia coli for the measurement of calcium transport. Methods Enzymol 56:233–241. https://doi.org/10.1016/0076-6879(79)56026-1.

25. Chen J, Madegowda M, Bhattacharjee H, Rosen BP. 2015. ArsP: a methylar senite efflux permease. Mol Microbiol 98:625–635. https://doi.org/10.1111/ mmi.13145.

26. Garbinski LD, Rosen BP, Chen J. 2019. Pathways of arsenic uptake and efflux. Environ Int 126:585–597. https://doi.org/10.1016/j.envint.2019.02 .058.

27. Zhang Y, Zhu X, Torelli AT, Lee M, Dzikovski B, Koralewski RM, Wang E, Freed J, Krebs C, Ealick SE, Lin H. 2010. Diphthamide biosynthesis requires an or ganic radical generated by an iron-sulphur enzyme. Nature 465:891–896. https://doi.org/10.1038/nature09138.

28. Broderick JB, Duffus BR, Duschene KS, Shepard EM. 2014. Radical S-adeno sylmethionine enzymes. Chem Rev 114:4229–4317. https://doi.org/10 .1021/cr4004709.

29. Li X-Z, Plésiat P, Nikaido H. 2015. The challenge of efflux-mediated antibiotic resistance in Gram-negative bacteria. Clin Microbiol Rev 28:337–418. https://doi.org/10.1128/CMR.00117-14.

30. Sambrook J, Fritsch EF, Maniatis T. 1989. Molecular cloning, a laboratory manual, 2nd ed. Cold Spring Harbor Laboratory, Cold Spring Harbor, NY.

31. Maki T, Hasegawa H, Watarai H, Ueda K. 2004. Classification for dimethylarsenate-decomposing bacteria using a restrict fragment length poly morphism analysis of 16S rRNA genes. Anal Sci 20:61–68. https://doi.org/ 10.2116/analsci.20.61.

32. Bankevich A, Nurk S, Antipov D, Gurevich AA, Dvorkin M, Kulikov AS, Lesin VM, Nikolenko SI, Pham S, Prjibelski AD, Pyshkin AV, Sirotkin AV, Vyahhi N, Tesler G, Alekseyev MA, Pevzner PA. 2012. SPAdes: a new genome assembly

algorithm and its applications to single-cell sequenc ing. J Comput Biol 19:455–477. https://doi.org/10.1089/cmb.2012.0021.

33. Simpson JT, Wong K, Jackman SD, Schein JE, Jones SJM, Birol I. 2009. ABySS: a parallel assembler for short read sequence data. Genome Res 19:1117–1123. https://doi.org/10.1101/gr.089532.108.

34. Utturkar SM, Klingeman DM, Land ML, Schadt CW, Doktycz MJ, Pelletier DA, Brown SD. 2014. Evaluation and validation of de novo and hybrid as sembly techniques to derive high-quality genome sequences. Bioinfor matics 30:2709–2716. https://doi.org/10.1093/bioinformatics/btu391.

35. Tatusova T, DiCuccio M, Badretdin A, Chetvernin V, Nawrocki EP, Zaslavsky L, Lomsadze A, Pruitt KD, Borodovsky M, Ostell J. 2016. NCBI prokaryotic ge nome annotation pipeline. Nucleic Acids Res 44:6614–6624. https://doi.org/10.1093/nar/gkw569.

36. Camacho C, Coulouris G, Avagyan V, Ma N, Papadopoulos J, Bealer K, Madden TL. 2009. BLAST1: architecture and applications. BMC Bioinfor matics 10:421. https://doi.org/10.1186/1471-2105-10-421.

37. Li L, Stoeckert CJ, Roos DS. 2003. OrthoMCL: identification of ortholog groups for eukaryotic genomes. Genome Res 13:2178–2189. https://doi.org/10.1101/gr.1224503.

38. Villadangos AF, Fu HL, Gil JA, Messens J, Rosen BP, Mateos LM. 2012. Efflux permease CgAcr3-1 of Corynebacterium glutamicum is an arsenite specific antiporter. J Biol Chem 287:723–735. https://doi.org/10.1074/jbc .M111.263335.

39. Notredame C, Higgins DG, Heringa J. 2000. T-Coffee: a novel method for fast and accurate multiple sequence alignment. J Mol Biol 302:205–217. https://doi.org/10.1006/jmbi.2000.4042.

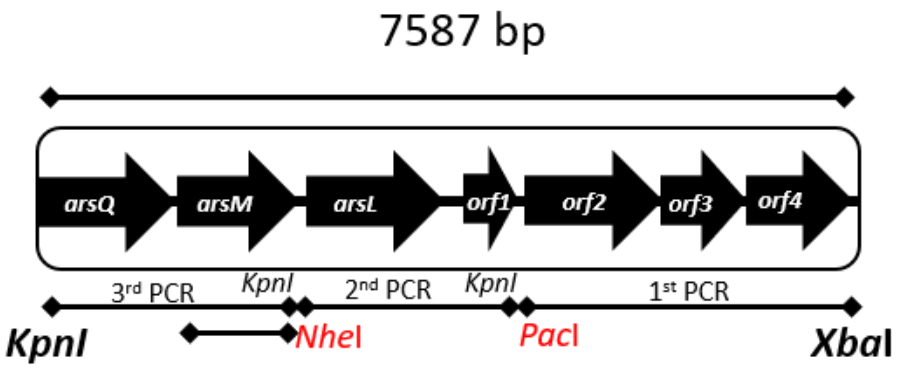

Figure S1. Diagram of the sequential cloning of the AST BGC genes. DNA fragments of no more than 3.2 kb were sequentially amplified by PCR with the indicated restriction sites. The PCR products were inserted into plasmid pUC118. The first amplified PCR fragment included *orf2-4* cloned between the *Kpn*I and *Xba*I sites. In the second step *arsL* and *orf1* were amplified and cloned between the *Kpn*I and *Pac*I sites, resulting in plasmid pUC*arsL-orf1-4*. For the construction of pUC*arsML-orf1-4* or pUC*arsQML-orf1-4*, a third fragment including *arsM* or *arsQ-arsM* genes, respectively, was cloned between the *Kpn*I and *Nhe*I sites.

Figure S2. Genome sequencing of *B. gladioli* GSRB05
After quality trimming and filtering, >64% of reads were retained that represent >160X genome coverage for *B. gladioli* GSRB05. Optimal genome assembly obtained through SPAdes was comprised of 171 contigs in 9.2 MB with N50 contigs size 132 KB and average contig length 54 KB.

Sample_ID	file_name	Total Reads	Read Counts after quality filtering	Percentage of Reads after quality filtering
Burkholderia GSRB05	Bgladio_1.fastq	7,879,185	5,083,214	64.51%
	Bgladio_2.fastq	7,879,185	5,083,214	64.51%

Tool	KMER	Contigs	Minimum Conting Length	Maximum Conting Length	Average Contig Length	Contig N50	Assembly Size
SPAdes version 3.13.0	21,33,55,77,99,127	171	512	445,577	54,067	132,483	9,245,390
AByss version 2.1.5	31	522	507	149,544	17,564	39,307	9,168,461
	41	387	501	196,023	23,919	52,853	9,256,639
	51	364	509	198,283	25,481	53,516	9,275,193
	61	343	508	196,909	27,148	57,530	9,311,829
	71	343	505	198,297	27,150	58,494	9,312,489
	81	350	500	216,645	26,806	51,115	9,381,985
	91	408	504	150,616	22,918	45,268	9,350,690
	101	584	500	95,090	15,859	30,938	9,261,652
	111	1,316	500	62,372	6,935	14,061	9,126,425
	121	3,793	500	33,284	2,147	3,484	8,144,987

Figure S3. Multiple alignment of BgArsM orthologs (accession numbers in parentheses). The protein sequence of BgArsM identified from *B. gladioli* GSBR05 (BurGSRB05_34905) is compared with putative orthologs from *Burkholderia oklahomensis* (WP_010121994.1), *Burkholderia cepacia* (WP_059666519.1), *Pseudomonas aeruginosa* (WP_174517314.1), *Pseudomonas fluorescens* (WP_064119070.1), *Pseudomonas amygdali* (WP_054068373.1), *Actibacterium* sp. (WP_204414387.1) and *Rhodobacter* sp. (PCJ07719.1). The four conserved cysteines are indicated (*). Identities are shaded in black, and conservative replacements are shaded in grey. The multiple alignment was calculated with CLUSTAL W.

.

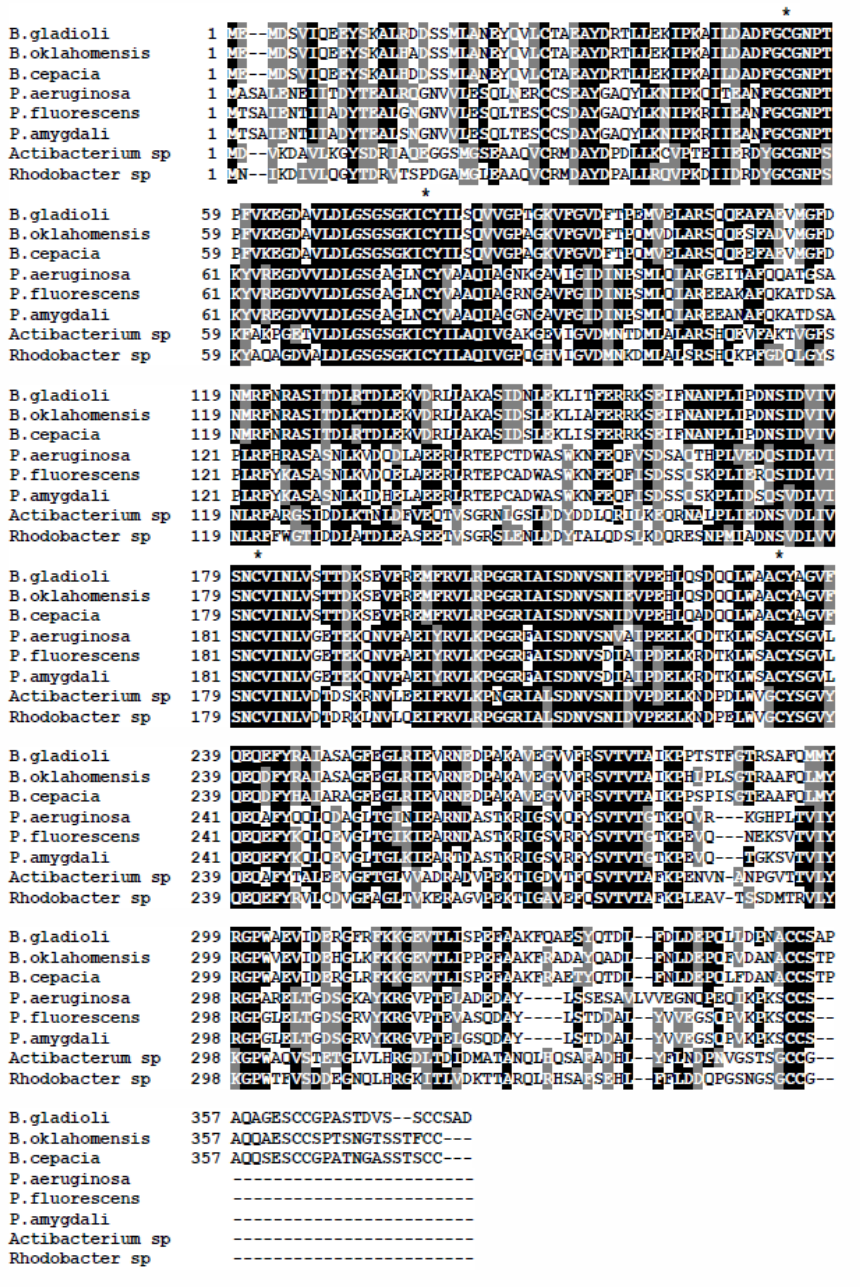

Figure S4. Multiple alignment of BgArsL orthologs (accession numbers in parentheses). The protein sequence of BgArsL identified from *B. gladioli* GSBR05 (BurGSRB05_34900) is compared with putattive orthologs from *Burkholderia oklahomensis* (WP_038802160.1), *Burkholderia cepacia* (WP_059666518.1), *Pseudomonas aeruginosa* (WP_174517312.1), *Pseudomonas fluorescens* (WP_064119068.1), *Pseudomonas amygdali* (WP_054068372.1), *Actibacterium* sp. (WP_204414396.1) and *Rhodobacter* sp. (PCJ07718.1). Identities are shaded in black, and conservative replacements are shaded in grey. The cysteines of the conserved CX_3CX_2C motif are identified (*). The multiple alignment was calculated with CLUSTAL W.

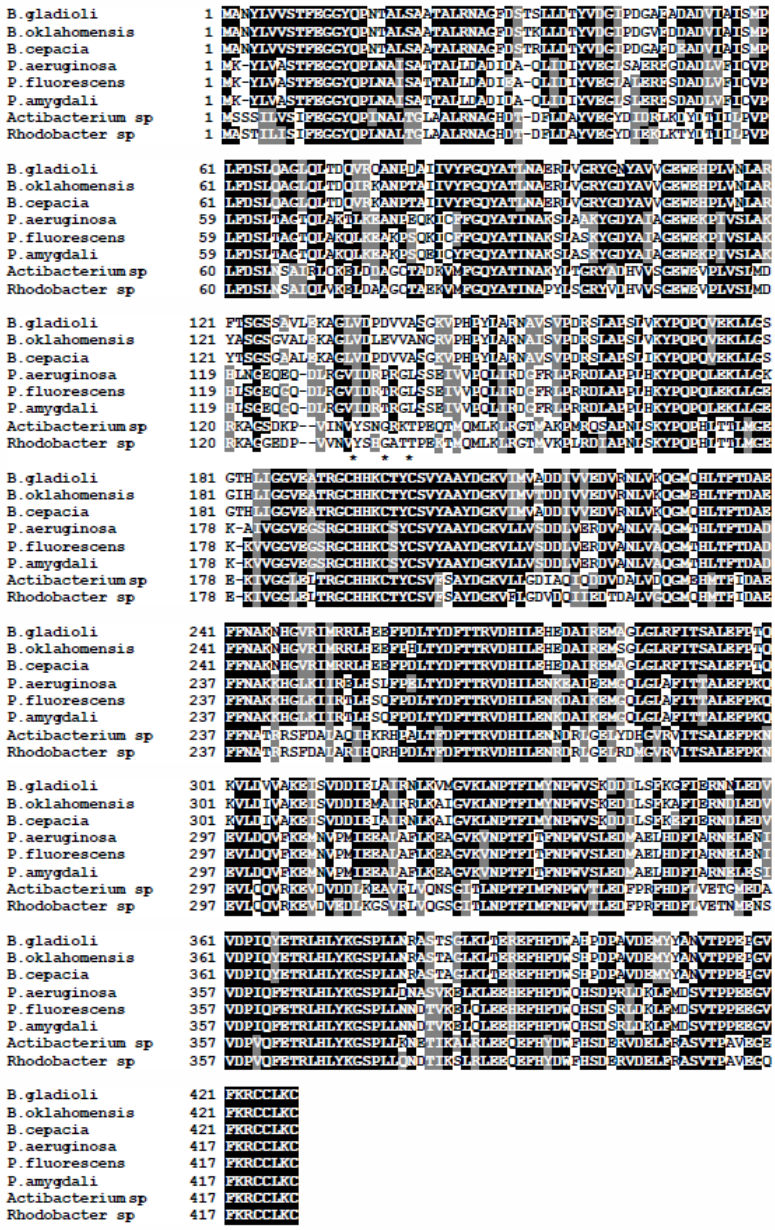

Figure S5. Multiple alignment of BgArsQ orthologs (accession numbers in parentheses). The protein sequence of BgArsQ identified from *B. gladioli* GSBR05 (BurGSRB05_34910) is compared with putative orthologs from *Burkholderia oklahomensis* (WP_010121992.1), *Burkholderia cepacia* (WP_081062335.1), *Pseudomonas aeruginosa* (WP_174517311.1), *Pseudomonas fluorescens* (WP_064119067.1), *Pseudomonas amygdali* (WP_054068371.1), *Actibacterium* sp. (WP_204414385.1) and *Rhodobacter* sp. (PCJ07720.1). Identities are shaded in black, and conservative replacements are shaded in grey. The multiple alignment was calculated with CLUSTAL W.

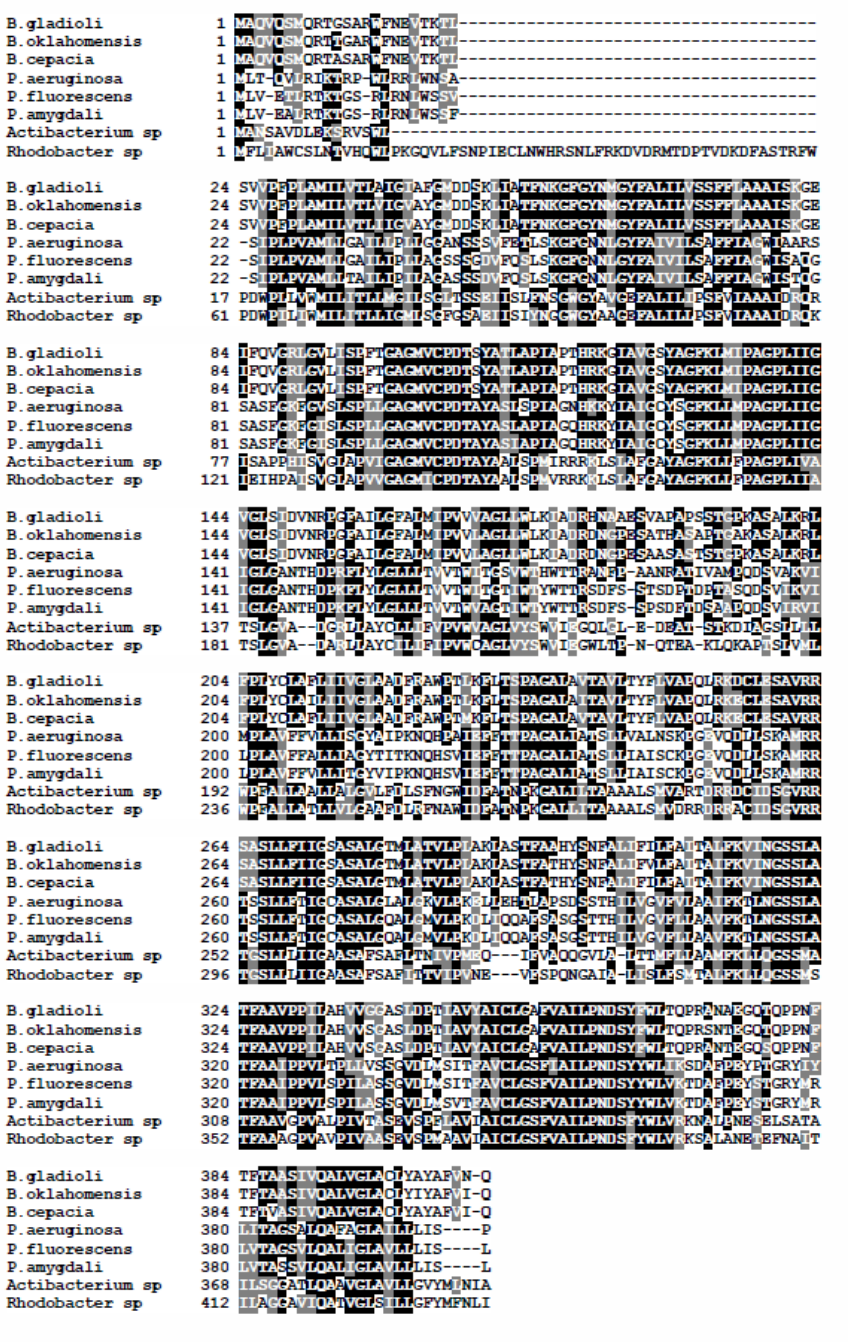

Table S1. Bacterial strains and plasmids

	Genotype/Description	References
Strain		
B. gladioli GSRB05	Soil isolated. AST producer	
E. coli Top10	F$^-$ *mcr*A Δ(*mrr-hsd*RMS-*mcr*BC) φ80*lac*ZΔM15 Δ*lac*X74 *rec*A1 *ara*D139 Δ(*ara-leu*)7697 *gal*U *gal*K λ$^-$ *rps*L(Str^R) *end*A1 *nup*G. Sm^r	Invitrogen
E. coli BL21 (DE3)	F$^-$ *omp*T *hsd*S$_B$ (r$_B^-$, m$_B^-$) *gal dcm* (DE3)	Novagen
E. coli AW3110	*ars*::*cam* F- IN(*rrnD-rrnE*). Cm^r	(1)
Plasmid		
pUC118	*E. coli* cloning and expression using *lac* promoter. Ap^r	Takara Bio USA
pUC*arsL-orf1-4*	PCR amplified *arsL* and orf1-4 genes inserted into the *Kpn*I and *Xba*I sites of pUC118.	This study
pUC*arsML-orf1-4*	PCR amplified *arsM-arsL* and orf1-4 genes inserted into the *Kpn*I and *Xba*I sites of pUC118	This study
pUC*arsQML-orf1-4*	PCR amplified *arsQ-arsM-arsL* and orf1-4 genes inserted into the *Kpn*I and *Xba*I sites of pUC118	This study
pETDuet-1	*E. coli* expression vector. Ap^r	Novagen
pETDuet-1*arsL*	*arsM* gene cloned in MCSI	This study
pETDuet-1*arsML*	*arsM* gene cloned in MCSI and *arsL* gene cloned in MCSII	This study
pTrcHisA	*E. coli* expression vector. Ap^r	Thermo Fisher Scientific Inc
pTrcHisA*arsQ*	*arsQ* genes inserted into the *Nco*I and *Sal*I sites of pTrcHisA.	This study

Abbreviations: Sm^r, streptomycin resistant. Cm^r, chloramphenicol resistant. Ap^r, ampicillin resistant.

1. Carlin, A.; Shi, W.; Dey, S.; Rosen, B. P., The *ars* operon of *Escherichia coli* confers arsenical and antimonial resistance. J. Bacteriol. 1995, 177, (4), 981-6.

Table S2. Primers

Cloning primers	Sequence
Bg_ars_XbaI_Rv	5’ ACCACCACCTCTAGATGGGGCATAGCGATAG 3’
Bg_ars_KpnI PacI_Fw	5’ GGTGGTGGTACCTTAATTAAGTGATAGCACGTCCGTCATTG 3’
Bg_ars_PacI_Rv	5’ ACCACCTTAATTAAGTGGCGCATGCCGGAGG 3’
Bg_ars_KpnI_NheI _Fw	5’ GGTGGTGGTACCGCTAGCTGAATAGATCAACAGACGACTTCAAG 3’
Bg_ars_NheI_Rv	5’ ACCACCGCTAGCATCAGCCGAGCAGCAG 3’
Bg_arsL_KpnI_Fw	5’ GGTGGTGGTACCTGGCCCAGGTTCAATC 3’
Bg_arsM_KpnI_Fw	5’ GGTGGTGGTACCAATGGAAATGGATTCTGTTATTC 3’

Red: unique site introduced for the sequentially cloning

Site-mutant primers	
arsL-G31T-Fwd	5’ CTGATATCCACCTTAAAAAGTGGAAACGACTAGATAGTTGG 3’
arsL-G31T-Rev	5’ CCAACTATCTAGTCGTTTCCACTTTTTAAGGTGGATATCAG 3’
orf1-C55T-Fwd	5’ CATCGAGCATTTCCTACACGGGGTCTATCGC 3’
orf1-C55T-Rev	5’ GCGATAGACCCCGTGTAGGAAATGCTCGATG 3’
orf2 -G28T-Fwd	5’ GCGACCGGTTATTCCTTGGCGAGTGCTGC 3’
orf2 -G28T-Rev	5’ GCAGCACTCGCCAAGGAATAACCGGTCGC 3’
orf3-G31T-Fwd	5’ CGGTATAGAAGAGCTAAACCCCGTCGTTAGTTCT 3’
orf3-G31T-Rev	5’ AGAACTAACGACGGGGTTTAGCTCTTCTATACCG 3’
orf4-C28T-Fwd	5’ CGCGTCGGGCTAGGCGCTGCTGA 3’
orf4-C28T-Rev	5’ TCAGCAGCGCCTAGCCCGACGCG 3’

Primers used in *ars* operon identification by RT-qPCR	
1F	5’ ATGGCCCAGGTTCAATCGATG 3’
1R	5’ CCTGAATAACAGAATCCATTTCC 3’
2F	5’ ATGGAAATGGATTCTGTTATTCAG 3’
2R	5’ GTGGAAACGACTAGATAGTTG 3’
3F	5’ ATGGCCAACTATCTAGTCGTTTC 3’
3R	5’ TCAGCATTTGAGGCAGCATCG 3’
4R	5’ GAAAACGCCGATGCCGTAC 3’
5R	5’ AGAGTGAAATCGTCATCGATTG 3’
27F-16S	5’ AGAGTTTGATCTGGCTCAG 3’
1492R-16S	5’ GGTTACCTTGTTACGACTT 3’

CHAPTER 3: THE ARSQ PERMEASE AND TRANSPORT OF THE ANTIBIOTIC ARSINOTHRICIN

3.1 Abstract

The pentavalent organoarsenical arsinothricin (AST) is a natural product synthesized by the rhizosphere bacterium *Burkholderia gladioli* GSRB05. AST is a broad-spectrum antibiotic effective against human pathogens such as carbapenem-resistant *Enterobacter cloacae.* It is a non-proteogenic amino acid and glutamate mimetic that inhibits bacterial glutamine synthetase. The AST biosynthetic pathway is composed of a three-gene cluster, *arsQML.* ArsL catalyzes synthesis of reduced trivalent hydroxyarsinothricin (R-AST-OH), which is methylated by ArsM to the reduced trivalent form of AST (R-AST). In the culture medium of *B. gladioli* both trivalent species appear as corresponding pentavalent arsenicals, likely due to oxidation in air. ArsQ is an efflux permease that is proposed to transport AST or related species out of the cells, but the chemical nature of the actual transport substrate is unclear. In this study *B. gladioli arsQ* was expressed in *Escherichia coli* and shown to confer resistance to AST and its derivatives. Cells of *E. coli* accumulate R-AST, and exponentially-growing cells expressing *arsQ* take up less R-AST. The cells exhibit little transport of their pentavalent forms. Transport was independent of cellular energy and appears to be equilibrative. A homology model of ArsQ suggests that Ser320 is in the substrate binding site. A S320A mutant exhibits reduced R-AST-OH transport, suggesting that it plays a role in ArsQ function. The ArsQ permease is proposed

to be an energy-independent uniporter responsible for downhill transport of the trivalent form of AST out of cells, which is oxidized extracellularly to the active form of the antibiotic.

Key words: Arsinothricin, antibiotic, resistance, efflux permease

3.2 Introduction

Arsenic is the most prevalent environmental toxic substance. It comes primarily from geochemical sources, with lower amounts contributed by human activities (Zhu *et al.*, 2014). Arsenic enters our food supply from water, air and soil (Naujokas *et al.*, 2013). It has no nutritional value and is both a carcinogen and a toxin. In fact, arsenic has been called the King of Poisons (Paul *et al.*, 2022). Soon after the origin of life, microbes adapted to the presence of environmental arsenic through the evolution of pathways for its detoxification (Liu *et al.*, 2013), with resistance genes organized in *ars* operons (Yang *et al.*, 2012). Even more striking is the ability of microbes to utilize this toxic metalloid to gain a competitive advantage over other microbes. Early in evolution, bacteria evolved the *arsM* gene encoding the ArsM As(III) *S*-adenosine methionine (SAM) methyltransferase, which catalyzes methylation of inorganic arsenic to form highly toxic methylarsenite (MAs(III) (Chen *et al.*, 2019), which has antibiotic properties in extant microbial communities (Yoshinaga *et al.*, 2011).

A more recent example of the adaptation of arsenic as a weapon in microbial warfare is synthesis of the natural product arsinothricin (2-amino-4-

(hydroxymethylarsinoyl)butanoic acid or AST) by the soil bacterium *Burkholderia gladioli* GSRB05. AST has broad-spectrum antibiotic action and is effective against both gram-positive and gram-negative bacteria, including some of the most dangerous human pathogens (Nadar *et al.*, 2019). AST is a non-proteogenic amino acid with a chemical structure similar to that of glutamate, where the γ-carboxyl group of glutamate is replaced with a methylarsenate moiety through a C-As bond. AST is unusual in that the arsenic atom has a pentavalent oxidation state. Pentavalent arsenicals in general have relatively low toxicity, and yet AST is as toxic as trivalent methylarsenite, one of the most toxic organoarsenicals. This is because the predicted mechanism of action of pentavalent AST is through inhibition of the enzyme glutamine synthetase, an essential enzyme in most bacteria. This is in contrast with trivalent arsenicals that disrupt metabolism by reaction with thiol groups in proteins and formation of complexes with small molecular weight thiols such as glutathione (Shen *et al.*, 2013).

Recently the AST biosynthetic gene cluster of *B. gladioli* GSRB05 was shown to consist of three genes, *arsQML,* that are transcriptionally controlled by the product of the *arsR* gene*.* ArsL catalyzes the formation of R-AST-OH, the reduced trivalent form of hydroxyarsinothricin (AST-OH), the unmethylated precursor of AST, from inorganic As(III) and the 3-amino-3-carboxypropyl (ACP) group of *S*-adenosylmethionine (SAM) (Fig. S1). R-AST-OH is methylated to reduced trivalent AST (R-AST) by ArsM, an As(III) SAM methyltransferase. ArsQ is proposed to be an efflux permease that extrudes AST-related species from the cells. Efflux is a

common final step in bacteria that produce antibiotics because the transporter puts the antibiotic into the medium, where it kills susceptible bacteria and simultaneously protects the producer from its own antimicrobial agent. In this study we characterized ArsQ to identify its substrate(s) and determine its transport properties. We propose that the physiological substrate of ArsQ is the reduced trivalent form of the antibiotic, R-AST that is oxidized in air to the pentavalent form, AST. *B. gladioli* GSRB05 *arsQ* was cloned and heterologously expressed in the As(III)-hypersensitive strain *E. coli* AW3110, in which the chromosomal *arsRBC* operon had been deleted (Carlin *et al.*, 1995). ArsQ confers resistance to AST and R-AST. Cells of *E. coli* are not very sensitive to AST-OH or R-AST-OH, but ArsQ increases resistance. Cells of *E. coli* expressing *arsQ* selectively transport R-AST-OH and R-AST. Transport is independent of cellular energy and appears to be equilibrative. Examination of a homology model of ArsQ based on the structure of the divalent anion sodium symporter (DASS) family member VcINDY (PDB ID: 5ULD) suggested that Ser320 contributes to the substrate binding site. Cells of a S320A mutant exhibited reduced uptake of R-AST-OH, consistent with a role in ArsQ function. We propose that the ArsQ permease is an energy-independent bidirectional uniporter that is responsible for downhill transport of the trivalent form of AST in AST-producing *B. gladioli* GSRB05. R-AST is oxidized extracellularly to the active pentavalent form of the antibiotic.

3.3 Results

ArsQ confers resistance to a broad range of arsenicals. Four families of organoarsenical efflux permeases, ArsJ (Chen *et al.*, 2016), ArsK (Shi *et al.*, 2018), ArsP (Chen *et al.*, 2015) and ArsW (Chen *et al.*, 2021), have previously been identified (Fig. 1). Here we identify *B. gladioli* GSRB05 ArsQ as a member of a different group of organoarsenical permeases (Fig. 1). Previously, it appeared that ArsQ transports AST, but the true substrate was not identified in that study (Galvan *et al.*, 2021). Here the substrate specificity of ArsQ was examined by transgenic expression in the As(III)-hypersensitive strain *E. coli* AW3110 in which the chromosomal *arsRBC* operon had been deleted (Carlin *et al.*, 1995). *E. coli* cells expressing *arsQ* have been shown to confer resistance to AST (Galvan *et al.*, 2021).

In this study, we extend the resistance studies to include trivalent R-AST and R-AST-OH, as well as pentavalent AST and AST-OH (Fig. 2). In general bacteria are resistant to low concentrations of pentavalent arsenicals. The antibiotic activity of AST is due to its ability to inhibit glutamine synthetase, an essential enzyme in nitrogen metabolism (Nadar *et al.*, 2019), while trivalent arsenicals exhibit toxicity by binding to protein and small molecule thiols. Both pentavalent AST and trivalent R-AST produced substantial inhibition of growth of cells of *E. coli* AW3110 at a concentration of 10 μM, and expression of *arsQ* conferred resistance to both. In contrast, compared with AST, *E. coli* cells are relatively resistant to the AST precursor R-AST-OH and its pentavalent form AST-OH at concentrations as high

as 50 μM, but, even so, resistance is increased by *arsQ* expression. AST did not confer resistance to MAs(III) (Fig. S2). indicating that ArsQ is specific for substrates in the AST biosynthetic pathway. AST-OH does not inhibit glutamine synthetase, which may explain its lower growth inhibition. The results from heterologous expression in *E. coli* are consistent with a physiological role of ArsQ in efflux of reduced AST in the producer, *B. gladioli* GSRB05.

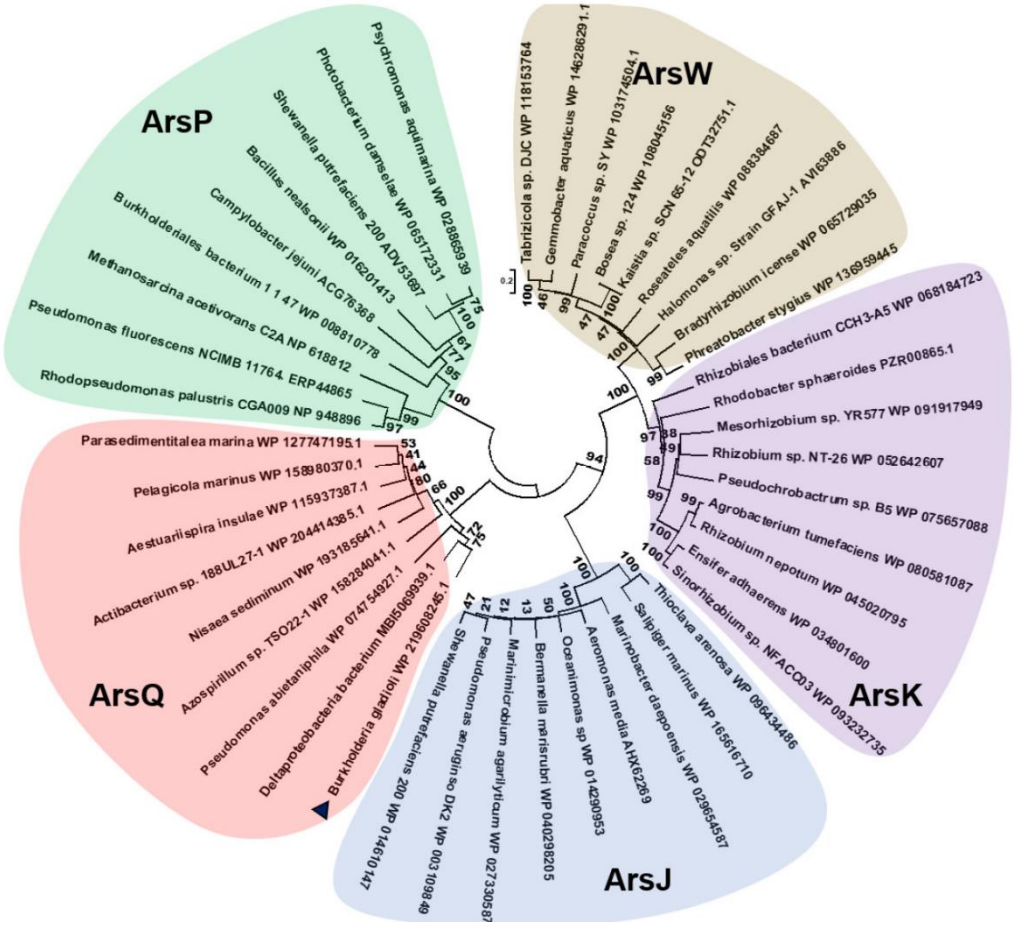

Fig. 1. Evolutionary relatedness of ArsQ to other organoarsenical efflux permeases. The five phylogenetic trees show that ArsQ forms an evolutionarily separate family from the four other known families of organoarsenical efflux permeases. *B. gladioli* ArsQ is indicated (►). ArsK and ArsP both transport and confer resistance to trivalent MAs(III). ArsW transports pentavalent MAs(V) and confers resistance to MAs(III) by coupling to the ArsV MAs(III) oxidase (Zhang *et al.*, 2022, Chen *et al.*, 2021). ArsJ is an efflux permease for 1-arseno-3-phosphoglycerate and couples to glyceraldehyde-3-phosphate dehydrogenase to confer resistance to arsenate (Chen *et al.*, 2016). NCBI accession numbers are indicated.

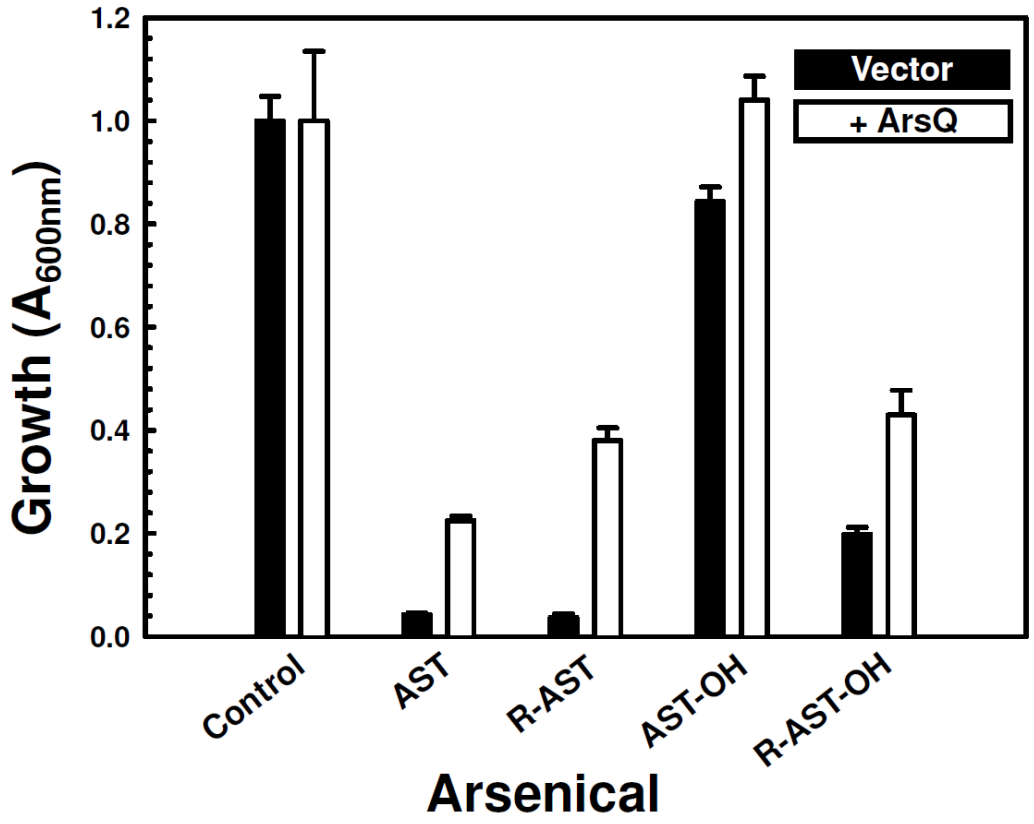

Fig. 2. ArsQ confers resistance to arsenicals in cells of *E. coli* AW3110. Resistance in cells of *E. coli* AW3110 heterologously expressing ArsQ (white fill) was compared with cells with vector plasmid pTrcHisA (black fill). Growth was assayed after overnight incubation at 37 °C in the presence of 10 µM AST, 10 µM R-AST, 50 µM AST-OH or 50 µM R-AST-OH. Growth was normalized to the density of the control cells without arsenicals. Data are the mean ± SD (n=3).

ArsQ facilitates uptake of R-AST-OH and R-AST in cells of *E. coli.* To examine the transport properties of ArsQ, uptake of AST and related organoarsenicals was examined in *E. coli* cells expressing *arsQ*. Stationary phase cells expressing *arsQ* accumulated considerably more R-AST-OH and R-AST compared to cells without the *arsQ* gene (Fig. 3). Little uptake of pentavalent AST or AST-OH was observed by *E. coli* cells with and without *arsQ* expression. Similarly, ArsQ did not catalyze uptake of MAs(III) or trivalent roxarsone (Rox(III)) (Fig. S3). The uptake data

suggests that R-AST-OH and R-AST are preferred substrates of ArsQ, with little uptake of the pentavalent species or other organoarsenicals. It was not clear how cells are sensitive to AST without substantial uptake. Resistance was assayed over 24 h or longer, while transport was assayed over a period of minutes, so enough AST may permeate over the longer time period to inhibit growth. We also considered the possibility that the endogenous *E. coli* uptake systems that take up R-AST adventitiously are not very active or well expressed in stationary phase cells, so additional uptake experiments were performed with cells in the exponential phase of growth and at a lower concentration of R-AST (10 μM). These cells accumulated approximately 3-fold more R-AST compared with stationary phase cells (Fig. S4A). Expression of the *arsQ* gene in these cells reduced accumulation (Fig. S4B), which confers resistance. As described below, these results are consistent with the function of ArsQ to facilitate bidirectional movement of R-AST.

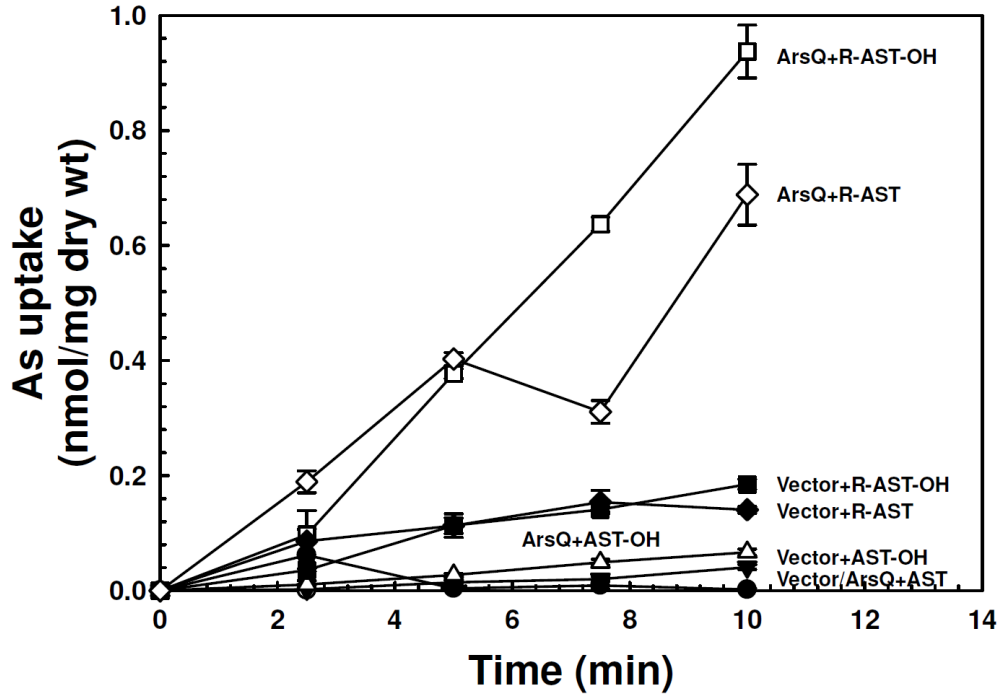

Fig. 3 ArsQ facilitates uptake of R-AST-OH and R-AST in cells of *E. coli* AW3110. Uptake of the following substrates was assayed in cells expressing ArsQ or vector plasmid pTrcHis2A: (□,■) R-AST-OH; (◊,◆), R-AST; (○,●) AST; (▼,Δ) AST-OH. All substrates were added at 25 μM, final concentration. (Note that (○) is visible only at 2.5 min and otherwise is obscured by the (●) symbols). Data are the mean ± SD (n=3).

GlpF does not transport R-AST or R-AST-OH

GlpF is a channel protein in the inner membrane of *E*. *coli* that is responsible for facilitated diffusion of polyols into the cells (Sweet *et al.*, 1990). It also serves as the major entry route of the trivalent As(III) (Yang *et al.*, 2005) and Sb(III) (Sanders *et al.*, 1997). In solution, arsenite is present as the trivalent trihydroxylated species $As(OH)_3$, which is likely recognized by GlpF as the inorganic equivalent of a polyol. Since our data suggest that ArsQ is specific for the transport of trivalent R-AST-OH and R-AST, we examined the possibility that GlpF also facilitates uptake of R-

AST or R-AST-OH. Uptake of R-AST-OH and R-AST was assayed in cells of *E*. *coli* strain OSBR1, a derivative of strain AW3110 in which *glpF* was inactivated and compared with cells of *E*. *coli* AW3110 expressing *arsQ*. Cells of both *E*. *coli* OSBR1 and AW3110 exhibited little accumulation of R-AST-OH (Fig. 4A) or R-AST (Fig. 4B) compared with cells of *E*. *coli* AW3110 expressing ArsQ. The level of accumulation of R-AST and R-AST-OH were similar in the two strains. In comparison, cells of *E*. *coli* OSBR1 accumulated little As(III) compared with cells of *E*. *coli* AW3110, as shown previously (Meng *et al.*, 2004), whether or not the cells expressed ArsQ (Fig. 4C). These results demonstrate that ArsQ catalyzes uptake of R-AST-OH or R-AST, but GlpF does not.

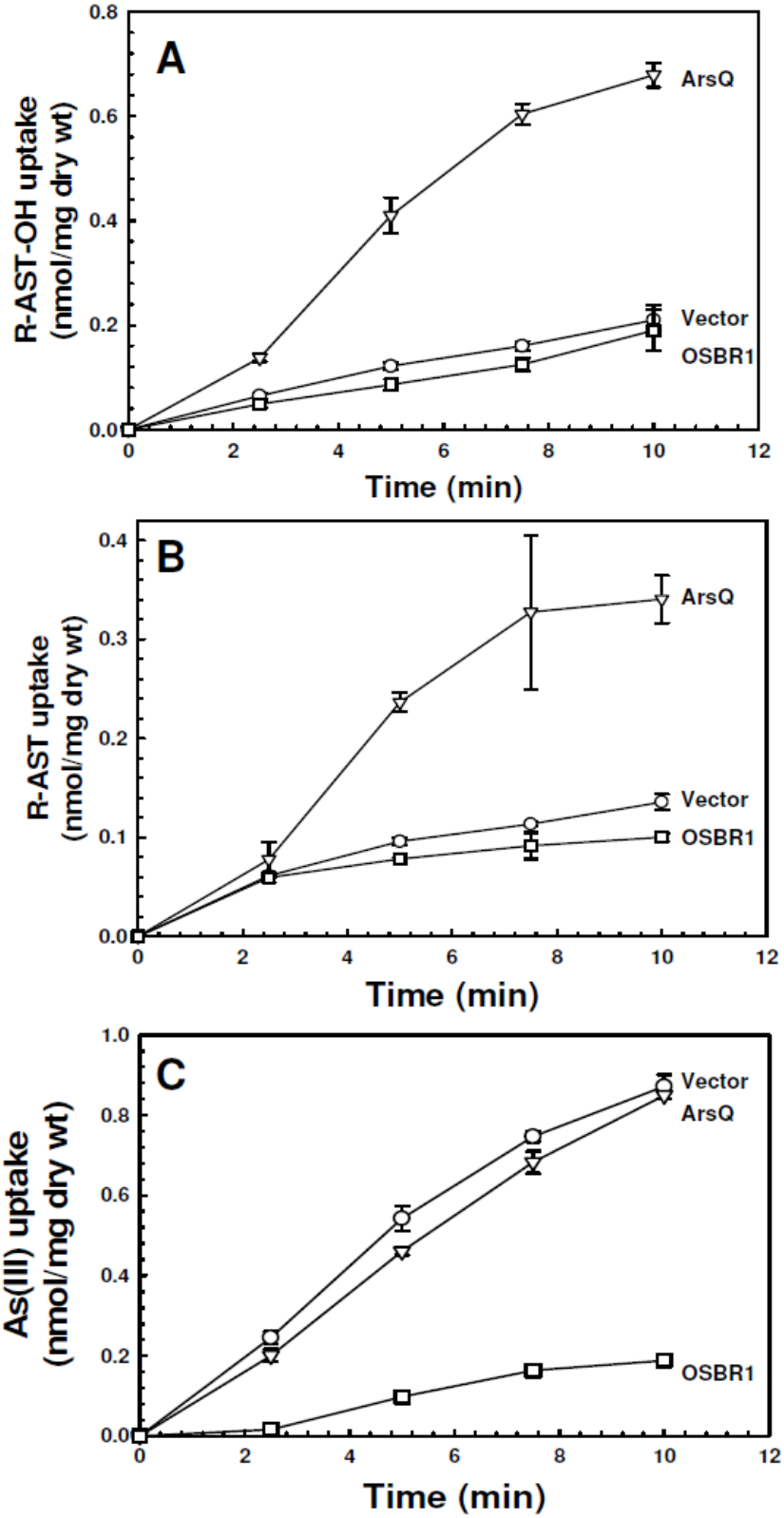
A
R-AST-OH uptake
(nmol/mg dry wt)
0.0
0.2
0.4
0.6
0.8
0
2
4
6
8
10
12
Time (min)
ArsQ
Vector
OSBR1
B
R-AST uptake
(nmol/mg dry wt)
0.0
0.1
0.2
0.3
0.4
0
2
4
6
8
10
12
Time (min)
ArsQ
Vector
OSBR1
C
As(III) uptake
(nmol/mg dry wt)
0.0
0.2
0.4
0.6
0.8
1.0
0
2
4
6
8
10
12
Time (min)
Vector
ArsQ
OSBR1

Fig. 4. GlpF does not transport R-AST or R-AST-OH. Uptake of (**A**) R-AST-OH, (**B**) R-AST, (**C**) inorganic As(III) was assayed in cells of *E. coli* AW3110 expressing ArsQ (▽) or vector plasmid pTrcHis2A (○), or in *E. coli* strain OSBR1, a derivative of strain AW3110 in which *glpF* was inactivated (□). All substrates were added at 25 μM. Data are the mean ± SD (n=3).

ArsQ is an energy-independent permease

The resistance data suggest that ArsQ catalyzes efflux of R-AST-OH or R-AST (Fig. 2), as shown in exponentially-growing cells expressing ArsQ (Fig. S4B). On the other hand, stationary phase cells expressing ArsQ catalyze uptake of R-AST-OH or R-AST (Fig. 3). Taken together, these two sets of data suggest that ArsQ catalyzes bidirectional transport of R-AST-OH or R-AST. To examine the energy dependence of ArsQ, the effect of the uncoupler carbonyl cyanide 4-(trifluoromethoxy)phenylhydrazone (FCCP) on uptake of R-AST-OH was assayed in cells of *E. coli* with or without *arsQ* (Fig. 5A). Uptake of R-AST-OH in ArsQ-expressing cells was insensitive to FCCP. As a control, ArsQ transport activity was compared with that of the known transmembrane arsenite antiporter Acr3, which is coupled to the protonmotive force (Fu *et al.*, 2009, Villadangos *et al.*, 2012). The *acr3* gene from *Alkaliphilus metalliredigens* was expressed in *E. coli* AW3110, and uptake of As(III) into cells of *E. coli* AW3110 was reduced by FCCP (Fig. 5B). Clearly Acr3 transport activity is uncoupled by FCCP, while ArsQ activity is not. These results demonstrate that ArsQ is not coupled to cellular energy and is a uniporter that facilitates bidirectional movement of R-AST-OH and R-AST.

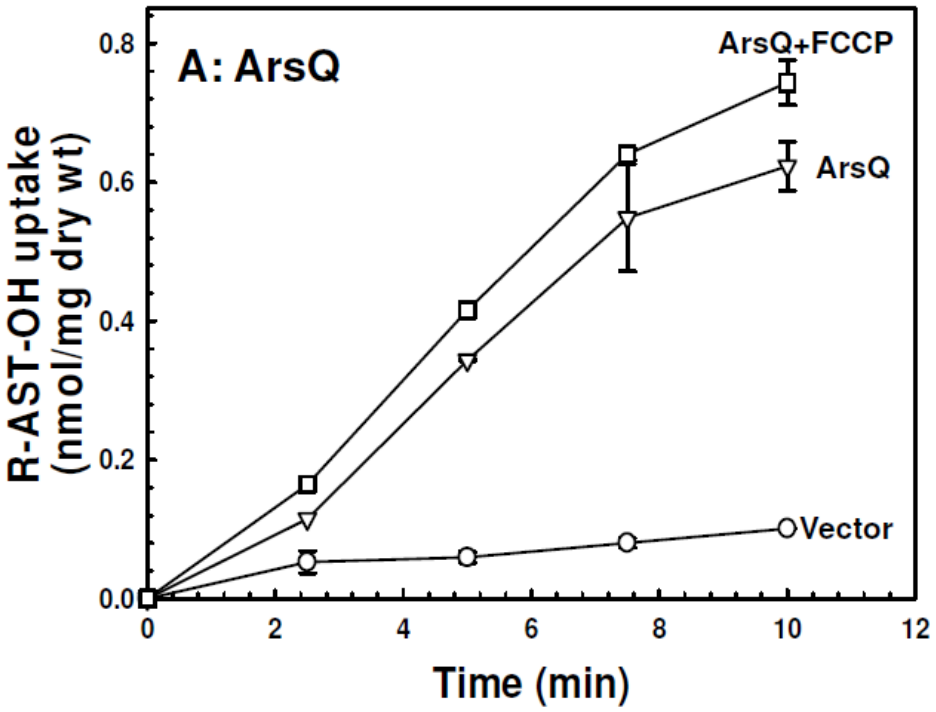
A: ArsQ
ArsQ+FCCP
ArsQ
Vector
R-AST-OH uptake
(nmol/mg dry wt)
Time (min)
0.0
0.2
0.4
0.6
0.8
0
2
4
6
8
10
12

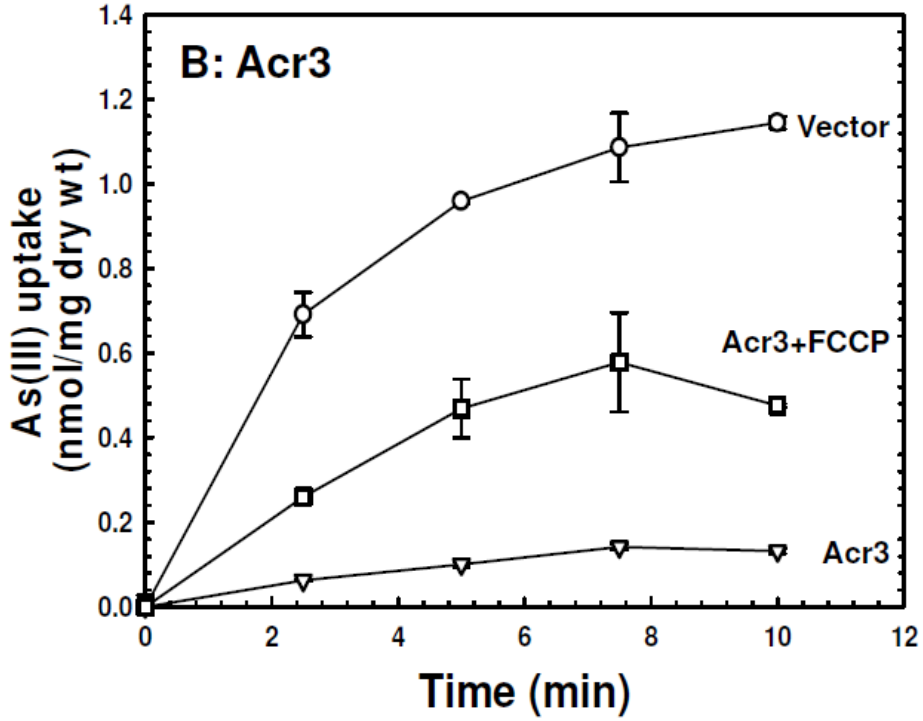
B: Acr3
Vector
Acr3+FCCP
Acr3
As(III) uptake
(nmol/mg dry wt)
Time (min)
0.0
0.2
0.4
0.6
0.8
1.0
1.2
1.4
0
2
4
6
8
10
12

Fig. 5. R-AST-OH uptake is not energy dependent. (A) Uptake of R-AST-OH was assayed in stationary phase cells of *E. coli* AW3110 expressing ArsQ in the (□) presence or (▽) absence of FCCP or (o) vector plasmid pTrcHis2A. (**B**) Uptake of inorganic As(III) was assayed in stationary phase cells of *E. coli* AW3110 expressing Acr3 in the (□).presence or (▽) absence of FCCP or (o) vector plasmid pTrcHis2A. Substrates were added at 25 μM, and FCCP was added at 10 μM, final concentrations. Data are the mean ± SD (n=3).

An ArsQ structural model

Structural information will be useful to understand the mechanism of ArsQ transport and substrate specificity. At this time, there are no structures for ArsQ family proteins, but a transmembrane topological analysis predicts that ArsQ has 11 transmembrane segments (TMs) (Fig. S5). In the NCBI database, ArsQ is annotated as a putative member of the GntP family of permeases that transport gluconate (Peekhaus *et al.*, 1997). However, no protein structural data are available for any member of the GntP family. A search for structural homologs of ArsQ identified the divalent anion sodium symporter (DASS) family of divalent anion/Na^+ symporters that transport di- and tricarboxylic acids or sulfate coupled to a Na^+ gradient (Nie *et al.*, 2017). An alignment of ArsQ with the 445-residue divalent anion/Na^+ symporter VcINDY (PDB ID: 5ULD) from *Vibrio cholerae* (Nie *et al.*, 2017), which also has 11 TMs, indicates that the two proteins have 19% identity and 31% overall similarity (Fig. 6). A homology structural model based on the VcINDY structure with bound terephthalate (Sauer *et al.*, 2020) was constructed (Fig. 7A and B). The model includes ArsQ residues 24 to 381 and shows 10 TMs (Fig. 7C). Topological connectivity indicates that TM3, 8 and 10 are discontinuous and composed of two shorter helices (Fig. S6). Predicted TM11

includes residues 283-402, but the model does not extend to those residues, so TM11 is not visible in the structural model.

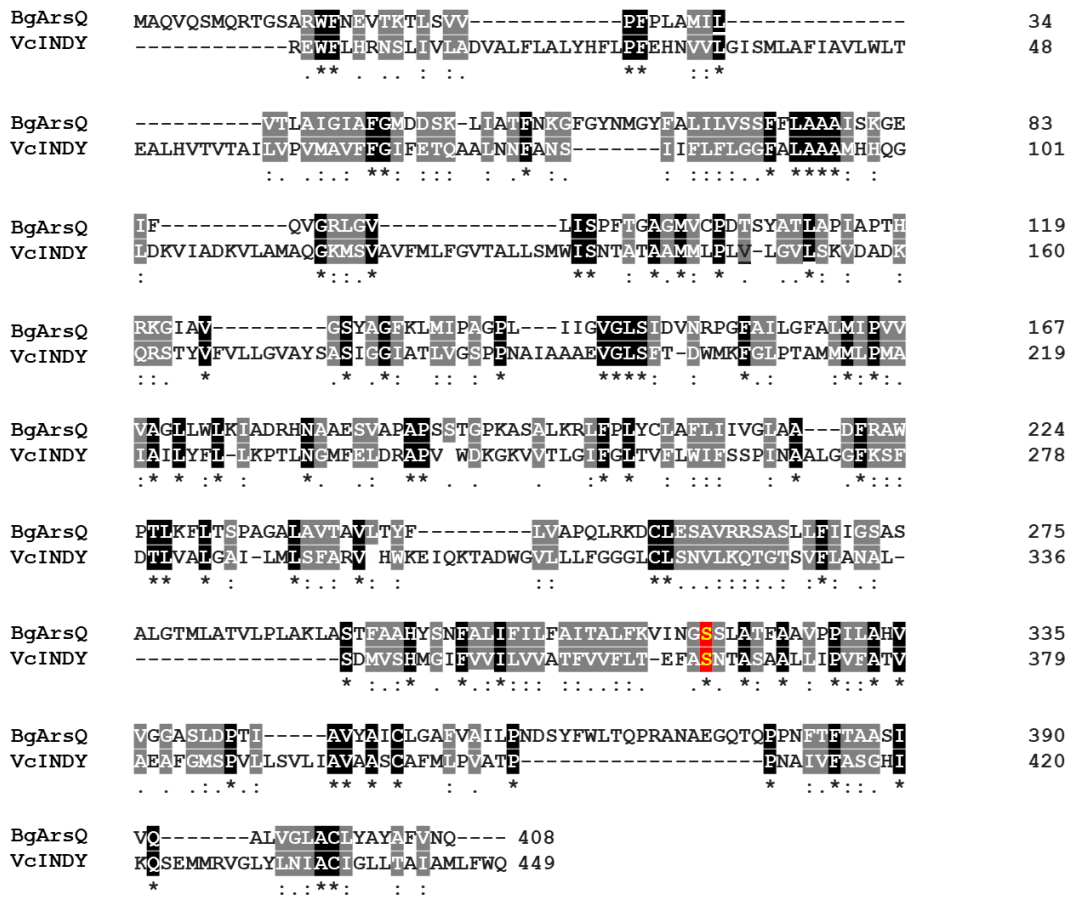

Fig. 6. Sequence alignment of ArsQ and VcINDY. ArsQ from *Burkholderia gladioli* GSRB05 (BgArsQ, accession number: WP_219608245.1) was aligned with the Na+/succinate transporter INDY from *Vibrio cholerae* (VcINDY, accession number: WP_071919799.1). Identical residues (*) are highlighted in black, and related residues (:,.) are highlighted in gray. Ser320 in BgArsQ and Ser377 in VcINDY are highlighted in red. The multiple alignment was calculated with CLUSTAL W.

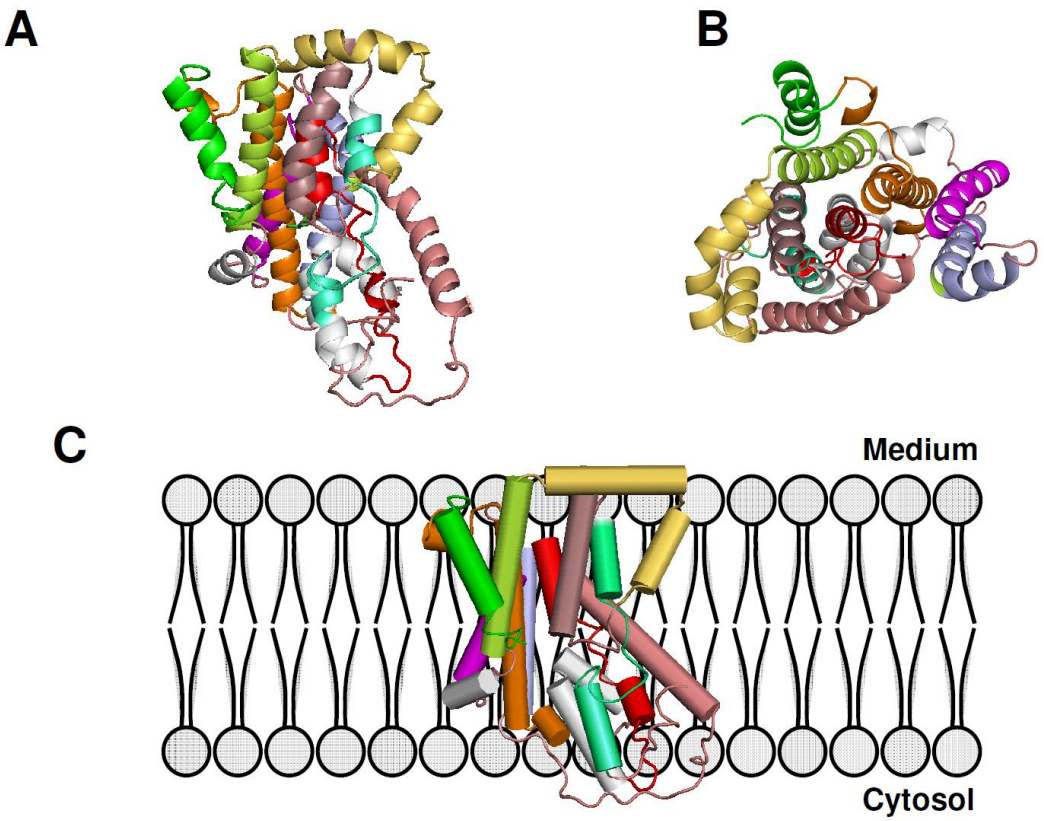

Fig. 7. ArsQ homology structural model. The predicted ArsQ structural model is shown as cartoon representation. Transmembrane segments (TMs) are shown as α-helices in different colors from the side (**A**) or top (**B**) relative to the plasma membrane. **C**, TMs are shown in cylindrical representation in a membrane to illustrate topological connectivity. Models were visualized with PyMOL.

A putative contribution of Ser320 in ArsQ catalysis

In the VcINDY structure the terephthalate binding site includes Ser377, which is considered crucial for substrate binding and transport. That residue corresponds to Ser320 in ArsQ (Fig. 6). To examine whether Ser320 plays a role in ArsQ activity, it was changed to an alanine residue. The level of expression of histagged

wild type ArsQ and the S320A protein in cells of *E. coli* AW3110 was estimated by immunoblot analysis using anti-histag antibodies (Fig. S7). The altered protein was present in the membrane in approximately the same amount and migrated with the same mobility as wild type ArsQ, indicating that the mutation did not affect expression. Expression of $arsQ_{S320A}$ led to a decrease in transport of R-AST-OH by about 80% (Fig. 8A). Interestingly, there was little change in R-AST transport activity (Fig. 8B). Serine and alanine differ only by the presence of a hydroxyl group, and R-AST-OH and R-AST differ only by the substitution of a methyl group for a hydroxyl group. We hypothesize that this apparent change in substrate specificity might be influenced by a change in polarity in the binding site, leading to loss of a hydrogen bond to R-AST-OH. This will be tested in future experiments by substitutions with other polar residues of similar size such as threonine or cysteine, or with larger amino acid residues. The structural model also allows identification of other residues in the predicted substrate binding site.

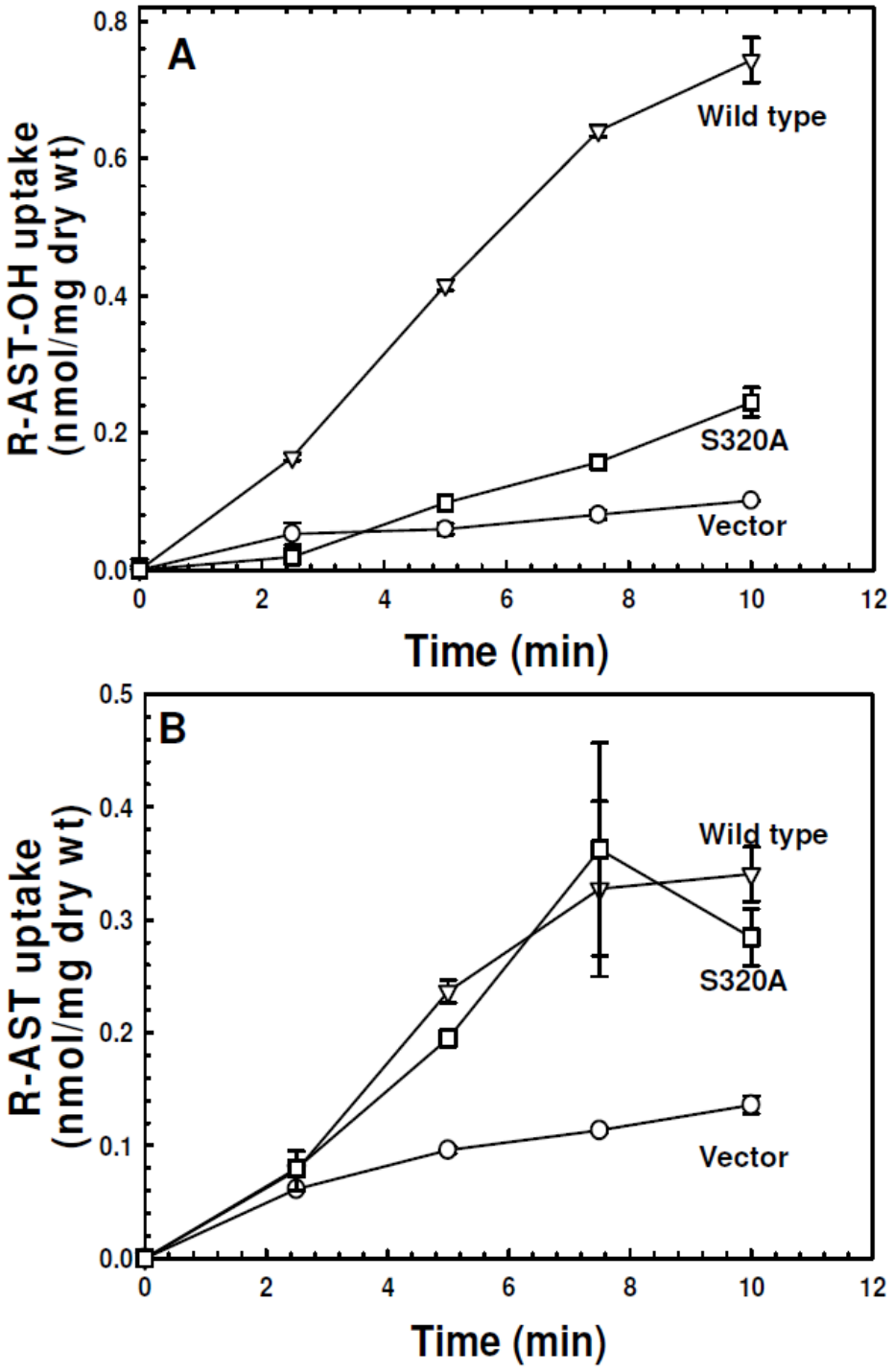

Fig. 8 Effect of S32A substitution on transport of R-AST-OH and R-AST. Uptake of (**A**) R-AST-OH or (**B**) R-AST was assayed in stationary phase cells expressing ArsQ (▽), S320A (□) or with vector plasmid pTrcHis2A (o). Substrates were added at 25 μM, final concentration. Data are the mean ± SD (n=3).

3.4 Discussion

The bacterium *Burkholderia gladioli* GSRB05 found in the rice rhizosphere produces AST, an arsenic-containing natural product (Kuramata *et al.*, 2016). AST possesses a broad-spectrum antibiotic activity and acts by the inhibition of bacterial glutamine synthetase (Nadar *et al.*, 2019). Recently, the gene cluster for AST biosynthesis was shown to be a three gene cluster, *arsQML*. The *arsL* and *arsM* gene products are sufficient to catalyze sequential steps in the biosynthesis of AST. ArsL is proposed to be a non-canonical radical SAM enzyme that catalyzes synthesis of the precursor, R-AST-OH from inorganic arsenite and the ACP moiety from SAM. The second step is catalyzed by ArsM, a SAM methyltransferase that methylates the R-AST-OH to the reduced trivalent form of AST (R-AST). ArsQ is proposed to be an efflux permease responsible for the transport of the antibiotic out of the cell (Galvan *et al.*, 2021). However, it is not clear whether the physiological substrate of ArsQ is the pentavalent or the trivalent species. In this study, we characterized the substrate specificity and transport properties of ArsQ.

Antibiotic-producing bacteria usually extrude the antibiotic from the cell, both to confer resistance to the producer and to inhibit growth of competitors (Li *et al.*, 2015). Since ArsQ is found in the AST biosynthetic gene cluster, it is reasonable to expect that it serves as an efflux permease for substrates, intermediates or products in the AST biosynthetic pathway. Although ArsQ confers moderate resistance to a variety of substrates and products in the pathway, data from our study suggests that it is specific for transport of the trivalent species, both R-AST-

OH and R-AST. We propose that trivalent R-AST, the end product of the *B*. *gladioli* biosynthetic pathway, is released into the medium by ArsQ and oxidized by air to the antibiotic AST, where it can kill competitors.

GlpF is a channel in the inner membrane of *E. coli* belonging to the major intrinsic protein (MIP) family of transmembrane channel proteins. It is a nonselective carrier protein that facilitates the diffusion of polyols such as glycerol in *E. coli* (Sweet et al., 1990). In addition to glycerol, GlpF serves as a channel for trivalent metalloids (Sanders et al., 1997, Yang et al., 2005). Our data show that GlpF is not a channel for trivalent R-AST-OH or R-AST.

However, similar to GlpF, ArsQ transports its substrate independent of energy, in contrast to Acr3, an $As(OH)_3/H^+$ exchanger. With ArsQ, R-AST-OH and R-AST flow out of cells down their concentration gradients following synthesis in *Burkholderia gladioli* GSRB05. R-AST is rapidly oxidized to AST, which prevents its reuptake. The extracellular R-AST-OH is oxidized more slowly and can re-enter the cells to be methylated to R-AST. Thus, by mass action, re-uptake of R-AST-OH results in conversion to AST. This is supported by the observation that AST-OH appears in the *B*. *gladioli* culture medium at early times, and then its levels decrease, while AST appears at later times and continues to increase, a clear precursor-product relationship (Kuramata *et al.*, 2016, Galvan *et al.*, 2021).

The situation in *E. coli* is different from that in the AST producer *B. gladioli*. We propose that *E. coli* takes up AST and derivatives adventitiously by one or more as-yet unidentified transport systems. Our data show that R-AST transport activity is low in stationary phase cells but substantially higher in exponentially growing cells (Fig. S4). The accumulated R-AST is released down its concentration gradient when ArsQ is expressed. Then why do stationary phase cells take up R-AST when ArsQ is expressed rather than releasing it (Fig. 2)? We assume that when stationary phase cells are exposed to 2.5-fold more R-AST, and uptake is low because the endogenous transporters have relatively poor activity, the extracellular concentration of R-AST is higher than the intracellular, so ArsQ would then facilitate uptake. In summary, ArsQ facilitates efflux of R-AST in exponential phase cells exposed to low R-AST, and facilitates uptake in stationary phase cells exposed to higher R-AST. Thus, the direction of R-AST movement catalyzed by the bidirectional ArsQ uniporter depends both on the activity of the uptake system(s) and the concentration of added R-AST. This hypothesis will be tested in future experiments, and the endogenous uptake systems for AST and derivatives will be identified.

ArsQ is annotated as a GntP family member in the NCBI database, but annotations do not always reflect functional similarities. ArsQ is smaller (408 amino acid residues) than the average GntP protein of approximately 445 residues. GntP family members are predicted to have 12-14 transmembrane α-helices (Peekhaus *et al.*, 1997), while ArsQ is predicted to have only 11. On the other hand, we

identified the 11-TM succinate transporter from V*ibrio cholerae* VcINDY (PDB ID: 5ULD) as a structural homolog of ArsQ. VcINDY is a member of the DASS family of transporters that includes cotransporters and exchangers that import di- and tricarboxylates into cells. The crystal structure of VcINDY with bound terephthalate was used as a template for construction of an ArsQ structural model. Ser377 in the terephthalate binding site of VcINDY corresponds to Ser320 in ArsQ, which led to the prediction that S320 may be involved in ArsQ catalysis. The serine to alanine substitution in ArsQ led to a significant decrease in transport of R-AST-OH. Interestingly, the S320A transported R-AST with nearly normal efficiency, suggesting that the ArsQ substrate binding site had a change in selectivity as a result of the mutation. The chemical difference between AST-OH and AST is replacement of a polar hydroxyl group in the former with a nonpolar methyl group in the latter. The hydroxyl and methyl groups are isosteric, both should fit equally well into the substrate binding site of ArsQ. We speculate that the nonpolar alanine residue is less able to interact with the hydroxyl group in R-AST-OH but retains the ability to interact with the methyl group in R-AST. Later experiments will include mutagenesis of other residues in the predicted substrate binding site of ArsQ to elucidate their contribution to ArsQ function. In summary, our data suggests that ArsQ is an energy-independent uniporter for trivalent R-AST. Future studies will focus on elucidating the structure of ArsQ and its relationship to function.

3.5 Materials and methods

Chemicals. Unless otherwise indicated, chemicals were purchased from Sigma-Aldrich. The L-enantiomer of arsinothricin (L-AST) was purified from cultures of *B. gladioli* GSRB05, whereas D,L-hydroxyarsinothricin (D,L-AST-OH) was chemically synthesized, as described previously (Kuramata *et al.*, 2016, Nadar *et al.*, 2019, Suzol *et al.*, 2020). In the experiments described below, the concentration of L-AST-OH was calculated as half of the total added D,L-AST-OH. Pentavalent arsenicals were reduced as described (Reay & Asher, 1977). The reduced species were analyzed by high pressure liquid chromatography (NexSar HPLC, Perkin Elmer, Waltham, MA) coupled with inductively coupled mass spectroscopy (ICP-MS) (NexION 1000; PerkinElmer) (Qin *et al.*, 2006).

Strains, media, and growth conditions. *E. coli* AW3110 (*Δars::cam F⁻ IN(rrn-rrnE)*) (Carlin *et al.*, 1995), which is As(III) hypersensitive, was used for most studies. OSBR1 (*Δars::cam F−IN(rrn-rrnE, ΔGlpF)*), an AW3110 derivative with a *glpF* disruption (Sanders *et al*., 1997), was used for transport assays. *E. coli* strains were grown aerobically at either 30 °C or 37 ˚C in either lysogeny broth (LB) medium or M9 basal salts medium (Sambrook *et al.*, 1989), as noted, supplemented with 0.4% glycerol, 0.1 mM $CaCl_2$ and 1 mM $MgSO_4$.

Preparation of wild type and mutant *arsQ* genes. *B. gladioli* wild type *arsQ* and mutant $arsQ_{S320A}$ genes GSRB05 *arsQ* was purchased from GenScript

(Piscataway, NJ, USA) and cloned in plasmid pTrcHisA (Thermo Fisher Scientific, Inc., Waltham, MA, USA).

Resistance assays. For resistance assays, competent cells of AW3110 were transformed with constructs bearing *arsQ* genes or the control vector. Cells were grown overnight with shaking at 37 °C in LB medium with antibiotics supplemented with 25 μg/ml chloramphenicol (Cm) and 100 μg/ml ampicillin (Ap), final concentrations. Overnight cultures were washed with and suspended in 0.9% NaCl, and diluted 100-fold or to an A_{600nm} = 0.05 in M9 medium containing various concentrations of organoarsenicals and incubated at 37 ˚C with shaking for an additional 24 h. Growth was estimated from the absorbance at 600nm.

Transport assays. Transport assays were performed with either exponential or stationary phase cells. Overnight cultures of *E. coli* cells were diluted 100-fold and grown to A_{600nm} = 0.5 (exponential phase) or A_{600nm} = 1 (stationary phase) at 37 ˚C with aeration in LB medium. The cells were harvested, washed and suspended in M9 medium at A_{600nm} = 10. To initiate the transport reaction, AST, R-AST, AST-OH or R-AST-OH was added at a final concentration of 25 μM to 2 ml of cell suspension. The uncoupler carbonyl cyanide 4-(trifluoromethoxy)phenylhydrazone (FCCP) was added at a final concentration of 10 μM. Portions (0.1 ml) from the cell suspension were withdrawn at the indicated times, filtered through nitrocellulose filters (0.2-μm pore diameter; EMD Millipore, Billerica, MA), and washed at room temperature with 5 ml of M9 medium. The

filters were digested with 0.2 ml of concentrated HNO_3 (70%, ≥ 99.999% trace metals basis) at 70 ˚C for 30 min. The dissolved filters were allowed to cool to room temperature and diluted with HPLC-grade water to produce a final HNO_3 concentration of 2%. Arsenic was quantified by ICP-MS. Standard solutions were made in the range of 1 - 50 ppb in 2% nitric acid using arsenic standard (Ultra Scientific, N. Kingstown, RI).

Immunological detection of ArsQ. Immunoblot analysis was used to detect expression of wild type and mutant ArsQ proteins. Membranes from *E. coli* were prepared for immunoblot analysis as described previously (Villadangos *et al.*, 2012). *E. coli* cultures were grown in 1 L of LB medium with 50 μM isopropyl β-d-1-thiogalactopyranoside as inducer at 37 ˚C to A_{600nm} = 0.6 for 2 h. Cells were harvested by centrifugation, and the pellet suspended in a buffer consisting of 75 mM HEPES-KOH, pH 7.5, 0.15 M KCl, 1 mM $MgSO_4$ and 0.25 M sucrose, and lysed by passage through a French pressure cell at 4000 psi. The lysate was treated with 0.5 mM diisopropyl fluorophosphate and 10 μg/ml DNase I, final concentrations, at 37 ˚C for 15 min, and centrifuged at 27,000 x *g* for 20 min at 4 ˚C to remove unbroken cells and cell debris. The supernatant suspension was centrifuged at 105,000 x *g* for 1 h, and the membrane fraction was suspended in the same buffer. Protein content was determined using a Pierce™ BCA Protein Assay Kit (Thermo Fisher Scientific, Inc.). Membrane proteins were separated by sodium dodecyl sulfate (SDS) polyacrylamide gel electrophoresis (PAGE) on 10% acrylamide gels and transferred to a Schleicher & Schuell Protran® nitrocellulose

transfer membrane (PerkinElmer). Immunoblot analysis was performed according to the manufacturer's directions using a Western Lighting Ultra Chemiluminescence Substrate Kit and an anti-mouse IgG to the six-histidine tag (PerkinElmer).

Phylogenetic analysis

Multiple alignment of ArsQ homolog sequences was performed using Clustal Omega (http://www.ebi.ac.uk/Tools/msa/clustalo/). Acquisition of ArsQ sequences was performed by searching the National Center for Biotechnology Information (NCBI) protein database using a BLASTP protein basic local alignment search (Johnson *et al.*, 2008). Phylogenetic analysis was performed to infer the evolutionary relationship among the ArsQ proteins from various organisms. The phylogenetic trees were constructed using the Neighbor-Joining method using MEGA 6.0.1 (Tamura *et al.*, 2013). The statistical significance of the branch patterns was estimated by conducting a 1000 bootstrap.

Topological analysis and construction of an ArsQ structural homology model. The prediction of the transmembrane helices (TMs) in *B. gladioli* ArsQ was calculated by the on-line TMHMM Server v. 2.0 (http://www.cbs.dtu.dk/services/TMHMM/). Based on this prediction, the intramembrane topological plot was constructed with Protter (http://wlab.ethz.ch/protter/) to analyze and illustrate the sequence, topology and annotations (Omasits *et al.*, 2014).

The ArsQ sequence was used for the prediction of the tertiary structure by CPHmodels 3.2 (http://www.cbs.dtu.dk/services/CPHmodels/), a comparative protein homology modeling server (Nielsen *et al.*, 2010). To examine the structure-function relationship of ArsQ, a homology model was generated using the SWISS-MODEL online tool (https://swissmodel.expasy.org/). The structure of VcINDY in complex with terephthalate (PDB ID: 6WTX) used as a template (Sauer *et al.*, 2020). The quality of the three-dimensional structure was assessed by PROCHECK (Laskowski *et al.*, 1996). The model was constructed by using PyMOL Molecular Graphics System, Version 1.3, Schrodinger LLC (http://www.pymol.org/).

3.6 Acknowledgements. This work was supported by the National Institutes of Health Grant R35 GM55425 to BPR and National Science Foundation BIO/MCB grant 1817962 to MY.

REFERENCES

Carlin, A., Shi, W., Dey, S., and Rosen, B.P. (1995) The *ars* operon of *Escherichia coli* confers arsenical and antimonial resistance. *J Bacteriol* **177**: 981-986.

Chen, J., Madegowda, M., Bhattacharjee, H., and Rosen, B.P. (2015) ArsP: a methylarsenite efflux permease. *Mol Microbiol* **98**: 625-635.

Chen, J., Yoshinaga, M., Garbinski, L.D., and Rosen, B.P. (2016) Synergistic interaction of glyceraldehydes-3-phosphate dehydrogenase and ArsJ, a novel organoarsenical efflux permease, confers arsenate resistance. *Mol Microbiol* **100**: 945-953.

Chen, J., Yoshinaga, M., and Rosen, B.P. (2019) The antibiotic action of methylarsenite is an emergent property of microbial communities. *Mol Microbiol* **111**: 487-494.

Chen, J., Zhang, J., Wu, Y.F., Zhao, F.J., and Rosen, B.P. (2021) ArsV and ArsW provide synergistic resistance to the antibiotic methylarsenite. *Environmental Microbiology* **23**: 7550-7562.

Fu, H.-L., Meng, Y., Ordóñez, E., Villadangos, A.F., Bhattacharjee, H., Gill, J.A., Mateos, L.M., and Rosen, B.P. (2009) Properties of arsenite efflux permeases (Acr3) from *Alkaliphilus metalliredigens* and *Corynebacterium glutamicum*. *J Biol Chem* **284**: 19887-19895.

Galvan, A.E., Paul, N.P., Chen, J., Yoshinaga-Sakurai, K., Utturkar, S.M., Rosen, B.P., and Yoshinaga, M. (2021) Identification of the Biosynthetic Gene Cluster for the Organoarsenical Antibiotic Arsinothricin. *Microbiol Spectr* **9**: e0050221.

Johnson, M., Zaretskaya, I., Raytselis, Y., Merezhuk, Y., McGinnis, S., and Madden, T.L. (2008) NCBIBLAST: a better web interface. *Nucleic Acids Res* **36**: W5-W9.

Kuramata, M., Sakakibara, F., Kataoka, R., Yamazaki, K., Baba, K., Ishizaka, M., Hiradate, S., Kamo, T., and Ishikawa, S. (2016) Arsinothricin, a novel organoarsenic species produced by a rice rhizosphere bacterium. *Environ Chem* **13**: 723-731.

Laskowski, R.A., Rullmannn, J.A., MacArthur, M.W., Kaptein, R., and Thornton, J.M. (1996) AQUA and PROCHECK-NMR: programs for checking the quality of protein structures solved by NMR. *Journal of biomolecular NMR* **8**: 477-486.

Li, X.Z., Plesiat, P., and Nikaido, H. (2015) The Challenge of Efflux-Mediated Antibiotic Resistance in Gram-Negative Bacteria. *Clin Microbiol Rev* **28**: 337-418.

Liu, Z., Rensing, C., and Rosen , B.P., (2013) Resistance pathways for metalloids and toxic metals. In: Metals in Cells. V. Culotta & R.A. Scott (eds). Hoboken, NJ Wiley & Sons, Inc., pp. 429-442.

Meng, Y.L., Liu, Z., and Rosen, B.P. (2004) As(III) and Sb(III) uptake by GlpF and efflux by ArsB in Escherichia coli. *J Biol Chem* **279**: 18334-18341.

Nadar, V.S., Chen, J., Dheeman, D.S., Galvan, A.E., Yoshinaga-Sakurai, K., Kandavelu, P., Sankaran, B., Kuramata, M., Ishikawa, S., Rosen, B.P., and Yoshinaga, M. (2019) Arsinothricin, an arsenic-containing non-proteinogenic amino acid analog of glutamate, is a broad-spectrum antibiotic. *Communications Biology* **2**.

Naujokas, M.F., Anderson, B., Ahsan, H., Aposhian, H.V., Graziano, J.H., Thompson, C., and Suk, W.A. (2013) The Broad Scope of Health Effects from Chronic Arsenic Exposure: Update on a Worldwide Public Health Problem. *Environmental Health Perspectives* **121**: 295-302.

Nie, R.X., Stark, S., Symersky, J., Kaplan, R.S., and Lu, M. (2017) Structure and function of the divalent anion/Na+ symporter from Vibrio cholerae and a humanized variant. *Nature Communications* **8**.

Nielsen, M., Lundegaard, C., Lund, O., and Petersen, T.N. (2010) CPHmodels-3.0--remote homology modeling using structure-guided sequence profiles. *Nucleic Acids Res* **38**: W576-581.

Omasits, U., Ahrens, C.H., Muller, S., and Wollscheid, B. (2014) Protter: interactive protein feature visualization and integration with experimental proteomic data. *Bioinformatics* **30**: 884-886.

Paul, N.P., Galvan, A.E., Yoshinaga-Sakurai, K., Rosen, B.P., and Yoshinaga, M. (2022) Arsenic in medicine: past, present, and future. *Biometals*.

Peekhaus, N., Tong, S.X., Reizer, J., Saier, M.H., Murray, E., and Conway, T. (1997) Characterization of a novel transporter family that includes multiple Escherichia coli gluconate transporters and their homologues. *Fems Microbiol Lett* **147**: 233-238.

Qin, J., Rosen, B.P., Zhang, Y., Wang, G., Franke, S., and Rensing, C. (2006) Arsenic detoxification and evolution of trimethylarsine gas by a microbial arsenite S-adenosylmethionine methyltransferase. *Proc Natl Acad Sci U S A* **103**: 2075-2080.

Reay, P.F., and Asher, C.J. (1977) Preparation and purification of ^{74}As-labeled arsenate and arsenite for use in biological experiments. *Anal Biochem* **78**: 557-560.

Sambrook, J., Fritsch, E.F., and Maniatis, T., (1989) *Molecular cloning, a laboratory manual*. Cold Spring Harbor Laboratory, New York.

Sanders, O.I., Rensing, C., Kuroda, M., Mitra, B., and Rosen, B.P. (1997) Antimonite is accumulated by the glycerol facilitator GlpF in *Escherichia coli*. *J Bacteriol* **179**: 3365-3367.

Sauer, D.B., Trebesch, N., Marden, J.J., Cocco, N., Song, J.M., Koide, A., Koide, S., Tajkhorshid, E., and Wang, D.N. (2020) Structural basis for the reaction cycle of DASS dicarboxylate transporters. *Elife* **9**.

Shen, S.W., Li, X.F., Cullen, W.R., Weinfeld, M., and Le, X.C. (2013) Arsenic Binding to Proteins. *Chem Rev* **113**: 7769-7792.

Shi, K.X., Li, C., Rensing, C., Dai, X.L., Fan, X., and Wang, G.J. (2018) Efflux Transporter ArsK Is Responsible for Bacterial Resistance to Arsenite, Antimonite, Trivalent Roxarsone, and Methylarsenite. *Appl Environ Microb* **84**.

Suzol, S.H., Hasan Howlader, A., Galvan, A.E., Radhakrishnan, M., Wnuk, S.F., Rosen, B.P., and Yoshinaga, M. (2020) Semisynthesis of the Organoarsenical Antibiotic Arsinothricin. *J Nat Prod* **83**: 2809-2813.

Sweet, G., Gandor, C., Voegele, R., Wittekindt, N., Beuerle, J., Truniger, V., Lin, E.C.C., and Boos, W. (1990) Glycerol Facilitator of Escherichia-Coli - Cloning of Glpf and Identification of the Glpf Product. *J Bacteriol* **172**: 424-430.

Tamura, K., Stecher, G., Peterson, D., Filipski, A., and Kumar, S. (2013) MEGA6: Molecular Evolutionary Genetics Analysis Version 6.0. *Mol Biol Evol* **30**: 2725-2729.

Villadangos, A.F., Fu, H.L., Gil, J.A., Messens, J., Rosen, B.P., and Mateos, L.M. (2012) Efflux Permease CgAcr3-1 of Corynebacterium glutamicum Is an Arsenite-specific Antiporter. *J Biol Chem* **287**: 723-735.

Yang, H.C., Cheng, J., Finan, T.M., Rosen, B.P., and Bhattacharjee, H. (2005) Novel pathway for arsenic detoxification in the legume symbiont *Sinorhizobium meliloti*. *J Bacteriol* **187**: 6991-6997.

Yang, H.C., Fu, H.L., Lin, Y.F., and Rosen, B.P. (2012) Pathways of arsenic uptake and efflux. *Curr Top Membr* **69**: 325-358.

Yoshinaga, M., Cai, Y., and Rosen, B.P. (2011) Demethylation of methylarsonic acid by a microbial community. *Environ Microbiol* **13**: 1205-1215.

Zhang, J., Chen, J., Wu, Y.F., Wang, Z.P., Qiu, J.G., Li, X.L., Cai, F., Xiao, K.Q., Sun, X.X., Rosen, B.P., and Zhao, F.J. (2022) Oxidation of organoarsenicals and antimonite by a novel flavin monooxygenase widely present in soil bacteria. *Environ Microbiol* **24**: 752-761.

Zhu, Y.G., Yoshinaga, M., Zhao, F.J., and Rosen, B.P. (2014) Earth abides arsenic biotransformations. *Annu Rev Earth and Planet Sci* **42**: 443-467.

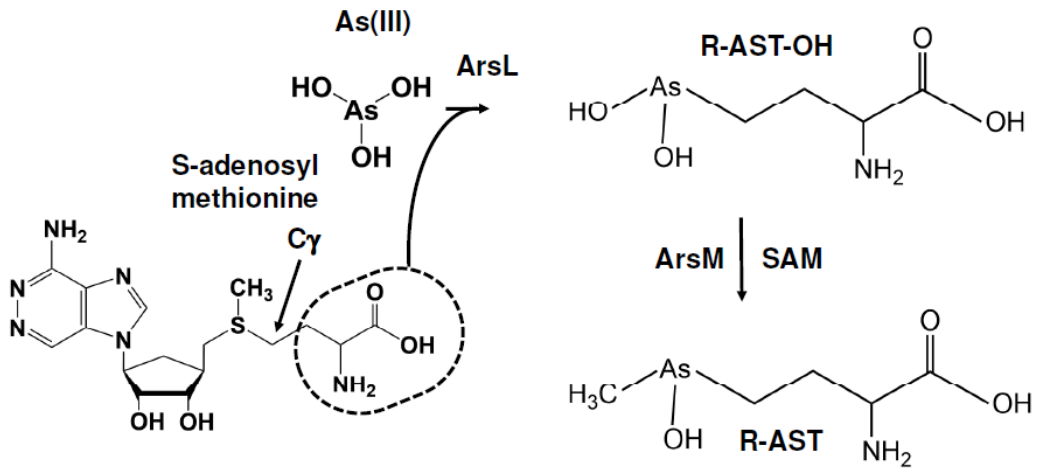

Fig. S1. ArsL reaction scheme. In the first step of AST biosynthesis, the radical SAM enzyme BgArsL cleaves the Cγ bond of SAM, forming a 3-amino-3-carboxypropyl (ACP) radical. This forms a C-As bond with As(III), producing R-AST-OH. In the second step, BgArsM uses a second molecule of SAM to methylate R-AST-OH, generating trivalent R-AST. ArsQ facilitates downhill efflux of R-AST, which spontaneously oxidizes nonenzymatically to the antibiotic pentavalent AST.

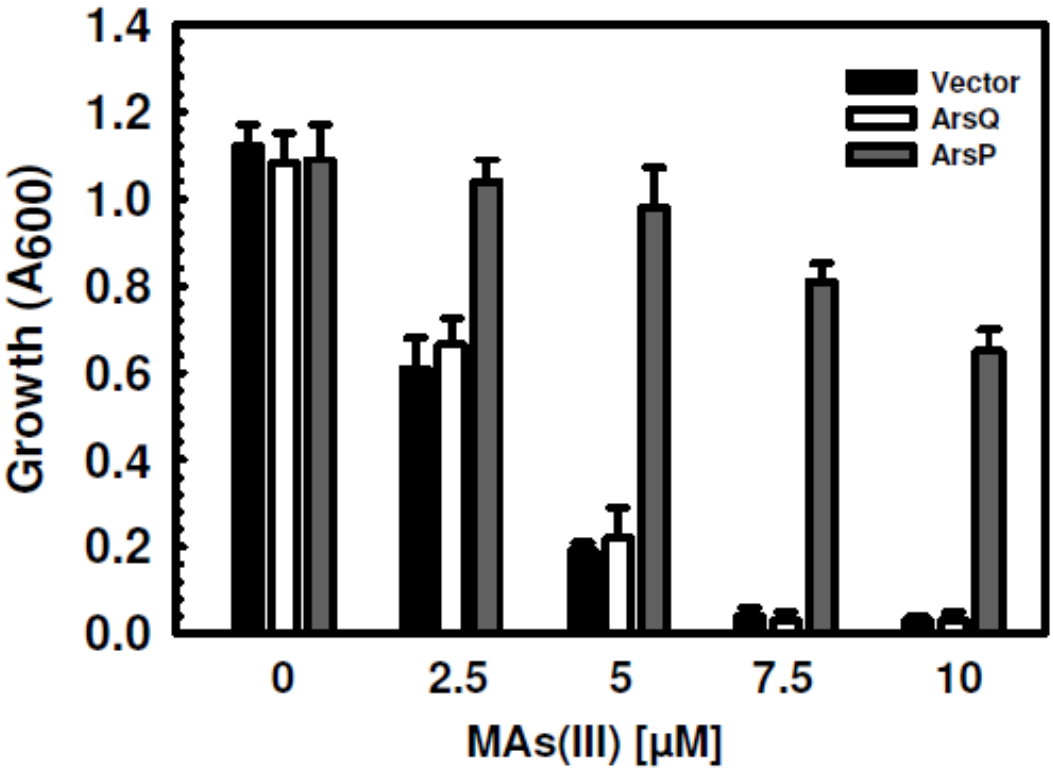

Fig. S2. ArsQ does not confer resistance to MAs(III) in cells of *E. coli* AW3110. Resistance in cells of *E. coli* AW3110 expressing ArsQ (white fill) was compared with cells with vector plasmid pTrcHisA (black fill) and cells expressing the ArsP MAs(III) efflux permease (grey fill). Growth was assayed after overnight incubation at 30 °C in the presence of the indicated concentrations of MAs(III). Data are the mean ± SD (n=3).

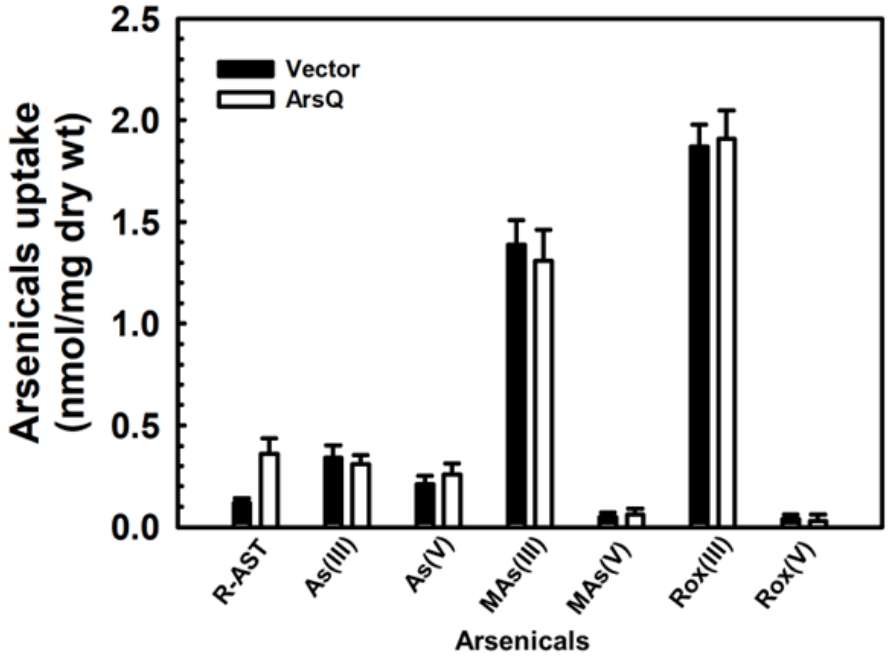

Fig. S3. ArsQ is specific for R-AST uptake. Uptake of the following substrates was assayed in stationary cells expressing ArsQ (white fill) or vector plasmid pTrcHis2A (black fill). All substrates were added at 25 μM, final concentration. Data are the mean ± SD (n=3).

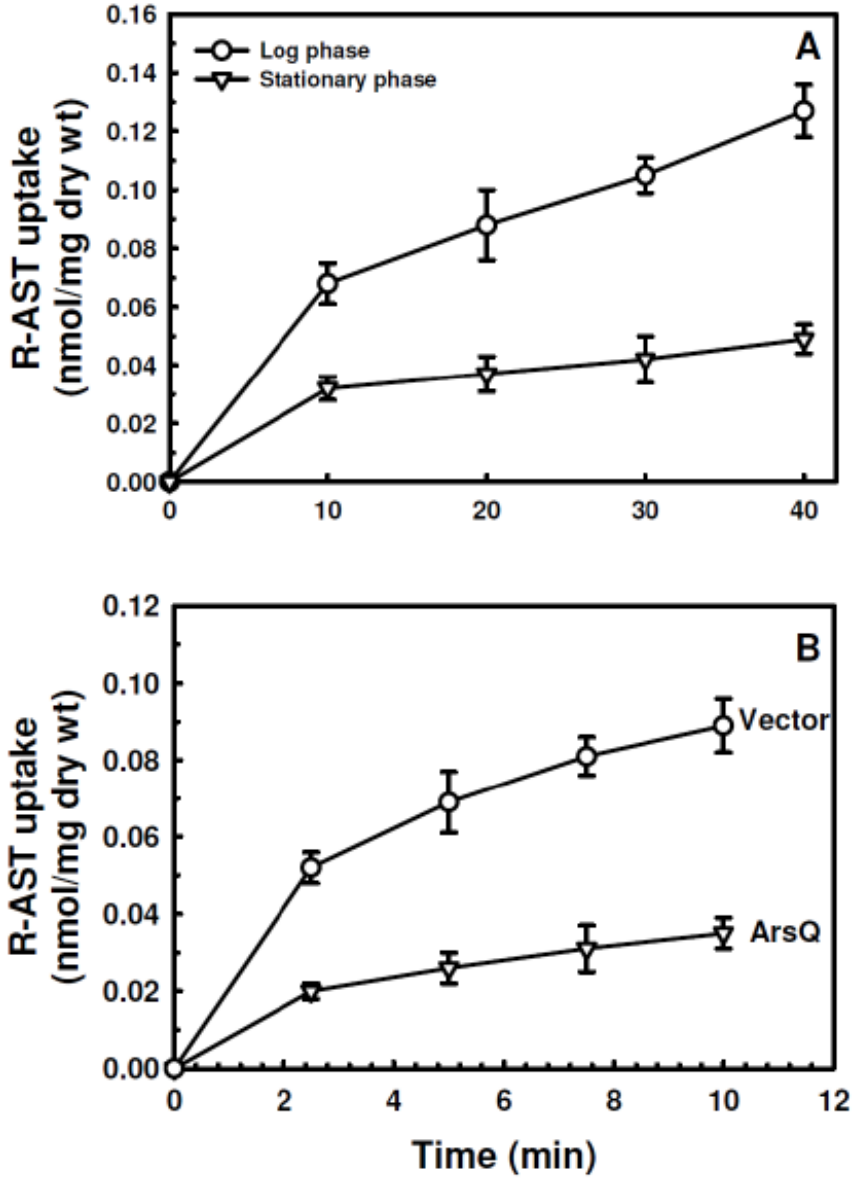

Fig. S4. ArsQ facilitates efflux of R-AST in exponential phase cells. A. R-AST uptake in cells differs in exponential and stationary phase cells of *E. coli*. Uptake of R-AST was assayed in cells of *E. coli* AW3110 expressing vector plasmid pTrcHis2A in log phase (o) and stationary phase(▽). R-AST was added at 10 μM, final concentration. **B. ArsQ confers resistance to R-AST by facilitating R-AST efflux in exponential phase cells of *E. coli* AW3110.** Uptake of the R-AST was assayed in exponential phase cells expressing ArsQ (▽) or vector plasmid pTrcHis2A (o). R-AST was added at 10 μM, final concentrations. Data are the mean ± SD (n=3).

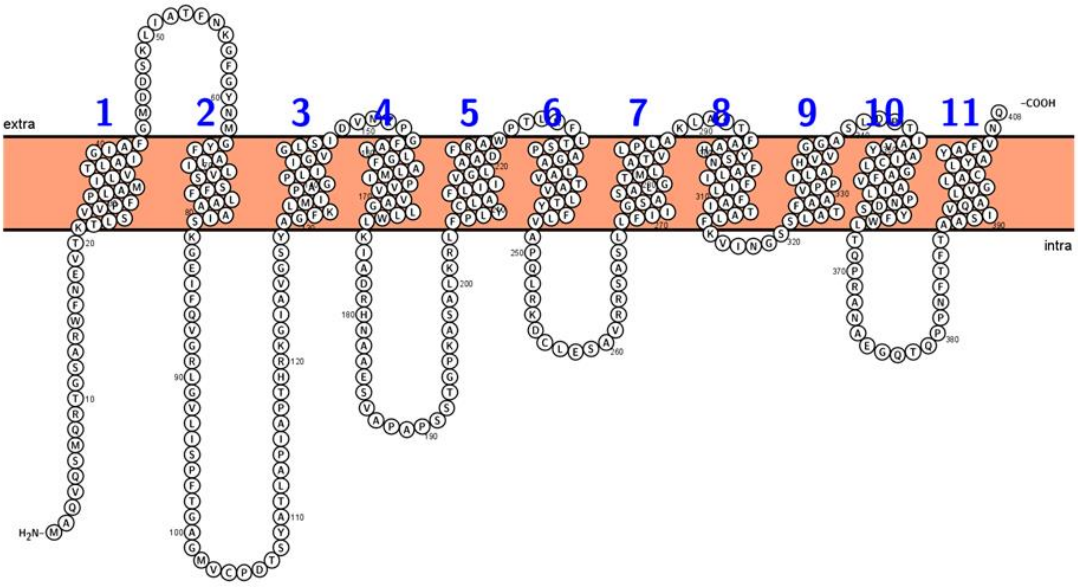

Fig. S5. Predicted ArsQ transmembrane topology. The secondary structural topology view was predicted using the Protter server (http://wlab.ethz.ch/protter/). The predicted TM regions are numbered 1-11.

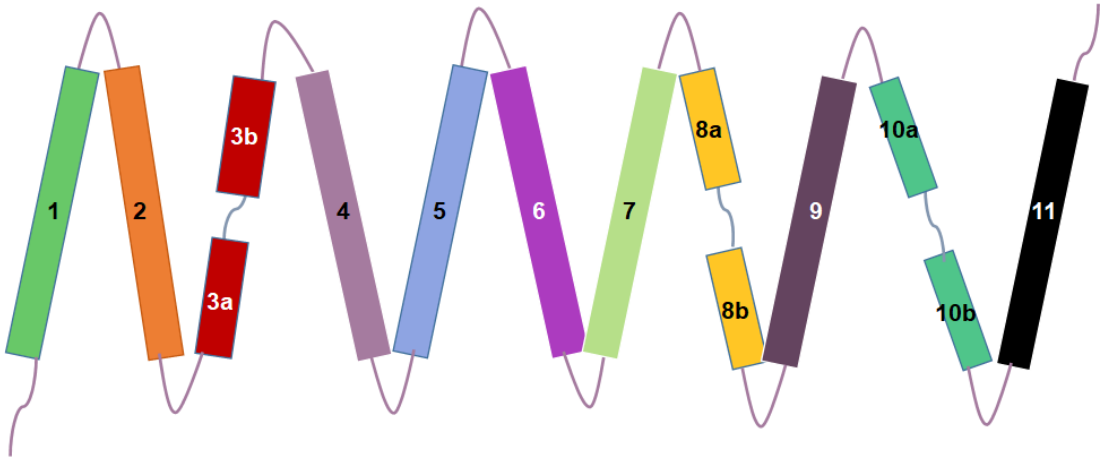

Figure S6. Structural modeling of ArsQ transmembrane topology. A manually-generated membrane topology of predicted TMs 1-11 is shown with each TM with residue

numbers shown in a different color. The TMs are based on the structural homology model except for TM11, which was not included in structural model.

Figure S7. Immunoblot analysis of ArsQ and S320A expression. Membrane proteins from cells of *E. coli* strain AW3110 harboring Acr3 (lane 1), vector plasmid pTrcHis2A (lane 2), plasmid pTrcHis2A-ArsQ (lane 3) or plasmid pTrcHis2A-ArsQ mutant (lane 4) were prepared, separated by SDS-PAGE and immunoblotted with an antimouse IgG to the six-histidine tag, as described under *Experimental Procedures.*

CHAPTER 4: IDENTIFICATION OF RESIDUES INVOLVED IN THE FUNCTION OF THE ARSQ PERMEASE

4.1 Introduction

In chapter 2 I reported that the biosynthetic gene cluster for arsinothricin (AST) contains the *arsQ* gene, which encodes a membrane protein with a predicted mass of 42.9 kDa (GenBank Accession No. MBW5287223), and we proposed that ArsQ is involved in the efflux of AST or related compounds (Galván et al., 2021). In chapter 3 I described the relationship of the ArsQ permease to the transport of the antibiotic arsinothricin. Phylogenetic analysis shows that ArsQ forms an evolutionarily separate family from the four other known families of organoarsenical efflux permeases. ArsQ confers resistance to AST and R-AST in cells of *E. coli* and selectively transports R-AST and R-AST-OH. The transport of these substrates was independent of cellular energy and appeared to be equilibrative. I proposed that the ArsQ permease is an energy-independent uniporter responsible for the downhill transport of the trivalent form of AST out of cells, which is oxidized extracellularly to the active form of the antibiotic (Paul et al., 2023).

Structural information is a major contributor to elucidating the function of a protein. I identified that ArsQ is structurally related to members of the DASS family of divalent anion/Na+ symporters. In collaboration with other members of my laboratory, I constructed a structural model of ArsQ based on the crystal structure

of a member of the DASS family, VcINDY (PDB ID: 5ULD) from *Vibrio cholerae,* with bound terephthalate, a substrate analog (Sauer et al., 2020). Ser377 in the terephthalate binding site of VcINDY corresponds to Ser320 in ArsQ, which led to the prediction that Ser320 may be involved in ArsQ catalysis. A serine-to-alanine substitution in ArsQ led to a significant decrease in R-AST-OH transport. Interestingly, the S320A derivative transported R-AST with nearly wild-type efficiency (Paul et al., 2023).

Protein cysteine residues are structurally and functionally crucial because of their ability to form disulfide bonds to stabilize proteins and maintain their integrity. Cysteines are used in the active site to bind substrates due to their ability to form intramolecular and extra molecular disulfide bonds. Cysteine residues often form two- and three-coordinate arsenic binding sites (Wang et al., 2014). Alignment of BgArsQ with other orthologs identified a conserved cysteine, Cys104, which was mutated to alanine to examine its contribution to ArsQ function. However, the $ArsQ_{C104A}$ mutant was not sufficiently expressed to draw any conclusions. Cys104 is more likely involved in ArsQ stability than a catalytic role in transport.

Using the ArsQ structural model, I identified other charged residues around Ser320 (Fig.1). Site-directed mutagenesis of these charged substrates in the predicted substrate-binding site was employed to elucidate their contribution to ArsQ function. These residues and the mutations include D106A, R262A, R263A, S320C, S320A, S321A, and D362A (Fig. 2). Currently, I am examining whether

the mutant proteins are expressed by immunoblotting analysis. In subsequent experiments, I will perform transport studies to analyze the possible contribution of each residue to ArsQ function.

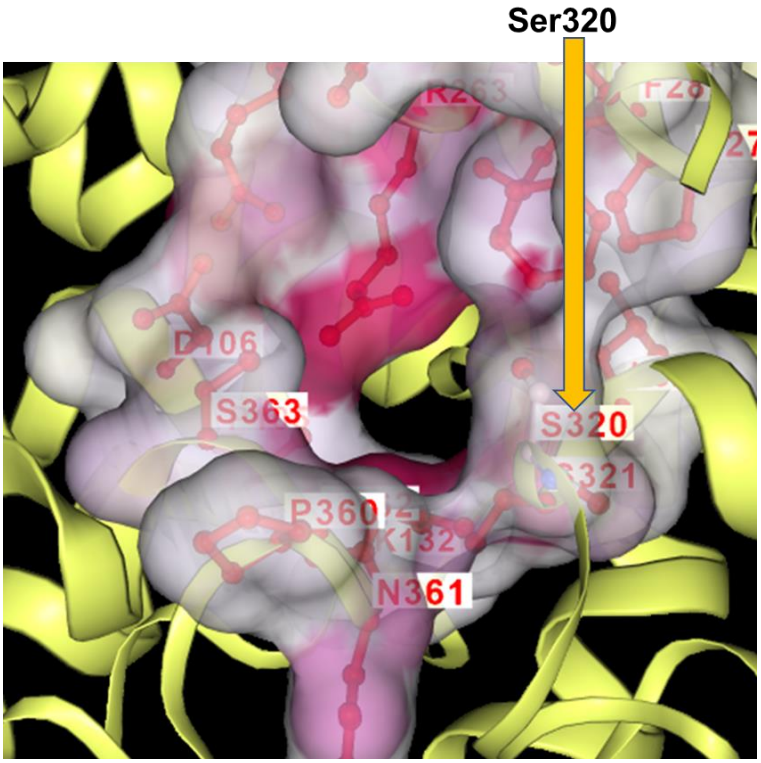

Fig. 1 S320 and other residues within the ArsQ predicted residue-binding site

Table 1: Primers used for site-directed mutagenesis

PRIMERS	SEQUENCE
ArsQ-D106A-Forward	5'-gcatggtttgccccgccacatcttacgccac-3'
ArsQ-D106A-Reverse	5'-gtggcgtaagatgtggcggggcaaaccatgc-3'
ArsQ-R262A-Forward	5'-ggagtcggcagtggcccgtagtgcatcg-3'
ArsQ-R262A-Reverse	5'-cgatgcactacgggccactgccgactcc-3'
ArsQ-R263A-Forward	5'-gtcggcagtgcgcgctagtgcatcgctc-3'
ArsQ-R263A-Reverse	5'-gagcgatgcactagcgcgcactgccgac-3'
ArsQ-S321A-Forward	5'-gtcatcaacggctcggcgctggcaacgtttg-3'
ArsQ-S321A-Reverse	5'-caaacgttgccagcgccgagccgttgatgac-3'
ArsQ-D362A-Forward	5'-gcgatccttccgaatgccagctacttttggctg-3'
ArsQ-D362A-Reverse	5'-cagccaaaagtagctggcattcggaaggatcgc-3'
ArsQ-S320C-Forward	5'-attattcaaagtcatcaacggctgctcgctggcaacgttt-3'
ArsQ-S320C-Reverse	5'-aaacgttgccagcgagcagccgttgatgactttgaataat-3'
ArsQ-S321C-Forward	5'-tcatcaacggctcgtgcctggcaacgtttgcg-3'
ArsQ-S321C-Reverse	5'-cgcaaacgttgccaggcacgagccgttgatga-3'


Seq_1 204 CCTCGTGTCCTCGTTTTTCCTCGCAGCGGCGATCAGCAAAGGCGAAATATTCCAAGTTGG 263
Seq_2 361 CCTCGTGTCCTCGTTTTTCCTCGCAGCGGCGATCAGCAAAGGCGAAATATTCCAAGTTGG 420
D106A
Seq_1 264 ACGGCTAGGGGTGTTGATTTCTCCCTTCACCGGAGCCGGCATGGTTTGCCCCGACACATC 323
Seq_2 421 ACGGCTAGGGGTGTTGATTTCTCCCTTCACCGGAGCCGGCATGGTTTGCCCCGCCACATC 480
Seq_1 324 TTACGCCACCCTTGCACCGATCGCTCCAACCCATCGTAAGGGCATCGCCGTTGGCAGCTA 383
Seq_2 481 TTACGCCACCCTTGCACCGATCGCTCCAACCCATCGTAAGGGCATCGCCGTTGGCAGCTA 540
Seq_1 891 TTACTCCAATTTCGCCCTGATATTTATACTGTTCGCGATCACTGCATTATTCAAAGTCAT 950
Seq_2 751 TTACTCCAATTTCGCCCTGATATTTATACTGTTCGCGATCACTGCATTATTCAAAGTCAT 810
S320C
Seq_1 951 CAACGGCTCGTCGCTGGCAACGTTTGCGGCCGTTCCTCCGATCCTCGCGCATGTTGTGGG 1010
Seq_2 811 CAACGGCTGCTCGCTGGCAACGTTTGCGGCCGTTCCTCCGATCCTCGCGCATGTTGTGGG 870
Seq_1 1011 CGGCGCATCGTTGGATCCAACGATCGCCGTATACGCGATCTGCCTGGGAGCATTCGTCGC 1070
Seq_2 871 CGGCGCATCGTTGGATCCAACGATCGCCGTATACGCGATCTGCCTGGGAGCATTCGTCGC 930
Seq_1 660 TTTTCGCGCATGGCCTACGCTGAAATTTCTTACTTCGCCAGCGGGGGCTCTCGCTGTCAC 719
Seq_2 552 TTTTCGCGCATGGCCTACGCTGAAATTTCTTACTTCGCCAGCGGGGGCTCTCGCTGTCAC 611
Seq_1 720 TGCCGTACTCACATACTTTCTCGTCGCACCGCAGCTACGCAAGGACTGTTTGGAGTCGGC 779
Seq_2 612 TGCCGTACTCACATACTTTCTCGTCGCACCGCAGCTACGCAAGGACTGTTTGGAGTCGGC 671
R262A
Seq_1 780 AGTGCGCCGTAGTGCATCGCTCCTGTTCATCATCGGCTCCGCGAGCGCCCTCGGGACGAT 839
Seq_2 672 AGTGGCCCGTAGTGCATCGCTCCTGTTCATCATCGGCTCCGCGAGCGCCCTCGGGACGAT 731
Seq_1 656 CTGATTTTCGCGCATGGCCTACGCTGAAATTTCTTACTTCGCCAGCGGGGGCTCTCGCTG 715
Seq_2 592 CTGATTTTCGCGCATGGCCTACGCTGAAATTTCTTACTTCGCCAGCGGGGGCTCTCGCTG 651
Seq_1 716 TCACTGCCGTACTCACATACTTTCTCGTCGCACCGCAGCTACGCAAGGACTGTTTGGAGT 775
Seq_2 652 TCACTGCCGTACTCACATACTTTCTCGTCGCACCGCAGCTACGCAAGGACTGTTTGGAGT 711
R263A
Seq_1 776 CGGCAGTGCGCCGTAGTGCATCGCTCCTGTTCATCATCGGCTCCGCGAGCGCCCTCGGGA 835
Seq_2 712 CGGCAGTGCGCGCTAGTGCATCGCTCCTGTTCATCATCGGCTCCGCGAGCGCCCTCGGGA 771

Fig. 2 Sequence alignment of wild-type ArsQ with mutants. Sections of alignments of wild-type ArsQ represented as Seq_1 with the ArsQ mutants, D106A, S320C, R262A, R263A, S321A, S321C, D362A represented as Seq_2.

4.2 Materials and methods

Media and growth conditions: Cells were grown aerobically at either 30 °C or 37 °C in lysogeny broth (LB) medium.

Cloning and expression: *B. gladioli* wild type *arsQ* and mutant $arsQ_{S320A}$ genes were purchased from GenScript (Piscataway, NJ, USA) and cloned in plasmid pTrcHisA (Thermo Fisher Scientific, Inc., Waltham, MA, USA).

Site-directed mutagenesis: Other ArsQ mutants were generated by site-directed mutagenesis. Mutations were introduced using a PCR protocol into plasmid using primers designed using the online QuikChange Primer Design program (https://www.agilent.com/store/primerDesignProgram.jsp) (Table 1). Unmutated plasmid pTrcHis2AarsQ was removed from the reaction mixture by digesting the methylated DNA with restriction enzyme DpnI (New England Biolabs, Ipswich, MA, USA). Each mutated plasmid was transformed into competent cells of *E. coli* AW3110, purified, and the presence of the mutation verified by sequencing using pTrc vector pSE3805 (forward and reverse) primers.

Immunological detection of mutant ArsQ: Immunoblot analysis was used to detect expression of wild-type and mutant ArsQ proteins. Membranes from *E. coli* were prepared for immunoblot analysis as described previously (Villadangos et al., 2012). *E. coli* cultures were grown in 1 L of LB medium with 50 μM isopropyl β-d-1-thiogalactopyranoside as inducer at 37 °C to A_{600nm} = 0.6 for 2 h. Cells were harvested by centrifugation, and the pellet suspended in a buffer consisting of 75 mM HEPES-KOH, pH 7.5, 0.15 M KCl, 1 mM $MgSO_4$, and 0.25 M sucrose, and

lysed by passage through a French pressure cell at 4000 psi. The lysate was treated with 0.5 mM diisopropyl fluorophosphate and 10 µg/mL DNase I, final concentrations, at 37°C for 15 min, and centrifuged at 27,000 x *g* for 20 min at 4°C to remove unbroken cells and cell debris. The supernatant suspension was centrifuged at 105,000 x *g* for 1 h, and the membrane fraction was suspended in the same buffer. Protein content was determined using a Pierce™ BCA Protein Assay Kit (Thermo Fisher Scientific, Inc.). Membrane proteins were separated by sodium dodecyl sulfate polyacrylamide gel electrophoresis (SDS PAGE) on 10% acrylamide gels and transferred to a Schleicher & Schuell Protran® nitrocellulose transfer membrane (PerkinElmer). Immunoblot analysis was performed according to the manufacturer's directions using a Western Lighting Ultra Chemiluminescence Substrate Kit and an anti-mouse IgG to the six-histidine tag (PerkinElmer).

REFERENCES

Galván, A. E., Paul, N. P., Chen, J., Yoshinaga-Sakurai, K., Utturkar, S. M., Rosen, B. P., & Yoshinaga, M. (2021). Identification of the Biosynthetic Gene Cluster for the Organoarsenical Antibiotic Arsinothricin. *Microbiology Spectrum*, *9*(1). https://doi.org/10.1128/spectrum.00502-21

J. Sambrock, E. F. Fritsch, T. M. (1989). Molecular cloning, a laboratory manual, 2nd ed. Cold Spring Harbor Laboratory, Cold Spring Harbor, NY

Paul, N. P., Viswanathan, T., Chen, J., Yoshinaga, M., & Rosen, B. P. (2023). *The ArsQ permease and transport of the antibiotic arsinothricin*. *January*, 1–10. https://doi.org/10.1111/mmi.15045

Sauer, D. B., Trebesch, N., Marden, J. J., Cocco, N., Song, J., Koide, A., Koide, S., Tajkhorshid, E., & Wang, D. N. (2020). Structural basis for the reaction cycle of dass dicarboxylate transporters. *ELife*, *9*, 1–74. https://doi.org/10.7554/ELIFE.61350

Villadangos, A. F., Fu, H. L., Gil, J. A., Messens, J., Rosen, B. P., & Mateos, L. M. (2012). Efflux permease CgAcr3-1 of Corynebacterium glutamicum is an arsenite-specific antiporter. *Journal of Biological Chemistry*, *287*(1), 723–735. https://doi.org/10.1074/jbc.M111.263335

Wang, S., Geng, Z., Shi, N., Li, X., & Wang, Z. (2014). The functions of crucial cysteine residues in the arsenite methylation catalyzed by recombinant human arsenic (III) methyltransferase. *PLoS ONE*, *9*(10), 1–13. https://doi.org/10.1371/journal.pone.0110924

CHAPTER 5: IDENTIFICATION OF AST UPTAKE SYSTEM(S)

5.1 Introduction

The exposure of microbes to arsenic since the origin of life was a driving force for the evolution of arsenic resistance (*ars*) operons. These operons contain specific genes for arsenic detoxification to protect the microbes (Yang & Rosen, 2016). However, there are no uptake pathways/systems specific to arsenic since arsenic is not essential for life. Therefore, all arsenic uptake pathways are adventitious via a variety of transporters for minerals and nutrients, such as phosphate, glycerol and glucose transporters (Garbinski et al., 2019).

AST is a pentavalent broad-spectrum antibiotic effective against Gram-positive and Gram-negative bacteria (Nadar et al., 2019). Our recent data suggested that the ArsQ permease is responsible for efflux of reduced trivalent AST out of the producer cell, which is then oxidized to the active form of the antibiotic (Galván et al., 2021; Paul et al., 2023). We propose that *E. coli* takes up AST and derivatives adventitiously by one or more transport systems. Given that the target of AST is cytosolic glutamine synthetase, it is likely that AST must enter the cell to exert its antibiotic activity. In other words, the binding and uptake of most antibiotics into the cell is the first step in antibiotic action. Based on its size and charge, AST probably cannot diffuse into the cell but is instead transported into the cell by membrane transporters. In an earlier study, our results suggest the presence of putative endogenous AST and R-AST transporters that show substantially higher transport activity in exponentially growing cells than in stationary phase cells.

However, we did not identify these transporters in that study (Paul et al., 2023). Identifying and understanding the AST uptake system(s) is crucial for its development as an effective antibiotic. For instance, the pharmacological upregulation of the identified AST transporter(s) could be employed to enhance its activity in bacteria.

This study aims to search for the gene(s) responsible for accumulation of AST in *Escherichia coli*, which is sensitive to AST. AST acts by the inhibition of bacterial glutamine synthetase (GS), similar to the sulfur and phosphorus mimetics of glutamate, methionine sulfoximine (MSO), and phosphinothricin (PT) (Nadar et al., 2019). L-MSO is a GS inhibitor effective against *Mycobacterium tuberculosis* (Harth & Horwitz, 1999). However, it is not in use as a treatment due to high rates of spontaneous resistance (Carroll et al., 2011). L-PT is a *Streptomyces* antibiotic commonly used as an effective broad-spectrum systemic herbicide commercially available with the trade name Glufosinate (Lamberth, 2016; Metcalf & Van Der Donk, 2009). The cyanobacterium *Nostoc muscorum* has a transport system for methionine and methionine/glutamate analogs, methionine sulfoximine and phosphinothricin (Singh et al., 2008). L-methionine and L-glutamine prevent growth inhibition by methionine sulfoximine by blocking the uptake of methionine sulfoximine into the cell (Meins & Abrams, 1972) - further evidence for the use of a common transport system by these GS inhibitors and their amino acid analogs.

5.1.1 Hypotheses

1. I hypothesize that, since it is chemically similar to glutamate, AST may be transported into the cells by transporters for glutamate or related amino acids. To examine this possibility, I analyzed AST's uptake and growth inhibitory activity in the presence and absence of structurally analogous amino acids.
2. Alternatively, AST uptake may use as-yet-unidentified transporters. I used random Tn5 mutagenesis in *E. coli* AW3110 to create AST-resistant mutants. I hypothesize that Tn5 inserted into gene(s) involved in uptake and, consequently, sensitivity to AST.

5.2 Preliminary Results

Growth inhibition by AST is reversed by glutamine and methionine, but not glutamate: The growth inhibition of AST was compared to PT and MSO in the presence or absence of three structurally analogous amino acids: glutamate, glutamine and methionine (Fig. 1A). AST completely inhibits growth at 25 µM, which is much lower than inhibitory concentrations of MSO or PT. In contrast to inhibition by MSO and PT, AST inhibition is not reversed by glutamate, indicating that it is not transported by glutamate permeases (Fig. 1B). These data suggest that AST is a more potent GS inhibitor than other known GS inhibitors. Inhibition by all three GS inhibitors is reversed by glutamine or methionine. It is not surprising that the inhibitory effect of MSO and PT is reversed by glutamate and glutamine, as these amino acids are analogs of the substrate and product, respectively, in the

glutamine biosynthetic pathway. AST is also a substrate of GS, and its inhibition is reversed by glutamine, so it is not clear why glutamate does not reverse inhibition. On the other hand, L-glutamine has been shown to prevent growth inhibition by MSO by blocking its uptake (Meins & Abrams, 1972), so perhaps AST is also taken up by a glutamine transporter.

Although methionine is not in the glutamine biosynthesis pathway, it has significant chemical similarity to the GS inhibitors. Methionine, MSO and PT are taken up by the same transporter, which explains why methionine reverses MSO and PT inhibition (Singh et al., 2008). I propose that AST might be taken up by this transporter. To test this hypothesis, I compared the uptake activity of AST in the presence and absence of methionine.

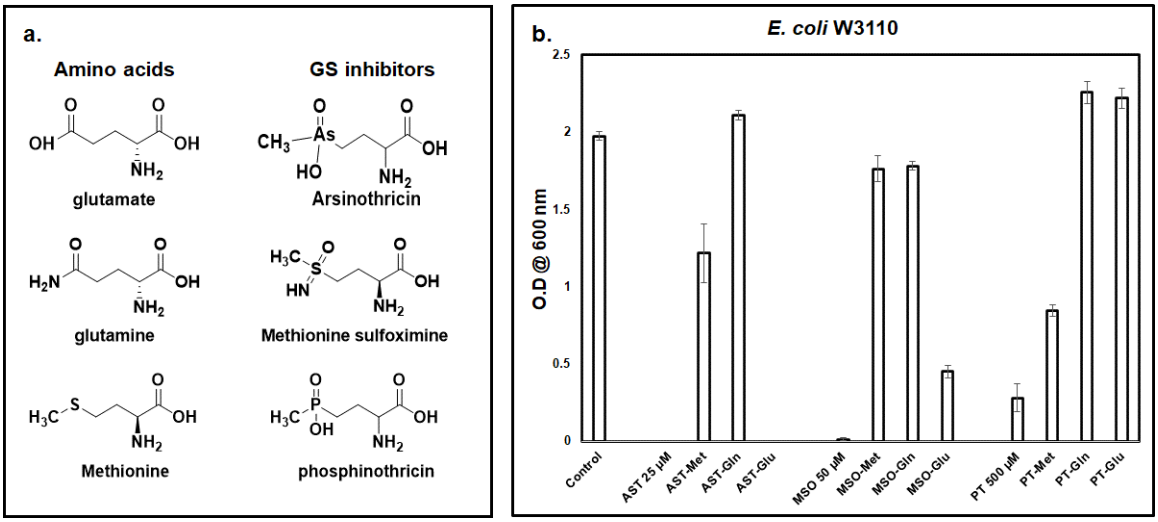

Fig. 1 Growth inhibition by AST is reversed by glutamine and methionine, but not glutamate. a. Chemical structures of amino acids and the GS inhibitors. b. Inhibition by AST, MSO and PT. Growth was assayed after overnight incubation at 37 °C in the presence of L-AST **(**25 µM), L-MSO (50 µM) or D,L-PT (500 µM) and with 1 mM of methionine, glutamine or glutamate. Data are the mean ± SD (n=3).

Methionine does not significantly inhibit AST uptake: I propose that AST is taken up by methionine permeases, so that the reversal of AST inhibition by methionine is due to inhibition of AST uptake. To test this idea, I assayed uptake of 25 µM AST in the presence or absence of 1 mM methionine but observed no significant difference in AST uptake with or without methionine (data not shown). To examine this question in more detail, I considered the possibility that any of the known methionine uptake systems can take up AST. At least two systems have been reported for methionine uptake in *E*. *coli*; the high-affinity system, MetD, and the lower affinity system, MetP (Kadner, 1974, 1975; Kadner & Watson, 1974). The *E*. *coli* *metD* operon encodes an ABC transporter with three subunits, *metN*, *metI,* and *metQ* (Merlin et al., 2002). My preliminary results with two mutants defective in a subunit of the *metD* locus (*ΔmetN* and *ΔmetQ*, table 1) showed no difference in AST uptake activity compared to the parent strains without the mutations, which seems to eliminate the possibility that MetD is involved in AST uptake. AST might use the low-affinity MetP methionine permease. I will perform further experiments with double mutants lacking both uptake systems to examine whether methionine permeases play any role in AST transport.

Tn5 random mutagenesis produces AST-resistant mutants: A different approach to identify AST uptake system(s) is by random mutagenesis of *E. coli* with selection for AST resistant mutants. I created a random transposon insertion library using bacterial conjugation between *E. coli* AW3110 - Cm^r (recipient) and *E. coli* S17-1 pSup102::Tn5B20 - Km^r (donor) (Fig. 2). Appropriate dilutions of the

mutant library were plated in M9 agar plates and agar broth containing 50 µM AST.

A few AST-resistant colonies were isolated (Fig. 3).

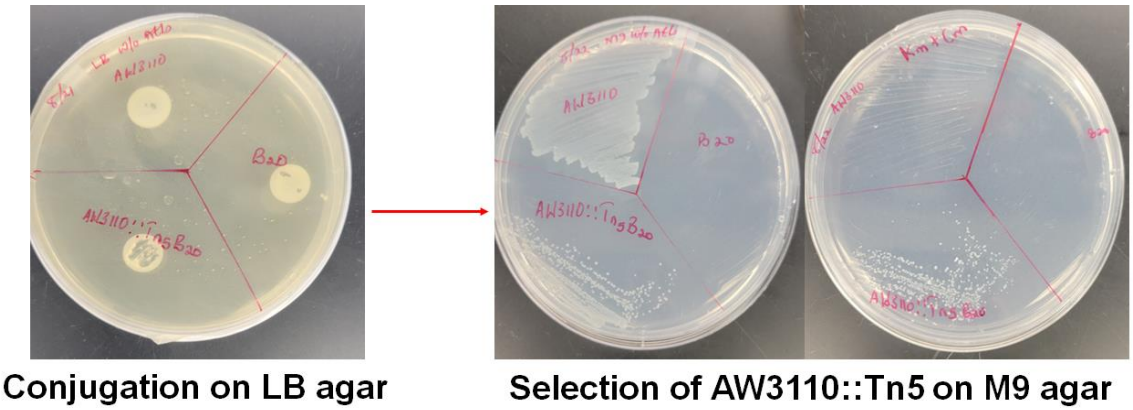

Fig. 2 Creation of a transposon insertion mutant library. The transposon insertion library was created using bacterial conjugation between *E*. *coli* AW3110 and *E*. *coli* S17-1, as described in Experimental Procedures.

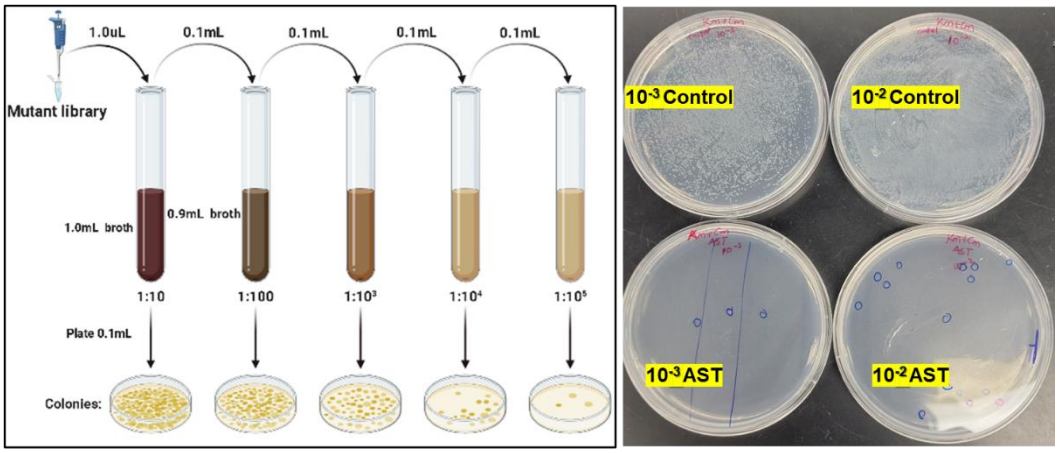

Fig. 3 Selection of AST-resistant mutants. Serial dilutions of the mutant library were plated on LB agar plates to determine the optimal number of cells per plate. The appropriate dilutions were plated on M9 agar plates with and without AST to select the AST-resistant colonies.

DNA sequence analysis of AST-resistant mutants: To identify the gene(s) into which Tn5 inserted, DNA was purified from AST-resistant mutants using OMEGA bio-tek E.Z.N.A® Bacterial DNA Kit according to manufacturer's manual, and sent to SeqCenter (SeqCenter, Pittsburg, PA, USA) for genome sequencing. Sequence analysis of one of the insertions identified a regulatory gene P*yjhI*. P*yjhI* is a transcription factor involved in the positive regulation of a D-xylonate-inducible operon, including a transporter gene *yjhF* (Bañares et al., 2019). I hypothesize that AST utilizes this transporter to get into the cell and that the disruption of P*yjhI* resulted in reduced expression of *yjhF*, leading to AST resistance. This hypothesis is plausible, and I will design experiments to test it.

Table1: Strains used in the study.

Strain	Description/genotype	Source/reference
***E. coli* W3110**	K12 F2 IN(*rrnD-rrnE*)	Bachman, B.J 1987
***E. coli* AW3110**	*ars*::*cam* F- IN(*rrnD-rrnE*). Cm^r	Carlin et al., 1995
***E. coli* S17-1**	pSup102::Tn5B20– Km^r	A gift from Dr. Timothy McDermott
***E. coli* k-12 BW25113**	*Δ(araD-araB)567*, *ΔlacZ4787*(::rrnB-3), λ^-, *rph-1*, *Δ(rhaD-rhaB)568*, *hsdR514*	Purchased from CGSC
***E. coli* JW0195-1 (*ΔmetN*)**	*Δ(araD-araB)567*, *ΔmetN724::kan*, *ΔlacZ4787*(::rrnB-3), λ^-, *rph-1*, *Δ(rhaD-rhaB)568*, *hsdR514*	Purchased from CGSC
***E. coli* JW0193-1(*ΔmetQ*)**	*Δ(araD-araB)567*, *ΔmetQ722::kan*, *ΔlacZ4787*(::rrnB-3), λ^-, *rph-1*, *Δ(rhaD-rhaB)568*, *hsdR514*	Purchased from CGSC

5.3 Materials and methods

Chemicals: AST was purified as previously described (Galván et al., 2021) as a modification of the original method (Kuramata et al., 2016). I determined the concentration and purity of purified AST by inductively coupled plasma mass spectrometry (ICP-MS) (NexION 1000; PerkinElmer, Waltham, MA, USA) and high-pressure liquid chromatography (HPLC) (NexSar HPLC, Perkin Elmer) coupled to ICP-MS, respectively. Biologically synthesized AST is assumed to be the L-enantiomeric form. Commercial MSO and PT were purchased from Sigma-Aldrich Co. LLC (St. Louis, MO, USA) as the L, and D, L-enantiomers, respectively. L-glutamic acid and L-methionine were from Sigma-Aldrich Co. LLC (St. Louis, MO, USA), while L-glutamine was purchased from *A*lfa *A*esar.

Strains and media: The strains used are described in Table 2. *E. coli* cultures were grown aerobically overnight with shaking in lysogeny broth (LB) medium at 37°C, respectively. M9 medium was supplemented with 0.4% glucose, 0.1 mM $CaCl_2$, and 1 mM $MgSO_4$. Antibiotics were supplemented at the following final concentrations: 25 µg/ml chloramphenicol (Cm) and 25 µg/ml kanamycin (Km).

Growth inhibition assays. For growth inhibition assays, *E*. *coli* W3110 (Bachmann, 1996) was grown overnight with shaking at 37 °C in LB medium without antibiotics. Overnight cultures were washed with and suspended in 0.9% NaCl and diluted 100-fold or to an A_{600nm} = 0.05 in M9 medium with 1 mM glutamate, glutamine, or methionine. The GS inhibitors were added at a final

concentration of 25 µM L-AST, 50 µM L-MSO or 500 µM D,L-PT and incubated at 37 ˚C with shaking for an additional 24 h. Growth was estimated from the absorbance at 600nm.

Transport assays. Overnight cultures of *E. coli* cells were diluted 10-fold and grown to A_{600nm} = 1 at 37 ˚C with aeration in LB medium. The cells were harvested, washed and suspended in M9 medium at A_{600nm} = 10, and methionine was added to a final concentration of 1 mM. To initiate the transport reaction, AST at a final concentration of 25 µM to 2 ml of cell suspension. Portions (0.1 ml) from the cell suspension were withdrawn at 5, 30, and 60 minutes, filtered through nitrocellulose filters (0.2-µm pore diameter; EMD Millipore, Billerica, MA), and washed at room temperature with 5 ml of M9 medium. The filters were digested with 0.2 ml of concentrated HNO_3 (70%, ≥ 99.999% trace metals basis) at 70 ˚C for 30 min. The dissolved filters were allowed to cool to room temperature and diluted with HPLC-grade water to produce a final HNO_3 concentration of 2%. Arsenic was quantified by ICP-MS. Standard solutions were made in the range of 1 - 50 ppb in 2% nitric acid using arsenic standard (Ultra Scientific, N. Kingstown, RI).

Random Tn5-mediated mutagenesis: Overnight cultures of *E. coli* AW3110 - Cm^r (recipient) (Carlin et al., 1995) and *E. coli* S17-1 pSup102::Tn5B20 - Km^r (donor) were diluted a hundred-fold and grown to A_{600nm} = 0.6 and 0.9, respectively. 3 ml of the recipient strain and 1.5 ml of the donor strain were centrifuged, mixed, and resuspended in 30 µL of LB. The mixture was spotted directly onto the surface

of LB agar and incubated overnight at 37 ˚C. A loopful of the conjugation mixture was streaked on M9 agar plates containing chloramphenicol and kanamycin to select the transconjugants. Transconjugants were pooled together to create a library of mutants, and appropriate dilutions of the mutant library were plated in M9 agar plates containing 50 µM AST, and colonies of AST-resistant mutants were isolated.

Genome sequence analysis: Illumina whole genome sequencing was performed by SeqCenter (SeqCenter, Pittsburg, PA, USA). Data quality control (Adapter removal, quality trimming, length filtering) was performed using fastp (Chen, 2023). Genome assembly and blast analysis was performed with the sequencing data. Briefly, 5 separate assemblies (LM1-LM5, based on the labelling of the DNA samples) were generated with SPAdes (Prjibelski et al, 2020)and annotated using Prokka (Seemann, 2014) . W3110 strain was used as a reference to improve the annotation quality. Next, the complete sequence of *Escherichia coli* transposon Tn5 (U00004) was used as a reference to perform blastN to check which predicted genes hit the transposon sequence. Similarly, blastN was performed using assembled contigs to determine hits with transposon reference. A contigs blast was performed to check for any hits in the intergenic region.

REFERENCES

Bachmann, B. J. (1987). Derivations and genotypes of some mutant derivatives of *Escherichia coli* K-12. In: Neidhardt FC, Ingraham JL, Low KB, Magasanik B, Schaechter M, Umbarger HE (eds) *Escherichia coli* and *Salmonella typhimurium* cellular and molecular biology. American Society for Microbiology, Washington DC, pp 1190–1219

Bañares AB, Valdehuesa KNG, Ramos KRM, Nisola GM, Lee WK, Chung WJ. Discovering a novel D-xylonate-responsive promoter: the P_{yjhI}-driven genetic switch towards better 1,2,4-butanetriol production. Appl Microbiol Biotechnol. 2019 Oct;103(19):8063-8074. doi: 10.1007/s00253-019-10073-0

Carlin, A., Shi, W., Dey, S., & Rosen, B. P. (1995). The ars operon of Escherichia coli confers arsenical and antimonial resistance. *Journal of Bacteriology*, *177*(4). https://doi.org/10.1128/jb.177.4.981-986.1995

Chen, S. (2023). Ultrafast one-pass FASTQ data preprocessing, quality control, and deduplication using fastp. *IMeta*, *2*(2), e107. https://doi.org/10.1002/imt2.107

Galván, A. E., Paul, N. P., Chen, J., Yoshinaga-Sakurai, K., Utturkar, S. M., Rosen, B. P., & Yoshinaga, M. (2021). Identification of the Biosynthetic Gene Cluster for the Organoarsenical Antibiotic Arsinothricin. *Microbiology Spectrum*, *9*(1). https://doi.org/10.1128/spectrum.00502-21

Garbinski, L. D., Rosen, B. P., & Chen, J. (2019). Pathways of arsenic uptake and efflux. *Environment International*, *126*, 585–597. https://doi.org/10.1016/j.envint.2019.02.058

Harth, G., & Horwitz, M. A. (1999). An inhibitor of exported Mycobacterium tuberculosis glutamine synthetase selectively blocks the growth of pathogenic mycobacteria in axenic culture and in human monocytes: Extracellular proteins as potential novel drug targets. *Journal of Experimental Medicine*, *189*(9). https://doi.org/10.1084/jem.189.9.1425

Kadner, R. J. (1974). Transport Systems for L-Methionine in Escherichia coli. In *journal of bacteriology* (Vol. 117, Issue 1). https://journals.asm.org/journal/jb

Kadner, R. J. (1975). Regulation of methionine transport activity in Escherichia coli. *Journal of Bacteriology*, *122*(1), 110–119. https://doi.org/10.1128/jb.122.1.110-119.1975

Kadner, R. J., & Watson, W. J. (1974). Methionine transport in Escherichia coli: physiological and genetic evidence for two uptake systems. *Journal of Bacteriology*, *119*(2), 401–409. https://doi.org/10.1128/jb.119.2.401-409.1974

Kumar Singh Mayashree B Syiem AE Rajkumar S Singh AE Samrat Adhikari AE Amar Nath Rai, A. A. (n.d.). *A Common Transport System for Methionine, L-methionine-DL-Sulfoximine (MSX), and Phosphinothricin (PPT) in the Diazotrophic Cyanobacterium Nostoc muscorum*. https://doi.org/10.1007/s00284-008-9111-2

Kuramata, M., Sakakibara, F., Kataoka, R., Yamazaki, K., Baba, K., Ishizaka, M., Hiradate, S., Kamo, T., & Ishikawa, S. (2016). Arsinothricin, a novel organoarsenic species produced by a rice rhizosphere bacterium. *Environmental Chemistry*, *13*(4). https://doi.org/10.1071/EN14247

Lamberth, C. (2016). Naturally occurring amino acid derivatives with herbicidal, fungicidal or insecticidal activity. In *Amino Acids* (Vol. 48, Issue 4). https://doi.org/10.1007/s00726-016-2176-5

Meins, F., & Abrams, M. L. (1972). How methionine and glutamine prevent inhibition of growth by methionine sulfoximine. *Biochimica et Biophysica Acta (BBA) - Biomembranes*, *266*(1), 307–311. https://doi.org/10.1016/0005-2736(72)90146-0

Merlin, C., Gardiner, G., Durand, S., & Masters, M. (2002). The Escherichia coli metD locus encodes an ABC transporter which includes Abc (MetN), YaeE (MetI), and YaeC (MetQ). *Journal of Bacteriology*, *184*(19). https://doi.org/10.1128/JB.184.19.5513-5517.2002

Metcalf, W. W., & Van Der Donk, W. A. (2009). Biosynthesis of phosphonic and phosphinic acid natural products. In *Annual Review of Biochemistry* (Vol. 78). https://doi.org/10.1146/annurev.biochem.78.091707.100215

Nadar, V. S., Chen, J., Dheeman, D. S., Galván, A. E., Yoshinaga-Sakurai, K., Kandavelu, P., Sankaran, B., Kuramata, M., Ishikawa, S., Rosen, B. P., & Yoshinaga, M. (2019). Arsinothricin, an arsenic-containing non-proteinogenic amino acid analog of glutamate, is a broad-spectrum antibiotic. *Communications Biology*, *2*(1). https://doi.org/10.1038/s42003-019-0365-y

Paul Carroll, Simon J. Waddell, Philip D. Butcher, and Tanya Parish (2011). Methionine Sulfoximine Resistance in *Mycobacterium tuberculosis* Is Due to a Single Nucleotide Deletion Resulting in Increased Expression of the Major Glutamine Synthetase, GlnA1. Microb Drug Resist. 2011 Sep;17(3):351-5. doi: 10.1089/mdr.2010.0125

Paul, N. P., Viswanathan, T., Chen, J., Yoshinaga, M., & Rosen, B. P. (2023). *The ArsQ permease and transport of the antibiotic arsinothricin*. *January*, 1–10. https://doi.org/10.1111/mmi.15045

Prjibelski, A., Antipov, D., Meleshko, D., Lapidus, A., & Korobeynikov, A. (2020). Using SPAdes De Novo Assembler. *Current Protocols in Bioinformatics*, *70*(1), e102. https://doi.org/10.1002/cpbi.102

Torsten Seemann, Prokka: rapid prokaryotic genome annotation, *Bioinformatics*, Volume 30, Issue 14, July 2014, Pages 2068–2069, https://doi.org/10.1093/bioinformatics/btu153

Yang, H. C., & Rosen, B. P. (2016). New mechanisms of bacterial arsenic resistance. In *Biomedical Journal* (Vol. 39, Issue 1). https://doi.org/10.1016/j.bj.2015.08.003

CONCLUSION AND FUTURE DIRECTIONS

Antimicrobial resistance is undoubtedly one of the greatest threats to global health. Unfortunately, there is a shortage of effective therapies, and the development of new drugs lags behind the emergence of these resistant pathogens. The major challenge with antibiotics is profitability, causing many pharmaceutical companies to abandon the market. The public health implications of a dwindling antibiotic pipeline are significant. Therefore, there is an urgent need to develop novel drugs to combat the global drug resistance crisis.

Arsenic is the most ubiquitous environmental toxin, and every organism has been exposed to this metalloid since the emergence of life on Earth. Behind its inglorious history as a poison, however, arsenic has an even more prestigious history as a pharmaceutical agent. Arsenic has been used as therapeutics since ancient times in the Greek and Roman civilizations and in Chinese and Indian traditional medicine. Various organic and inorganic arsenic compounds have been used as anticancer, antiviral, antiparasitic, and antibiotic agents. In Chapter 1, I reviewed the use of arsenic as a therapeutic agent in the past, present, and future.

Arsinothricin (2-amino-4-(hydroxymethylarsinoyl)butanoate, or AST) is a newly identified broad-spectrum organoarsenical antibiotic. AST was first discovered as a natural product synthesized by the rice rhizosphere bacterium *Burkholderia gladioli* strain GSRB05. Given AST's better antibiotic effectiveness

compared to known GS inhibitors, it has the potential to usher in a new class of organoarsenical antibiotics. This dissertation aims to identify the AST biosynthetic gene cluster and study its transport in and out of cells.

In Chapter 2, I described in detail our laboratory's study of the AST biosynthetic gene cluster (BGC). I showed that only three genes, two of which are novel, are required for the biosynthesis and transport of arsinothricin. The *arsQML* genes comprise an As(III)-responsive *ars* operon controlled by an ArsR repressor. The discovery of the AST BGC will provide insight for developing more effective organoarsenical antibiotics, illustrate the previously unknown complexity of the arsenic biogeochemical cycle, and bring a new perspective to environmental arsenic biochemistry.

Understanding drug transport is crucial for the development of effective antimicrobial therapy. One of the genes in the AST BCG, the *arsQ* gene, is a membrane protein involved in transporting the product(s) of the AST biosynthetic pathway. In Chapter 3, I described my study of ArsQ by heterogeneous expression of the *BgarsQ* gene in *E*. *coli.* My objective was to characterize the function of ArsQ and the chemical nature of its substrate(s). Expression of the *arsQ* gene confers resistance against the antibiotic. ArsQ selectively transports R-AST-OH and R-AST, the reduced trivalent counterparts of AST-OH and AST, respectively. Transport was not dependent on cellular energy. I propose that the ArsQ permease is an energy-independent bidirectional uniporter responsible for the downhill

transport of the trivalent form of AST in AST-producing *B. gladioli* GSRB05. R-AST is oxidized extracellularly to the active pentavalent form of the antibiotic. ArsQ is structurally homologous to the DASS family members. Transport analysis of a serine-to-alanine mutant suggested that the serine residue is in the ArsQ binding site. In an ongoing study described in Chapter 4, I generated ArsQ mutants by site-directed mutagenesis of specific charged residues within the predicted binding site. I will confirm the expression of these mutant proteins by immunoblot analysis. Detailed analysis of their resistance and transport activity will highlight the contribution of each residue to the transport function of ArsQ. The results will lead to a mechanistic understanding of this novel antibiotic transporter.

Finally, in Chapter 5, I describe another direction that I will pursue if time permits: identification of the uptake system(s) of AST into cells of sensitive bacteria. It is unlikely that they would have evolved a dedicated AST uptake system. It is more likely that AST is taken up adventitiously by other permeases such as transporters for structural analogous amino acids, or by an as-yet unidentified transporter. First, I am comparing the transport of AST in the presence and absence of structurally similar amino acids to test the possibility that AST and these amino acids use a common transporter. Next, using random Tn5 insertional mutagenesis, I generated AST-resistant mutants. I am analyzing the DNA sequences of these mutants to identify the insertion points. I hypothesize that the inserted genes will be involved in AST uptake into the cells of sensitive bacteria. Identifying and understanding the

AST uptake system(s) will aid in its development as an effective antibiotic and in the rationale design of other organoarsenical drugs yet to be discovered.

The next steps in this research include elucidating the structure of ArsQ and its relationship to function, chemical modification of AST to improve its efficacy, and further characterization of ArsL, the non-canonical radical SAM enzyme involve in AST biosynthesis. These projects will lead to the development of potent antibiotics to replenish our shrinking antibiotic reserve and extend the antibiotic era.

VITA

PATIENCE NGOZI PAUL

2010 – 2012	National Diploma, Science Laboratory Technology Federal Polytechnic Idah, Nigeria
2012 – 2016	Bachelor of Science, Microbiology University of Ilorin Ilorin, Nigeria
2017	National Youth Service Corps Benue, Nigeria
2019 – 2023	Doctoral Candidate Florida International University Miami, Florida

University Graduate School Dissertation Year Fellowship, Spring & Summer 2023

FIU Diversity, Equity, and Inclusion Doctoral Fellowship, Fall 2022 & Spring 2023

University Graduate School Dissertation Evidence Acquisition Fellowship, Fall, 2022

First South Florida Translational Science Research Symposium, First place Graduate Students Poster Presentation, April 13 & 14, 2022

FIU Student Government Association Graduate Scholarship, Spring 2022

PUBLICATIONS AND PRESENTATIONS

Paul NP, Thiruselvam Viswanathan, Jian Chen, Masafumi Yoshinaga and Barry P. Rosen. *The ArsQ permease and transport of the antibiotic arsinothricin*. 2022 October. Submitted to the Journal of Molecular Microbiology. Mol Microbiol. 2023 Feb 13. doi: 10.1111/mmi.15045. Epub ahead of print. PMID: 36*785875*

Paul NP, Galván AE, Yoshinaga-Sakurai K, Rosen BP, Yoshinaga M. *Arsenic in medicine: past, present and future*. Biometals. 2022 Feb 21:1–19. doi: 10.1007/s10534-022-00371-y. Epub ahead of print. PMID: 35190937; PMCID: PMC8860286

Galván AE, Paul NP, Chen J, Yoshinaga-Sakurai K, Utturkar SM, Rosen BP, Yoshinaga M. *Identification of the Biosynthetic Gene Cluster for the Organoarsenical Antibiotic Arsinothricin*. Microbiol Spectr. 2021 Sep

3;9(1):e0050221. doi: 10.1128/Spectrum.00502-21. Epub 2021 Aug 11. PMID: 34378964; PMCID: PMC8552651

Maria Esteban-Lopez, Marissa D. Perry, Luis D. Garbinski, Marko Manevski, Mickensone Andre, Yasemin Ceyhan, Allen Caobi, Paul NP, Lee Seng Lau, Julian Ramelow, Florida Owens, Joseph Souchak, Evan Ales, Nazira El-Hage*. Health effects and known pathology associated with the use of E-cigarettes*. Toxicology Reports,Volume 9, 2022, Pages 1357-1368, ISSN 2214-7500, https://doi.org/10.1016/j.toxrep.2022.06.006

Gordon Research Conference, Les Diablerets, Switzerland (June 17 – 23, 2023): *The ArsQ Permease and the Transport of the Antibiotic Arsinothricin*

FIU-HWCOM 8th Annual Research Symposium, Virtual Poster presentation (April 22, 2022): *Arsinothricin: an effective antibiotic against Mycobacterium tuberculosis*

Center for Translational Science Symposium – Virtual Poster Presentation (April 13 & 14, 2022): Arsinothricin: *an effective antibiotic against Mycobacterium tuberculosis*

Merck, Kenilworth, New Jersey Oral Research Presentation (April 6, 2022): Arsenic in medicine: *Arsinothricin, an effective antibiotic against Mycobacterium tuberculosis*

FIU-UGS Graduate Students Appreciation Week Scholarly Forum, Poster Presentation (April 5, 2022): *Arsinothricin: an effective antibiotic against Mycobacterium tuberculosis*

HWCOM First Diversity Leadership Series, Virtual Oral Presentation (February 24, 2022): Review of ‘Medical Apartheid’ by Harriet Washington and oral presentation on racism in Medicine

HWCOM Research in Progress Seminar Series, Virtual Oral Presentation (December 7, 2021): *Study of biosynthetic pathway of AST*